2012-11-28

An Optimization-Based Method of Traversing Dynamic s-Pareto Frontiers

Patrick K. Lewis
Brigham Young University - Provo

An Optimization-Based Method of Traversing Dynamic s-Pareto Frontiers

Patrick K. Lewis

A dissertation submitted to the faculty of
Brigham Young University
in partial fulfillment of the requirements for the degree of

Doctor of Philosophy

Christopher A. Mattson, Chair
Spencer P. Magleby
Randy S. Lewis
Brian D. Jensen
Steven K. Charles

Department of Mechanical Engineering

Brigham Young University

November 2012

ABSTRACT

An Optimization-Based Method of Traversing Dynamic s-Pareto Frontiers

Patrick K. Lewis
Department of Mechanical Engineering, BYU
Doctor of Philosophy

The use of multiobjective optimization in identifying systems that account for changes in customer needs, operating environments, system design concepts, and analysis models over time is generally not explored. Providing solutions that anticipate, account for, and allow for these changes over time is a significant challenge to manufacturers and design engineers. Products that adapt to these changes through the addition and/or subtraction of modules can reduce production costs through product commonality, and cater to customization and adaptation. In terms of identifying sets of non-dominated designs, these changes result in the concept of *dynamic Pareto frontiers*, or *dynamic s-Pareto frontiers* when *sets* of system concepts are simultaneously evaluated over time. In this dissertation, a five-step optimization-based design method identifying a set of optimal adaptive product designs that satisfy the predicted changes by moving from one location on the dynamic s-Pareto frontier to another through the addition of a module and/or through reconfiguration is developed. Development of this five-step method was separated into four phases. The first two phases of developments respectively focus on Pareto and s-Pareto cases, where changes in concepts, models, and environments that would effect the Pareto/s-Pareto frontier are ignored due to limitations in traditional optimization problem formulations. To overcome these limitations, and allow for these changes, the third phase of developments presents a generic optimization formulation capable of identifying a dynamic s-Pareto frontier, while the fourth phase adapts the phase three method to incorporate this new dynamic optimization formulation. Example implementations of the four phases of developments were respectively provided through the design of a modular UAV, a hurricane and flood resistant modular residential structure, a simple aircraft design example inspired by the Lockheed C-130 Hercules, and a modular truss system. Noting that modular products only represent one approach for dealing with changes in preferences, environments, models, and concepts, the final research contribution connects the presented method with parallel research developments in collaborative product design and design principles identification, followed by two case study implementations of this unifying design approach in the development of a modular irrigation pump and a modular plywood cart for developing countries.

Keywords: dynamic s-Pareto frontiers, multiobjective optimizaiton, modular systems design, Pareto traversing

ACKNOWLEDGMENTS

This work would not have been possible without the constant and unwavering support of my loving wife Dixie. Likewise, without the continual support, encouragement, and patient mentoring of Dr. Christopher A. Mattson, this work would not have been possible. I appreciate the many hours he has dedicated to teaching and mentoring me throughout this project. I would also like to express my appreciation to Dr. Spencer P. Magleby, Dr. Brian D. Jensen, Dr. Steven P. Charles, and Dr. Randy S. Lewis, my other committee members for their support and assistance throughout this research effort.

I would like to recognize the Fulton College of Engineering and Technology and the National Science Foundation Career Grant CMMI-0954580 for funding this research, as well as the support of my design colleagues at Rocketship, Inc. and the students in the Design Exploration Research Group.

I am grateful to both my and my wife's family for their support in working toward this degree. They have given me hope on a number of occasions when I was not sure I could accomplish what I had set out to do. Finally, I am grateful to a kind Heavenly Father who has answered many prayers, enlightened my understanding, guided my thoughts, and given me ideas of how to proceed in order to be successful.

TABLE OF CONTENTS

LIST OF TABLES

LIST OF FIGURES

NOMENCLATURE

δ	Matrix dictating the desired performance progression that each module provides
D_{a}	Set containing all design variable values of x_{a} and x_{p}
D_{m}	Set containing all design variable values of x_{m} and x_{p}
g	Vector of inequality constraints
h	Vector of equality constraints
J	Aggregate objective function
μ	Vector of design objectives
n_{d}	Number of designs comprising the adaptive design set
$\hat{\mu}^{(i)}$	Objective space performance of a design when used with the i-th module
$\Delta\hat{\mu}^{(i)}$	Change in objective space performance from the base design to $\hat{\mu}^{(i)}$
p	Vector of design parameters
$\hat{p}$	Vector of module design parameters
x	Vector of design variables or design objects
$\hat{x}$	Vector of module design objects
x_{a}	Vector of non-platform adjustable design variables
x_{m}	Vector of non-platform design variables that characterize the design of modules
x_{p}	Vector of platform design variables
y	Vector of independent design objects
y	Vector of dependent design objects
χ	Diagonal matrix of objective identifiers

Subscripts, superscripts, and other indicators

$[\,]^{(i)}$	indicates current design/module
$[\,]^{(k)}$	indicates current design conceptl
$n_{[\,]}$	indicates the number of [ ]
$[\,]_l$	indicates the lower limit of [ ]
$[\,]_u$	indicates the upper limit of [ ]
$[\,]^*$	indicates the optimal value of [ ]
$\hat{[\,]}$	indicates the modular-system [ ]

CHAPTER 1. INTRODUCTION

The needed performance of a product/system, commonly referred to as *customer needs* or *preferences*, tend to naturally change over time [1]. In addition, changes can also occur in operation environments, design concepts, and analysis models [2]. The decision of whether to account for these changes through the development of multiple systems, or adaptive/reconfigurable/modular systems is a complex decision. In addition, providing/developing solutions that anticipate, account for, and allow for any, or all of these types of changes, can be a significant challenge to manufacturers and design engineers.

1.1 Objective

It is observed that accounting for changes in environments, concepts, and models can be viewed as the need to balance competing design objectives [1]. In addition, preferences regarding the desired balance between design objectives have the potential to change over time [3] (e.g., views of affordability for those in poverty change over time as earning power increases due to successful use of products that generate additional income). As such, the objective of this research is to develop and illustrate application of a method that balances the trade-offs between competing design objectives over time, while simultaneously accounting for changes in preferences, operating environments, concepts, and analysis models over time through the identification of a *single* product or system that optimally adjusts to these new and changing needs.

1.2 Approach and Assumptions

In this dissertation, a multiobjective optimization design method identifying sets of non-dominated designs from changing (*dynamic*) sets of design models/concepts is developed. This dynamic set of non-dominated designs is then used to guide the identification of a set of optimal adaptive product

designs that account for changes in preferences, environments, design concepts, and analysis models over time. Assuming these changes are known a priori, the use of a multiobjective optimization method provides two key benefits: (1) The ability to leverage a dynamic set of non-dominated designs from changing design concepts and analysis models to enhance the selection of the modular/adaptive system configuration designs. (2) The ability to balance the competing nature of present customer needs against future needs. Figure 1.1 illustrates the concept of non-dominated designs (bold line) within feasible design spaces (shaded regions) based upon two design objectives (e.g. Cost, Output, etc.) represented by the horizontal and vertical axis. Figure 1.1(a) provides a generic representation of the non-dominated designs for a *single* design model, assuming that both Objective 1 and Objective 2 are to be minimized. Figure 1.1(b) provides a generic representation of the non-dominated designs in the presence of *multiple* design concepts. Figure 1.1(c) provides a generic representation of the non-dominated designs in the presence of changing (dynamic) sets of design concepts.

The novel outcome of the method presented herein is a product that adapts to changing preferences, environments, models, and concepts by moving from one non-dominated design to another through the addition of a module and/or through reconfiguration. Figure 1.2 provides a graphical illustration of the intent of the method in the context of the feasible design spaces and dynamic set of non-dominated designs of Figure 1.1(c). From this figure it is observed that in the development of the method presented in this dissertation there are two assumptions which the method is based upon:

(i) In selecting a product design, non-dominated designs are preferred above any other designs within the feasible design space.

(ii) The current and future needs used to select the optimal product design represent individual points (designs) among the non-dominated designs of a given design space.

Recognizing the complexities of creating an optimization-based modular product design method capable of simultaneously accounting for changing preferences, environments, models, and concepts, the developments presented in this dissertation were accomplished in four phases. The first phase focuses on design scenarios with a single design concept (see Figure 1.1(a)), where

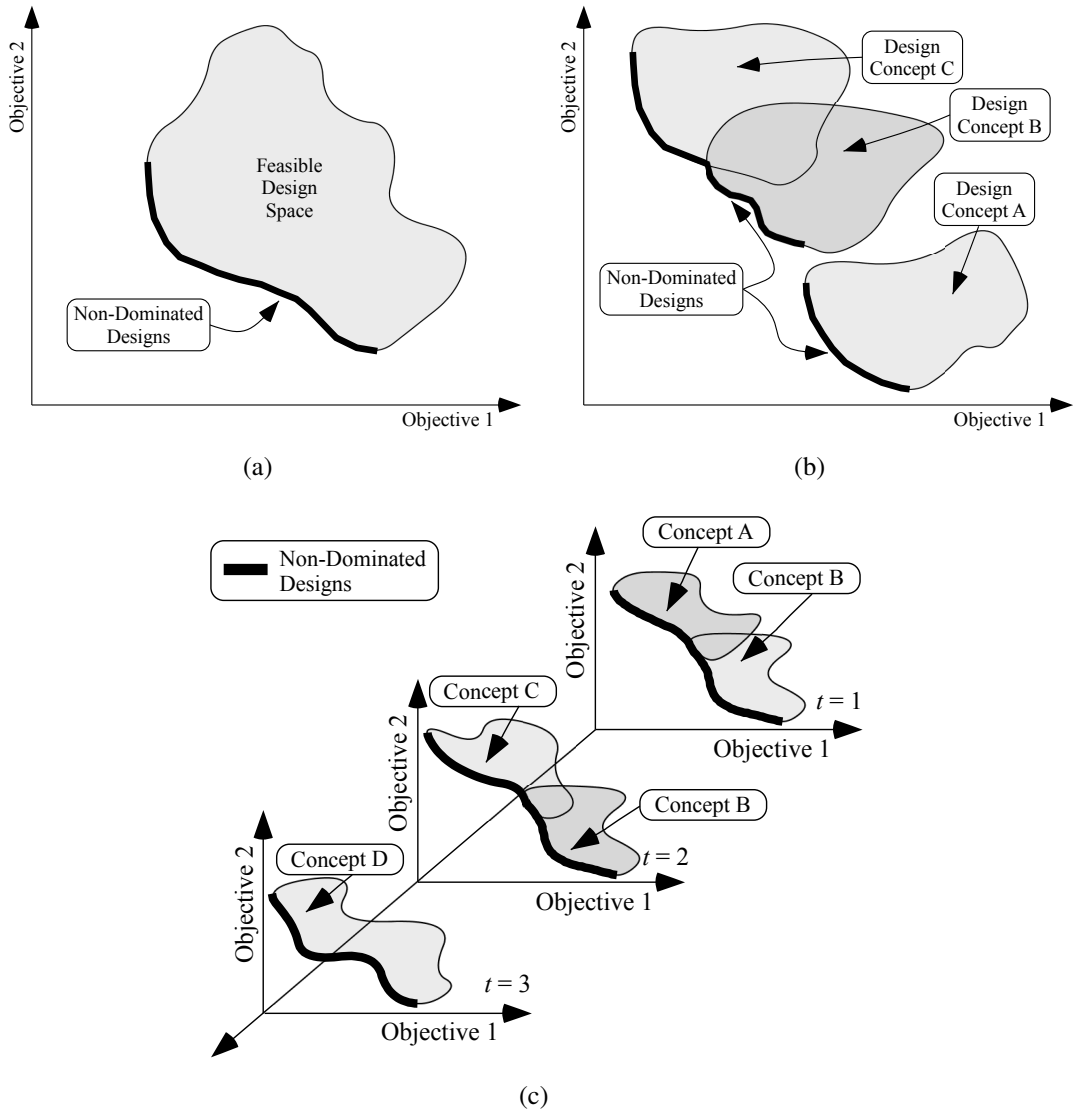

Figure 1.1: Illustration of the concept of non-dominated designs (bold line) within feasible design spaces (shaded regions) based upon minimizing two design objectives, where (a) illustrates a *single* design model, (b) illustrates *multiple* design concepts, and (c) illustrates changing (dynamic) sets of design concepts over time (t).

the only changes considered are the preferences and environment that affect the selection of non-dominated designs over time (i.e., non-dynamic design spaces). The second phase expands upon the first phase developments to consider non-dominated designs from *multiple* design concepts (see Figure 1.1(b)), and allows for more significant changes in the performance of the modular systems that are developed. The third phase focuses on developing a generic optimization formulation capable of identifying the dynamic set of non-dominated designs that results from changing environments, models, and concepts (see Figure 1.1(c)). Finally, the fourth phase adapts the method

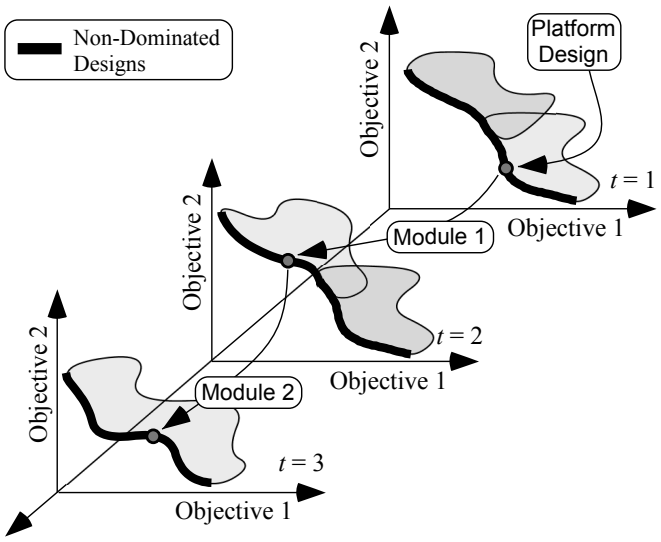

Figure 1.2: Graphical representation of the intent of the method developed in this dissertation to provide a product that expands from one non-dominated design to another through the addition of modules.

resulting from the phase two developments to incorporate the dynamic optimization formulation from the phase three developments, and allow for the identification of modular systems that account for changing preferences, environments, models, and concepts.

It is noted that modular/adaptive products only represent one approach for dealing with changes in preferences, environments, models, and concepts. As a result, in addition to these modular product optimization method developments, parallel research performed in the areas of Collaborative Products [4] (modular products created by combining two or more independently functional products) and Design Principle Identification [5] are also described in this dissertation. In light of these parallel developments, the final research contribution described in this dissertation gathers the presented research developments into a unifying design approach.

1.3 Outline

The remainder of this dissertation is presented as follows: A literature review is included in Chapter 2, along with summaries of the parallel research performed in the areas of Collaborative Products and Design Principle Identification. In Chapter 3, the first phase of the method development focused on traversing of Pareto frontiers is presented. In Chapter 4, the design of a simple unmanned air vehicle is used to demonstrate application of the phase one developments. In Chapter 5, the

second phase of the method development extending the method to traversing s-Pareto frontiers is presented, with Chapter 6 demonstrating the implementation of the phase two developments through the design of a hurricane and flood resistant modular residential structure. Phase three developments focused on dynamic s-Pareto frontier identification along with an example implementation using a simple aircraft design example are provided in Chapters 7 and 8 respectively. In Chapter 9, the fourth phase of the method development focused on traversing dynamic s-Pareto frontiers is presented, with implementation demonstrated through the development of a modular truss system in Chapter 10. In Chapter 11 the unifying design approach is presented, with case study implementations in the development of a manual irrigation pump, and a modular plywood cart for developing countries provided in Chapters 12-13, respectively. Concluding remarks and a discussion of future work are provided in Chapter 14. Additional information required for the aircraft example in Chapter 8, and the cart example in Chapter 13, is provided in Appendix A and Appendix B, respectively.

CHAPTER 2. LITERATURE SURVEY & PARALLEL RESEARCH DEVELOPMENTS

This chapter provides a review of published literature that establishes the foundation for the presented optimization-based method of designing modular/reconfigurable products, and a summary of research developments in collaborative product design and design principle identification. The technologies that form an enabling foundation for the design methodology are (i) product modularity and adaptability, and (ii) multiobjective optimization. The following literature review will first introduce (i) and (ii), followed by a review of the application of optimization techniques in modular product/system design.

2.1 Product Modularity and Adaptability

In order to develop modular systems that account for changing needs over time, there is a need for strategic module designs that make product platform designs progressively expandable [6–9]. To this end, published literature in the areas of product family and modular product design serve as a starting point [6, 7, 10–13]. Some of the noted benefits of modular designs include the following:

(i) The ability to serve the widest range of customers and changing product demands [9, 14, 15].

(ii) The ability to build upon existing process capabilities, experience, and knowledge (economies of scale) through the reusability/commonality of components [9, 16].

(iii) Have an increased number of product variants (product iterations/configurations) [14, 16].

(iv) Cost savings in inventory and logistics [16].

(v) Lower life cycle costs through easy maintenance [14, 16].

(vi) Potential for parallel manufacture of modules [16].

(vii) Shorter life cycles through incremental improvements like upgrades, add-ons, and adaptations [14, 16].

Modular products are defined in the literature as products, assemblies, and components that combine distinct building blocks (modules) to fulfill various functions [17]. Similarly, a module-based product family is defined in the literature as a group of related products derived from independent functional or geometric units [18–20], that differ through the addition or subtraction of modules [10, 19, 20]. Two common goals of product family design are to identify product families and platforms that maximize both variable commonality, and performance diversity [21, 22].

Product families are often used to address the challenge of satisfying a variety of needs through product performance diversity [9, 14, 23], while still maintaining product commonality as seen by manufacturers [12, 21]. Two platforms for building product families are identified within the literature: Scale-based and Module-based product platforms [12, 24]. The strength of product family approaches is in their ability to provide a range of products that satisfy the *current* variation in customer needs across *multiple market segments* [11]. One approach presented in the literature by Meyer [25] for accomplishing this is the product family beachhead approach illustrated in Figure 2.1.

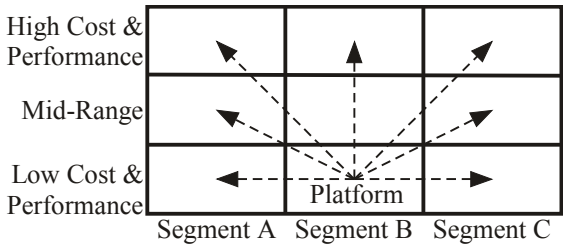

Figure 2.1: Representation of the product family beachhead approach as presented by Meyer [25].

From Figure 2.1 it is seen that product family approaches use customer needs of the various market segments to identify a product platform that is used to derive a variety of products to satisfy the needs of the various market segments [11, 25, 26]. However, it is observed that the effects of future operation environments, analysis models, design concepts, and needs of the various market segments represented by the movement of customers (groups of customers are indicated by the numbers 1-6) from one market segment to another, or the emergence of new market segments, is not considered in current design methods. This movement of customers to different or new market

segments is illustrated in Figure 2.2, and represents a gap in product family design methods that is addressed through the research presented in this dissertation.

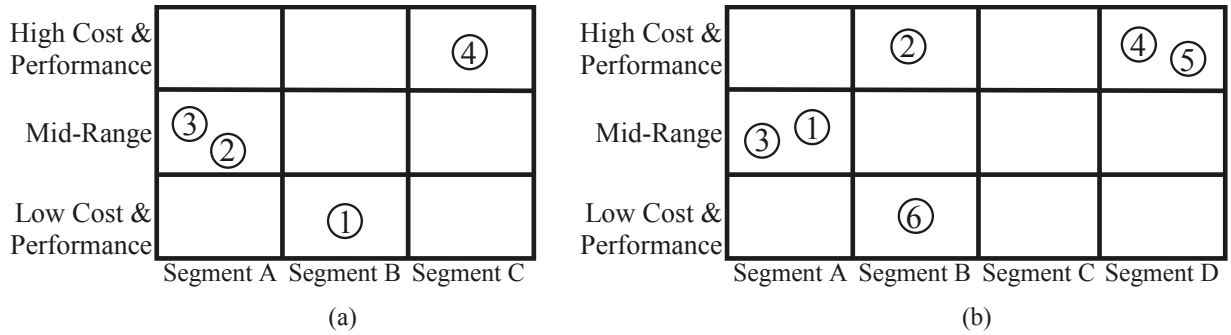

Figure 2.2: Illustration of the changes in market segment composition over time due to changing needs of customers (groups of customers are indicated by the numbers 1-6). The customers and market segments of (a) represent the current market segment compositions. The customers and market segments of (b) represent a future market segment composition.

In the development of modular systems, the literature also identifies four main modular architecture types [20, 27–29]. A description of these architectures is provided below, and the conceptual differences between them are illustrated in Figure 2.3.

1. *Slot-Modular* – provides each module with a unique interface in order to eliminate improper assembly [20, 27, 28].

2. *Bus-Modular* – implements interfacing that is the same for all modules, thus making the platform design behave as a common connection platform for all modules [20].

3. *Sectional-Modular* – similar to bus-modular in that all modules contain the same interface, but in this architecture no single element is identified as the platform that all modules attach to [20, 27].

4. *Type II Modular* – combination of slot and sectional-modular architectures in that each module interface is unique, and there is no identified platform that all modules attach to [29].

Building on these foundational elements, the research presented in this dissertation allows designers to leverage these existing developments in modular system classifications to specify the

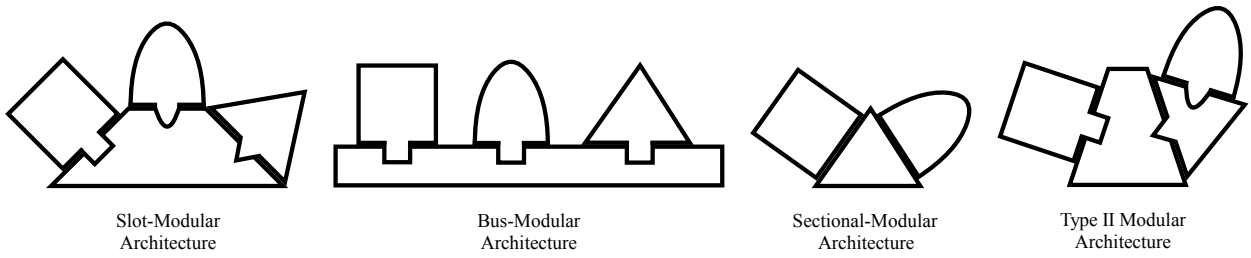

Figure 2.3: Representation of four modular architecture types as presented in Ulrich and Eppinger [20], and Strong et al. [29].

approach needed to develop module designs and interfaces. In addition, research in the areas of adaptive systems [30], flexible systems [31], and reconfigurable systems [32] can also be used to assist in the identification of platform and module design concepts.

It is noted that adaptive, flexible, and reconfigurable systems seek to address changes in preferences and environments by enabling a product to adapt/reconfigure based on these changes, or by designing the product to inherently/flexibly function in multiple scenarios. However, because these systems do not typically consider the addition/subtraction of modules to account for changes in design concepts or analysis models, the methods for developing these systems do not meet the objectives of this dissertation. In addition, the application of optimization approaches within these methods is described in Section 2.3.

Research Needs: An important element of the research presented in this dissertation is that changes in needs over time do not always require significant changes in product performance. As such, the objectives of traditional product family approaches to maximize both product family performance diversity and product commonality will not always be considered/satisfied. In particular, the presented research seeks to identify product family platforms that facilitate modularity, even if maximum variable commonality is not explicitly obtained. Additionally, the presented research also seeks to drive module-enabled performance as close to predicted future performance needs as possible, without regard to how diverse those future needs are.

2.2 Multiobjective Optimization

Fundamental within the presented research is the need to characterize/balance competing objectives or goals (customer product performance needs). Multiobjective optimization is a well-known,

well-accepted, means to quantify tradeoffs between competing design objectives [33–43]. One pertinent application of multiobjective optimization in the context of the research presented in this dissertation is that of identifying a set of non-dominated designs – Pareto frontier [44–46]. Figure 2.4 demonstrates a generic characterization of trade-offs between objectives through the identification of a Pareto frontier, assuming that objectives μ_1 and μ_2 are to be minimized. Each solution comprising the illustrated frontier is said to be *Pareto optimal* – no other designs better satisfy *all* design objectives [47–50]. These Pareto solutions are generally sought because they indicate that objectives have been improved as much as possible without sacrificing another design objective's performance.

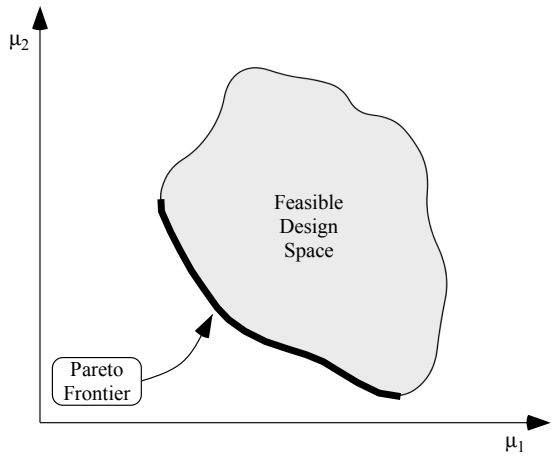

Figure 2.4: A feasible design space (shaded) for objectives 1 and 2. The Pareto frontier (bold line) represents the most desirable set of solutions in the feasible space for this minimization-minimization problem.

A generic multiobjective optimization problem (MOP) formulation yielding a set of optimal solutions – those belonging to the Pareto frontier – is presented as follows:

Problem 2.1: Generic multiobjective optimization problem statement

$$D := \{(x_1^*, x_2^*, ..., x_{n_x}^*)\} \tag{2.1}$$

x^* defined by:

$$\min_x \ \{\mu_1(x,p),\ \mu_2(x,p),\ ...,\ \mu_{n_\mu}(x,p)\} \quad (n_\mu \geq 2) \tag{2.2}$$

subject to:

$$g_q(x,p) \leq 0 \quad \forall\, q \in \{1,...,n_g\} \tag{2.3}$$

$$h_v(x,p) = 0 \quad \forall\, v \in \{1,...,n_h\} \tag{2.4}$$

$$x_{jl} \leq x_j \leq x_{ju} \quad \forall\, j \in \{1,...,n_x\} \tag{2.5}$$

where D is a set containing all values of x^* for each Pareto-optimal design obtained through the evaluation of the MOP; μ_i denotes the i-th generic design objective; x is a vector of design variables with upper/lower bounds of x_u and x_l respectively; p is a vector of fixed design parameters; g is a vector of inequality constraints; and h is a vector of equality constraints.

For multiobjective optimization approaches, the decision of which Pareto-optimal solution is to be used comes through the inclusion of objective function parameters, and sometimes constraints that capture customer needs or preferences for a single instance in time. As indicated in Problem 2.1 above, the presented MOP yields a set of solutions. In order to obtain a single optimal solution, the set of objectives in Equation 2.2 is often replaced by a scalar function that is optimized, where this scalar function is commonly referred to as an aggregate objective function [37, 51].

The concept of Pareto optimality is central to multiobjective optimization [47, 49, 50, 52], and within the presented method there is a need to characterize the competing nature of the Pareto frontiers of multiple design concepts. Within the literature, this characterization is obtained through the identification of a set of Pareto-optimal solutions through the use of Pareto filters that either reduce the set of Pareto optimal solutions, [34, 53–55] or eliminate non-Pareto and locally Pareto solutions [37, 56–59]. In particular, the concept of generating an s-Pareto frontier – reduction of the Pareto frontiers from a *set* of concepts into a single Pareto frontier – presented in Mattson et al [37] has direct application to the balancing of the tradeoffs of a set of design concepts needed within the presented method developments. Figure 2.5 illustrates the meaning of non-dominance in the presence of multiple system concepts (bold line), for the minimization of two objectives (μ_1 and μ_2), through the identification of a s-Pareto frontier. Similar to a Pareto frontier, each solution comprising the s-Pareto frontier, graphically demonstrated in Figure 2.5, is

said to be *s-Pareto-optimal* [37] because there are no other feasible designs from any other concept that are better in all objectives.

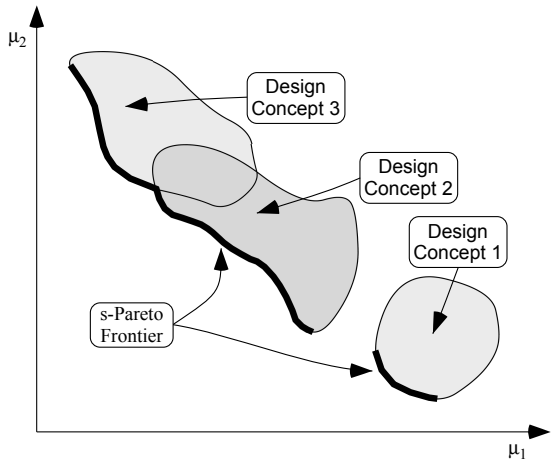

Figure 2.5: A feasible design space (shaded) for objectives 1 and 2. The s-Pareto frontier (bold line) represents the most desirable set of solutions in the feasible space for this minimization-minimization problem with three possible design concepts.

Within the literature, s-Pareto frontier identification methods include directly evaluating an MOP (see Problem 2.2 below), Pareto filters that find s-Pareto solutions among sets of Pareto optimal solutions [54, 55], eliminating non-Pareto and locally Pareto solutions with Pareto filters [37, 44, 58], and combinations of these methods. In particular, the method presented in Mattson and Messac 2003 [37] for generating an s-Pareto frontier by reducing the Pareto frontiers from disparate system concepts into a single s-Pareto frontier has direct application to the balancing of the tradeoffs of a set of system concepts needed within the presented research.

A generic MOP formulation yielding a set of optimal solutions – those belonging to a s-Pareto frontier – is presented as follows:

Problem 2.2: Generic s-Pareto multiobjective optimization problem statement

$$D := \{(x_1^{(k)*}, x_2^{(k)*}, ..., x_{n_x^{(k)}}^{(k)*})\} \tag{2.6}$$

$x^{(k)*}$ defined by:

$$\min_{k}\left\{\min_{x^{(k)}}\left\{\mu_1^{(k)}(x^{(k)},p^{(k)}),\ \mu_2^{(k)}(x^{(k)},p^{(k)}),\ ...,\ \mu_{n_\mu}^{(k)}(x^{(k)},p^{(k)})\right\}\quad (n_\mu \geq 2)\right\} \tag{2.7}$$

subject to:

$$g_q^{(k)}(x^{(k)},p^{(k)}) \leq 0 \quad \forall\, q \in \{1,...,n_g^{(k)}\} \tag{2.8}$$

$$h_v^{(k)}(x^{(k)},p^{(k)}) = 0 \quad \forall\, v \in \{1,...,n_h^{(k)}\} \tag{2.9}$$

$$x_{jl}^{(k)} \leq x_j^{(k)} \leq x_{ju}^{(k)} \quad \forall\, j \in \{1,...,n_x^{(k)}\} \tag{2.10}$$

where k denotes the k-th design model, D is now a set containing all values of $x^{(k)*}$ for each s-Pareto-optimal design obtained through the evaluation of the MOP; $\mu_i^{(k)}$ denotes the i-th generic design objective; $x^{(k)}$ is a vector of design variables for the k-th design model; and $p^{(k)}$ is a vector of design parameters for the k-th design model. It should be noted that, once again, the above MOP does not yield a unique solution, and that the common method to obtain a single optimal solution is to replace the right-hand-side of Equation 2.7 with an aggregate objective function [37].

It should be noted that although Figures 2.4 and 2.5 only provide 2-dimensional (2-objective) representations of the solutions to Problems 2.1 and 2.2 respectively, the presented MOP formulations are not limited to 2-dimensional cases. For problems where $n_{n_\mu} = 3$, the results of Problems 2.1 and 2.2 result in 3-dimensional surfaces. Figure 2.6 demonstrates this result for Problem 2.1, where Figure 2.6(a) illustrates a 3-dimensional feasible space, and Figure 2.6(b) illustrates the resulting 3-dimensional Pareto surface assuming all objectives are minimized. For problems where $n_{n_\mu} > 3$, the results of Problems 2.1 and 2.2 are hyper-surfaces, and are therefore ill-suited for graphical representation. For this reason, although the MOP formulations presented in this dissertation will be applicable in n-dimensions, all graphical representations of generic MOP formulations provided hereafter will be represented in 2-dimensions in order to remain consistent with Figures 2.4 and 2.5.

Fundamental in the optimization-based method described in this dissertation, is the need to balance the trade-off in product performance over time due to changes in preferences, environments, concepts, and analysis models. Recognizing that these changes over time can be viewed as

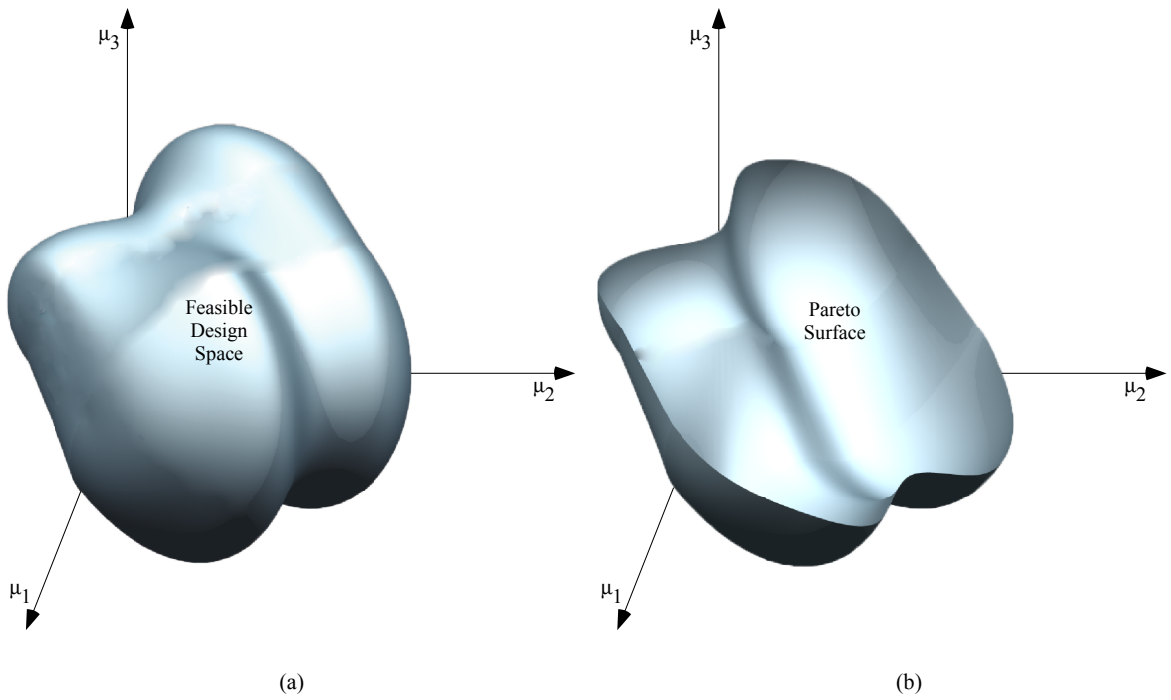

Figure 2.6: Representation of a 3-dimensional (3-objective) evaluation of Problem 2.1, where (a) illustrates a 3-dimensional feasible space, and (b) illustrates the resulting 3-dimensional Pareto surface for a minimization-minimization problem.

a series of anticipated optimization scenarios, a review of multi-scenario optimization literature is now provided.

With the rise of mass customization, the engineering and science communities are being compelled to look for designs that are appropriate for groups of applications, rather than a single application [60, 61]. In order to address this need to consider multiple scenarios simultaneously, three approaches are observed in the literature.

1. *Optimize an aggregate performance function:* This approach is characterized by the use of a function that seeks to combine the performance of the product/system for each of the scenarios being considered into a single aggregate performance value that is then optimized [62–67]. The result of this approach is a single-objective optimization that only returns a single optimal design.

2. *Optimize the worst case scenario:* This approach evaluates the performance of the product/system for each scenario, identifies the scenario where the system has the worst performance, and then optimizes the performance of that scenario [60,68]. For cases where there is

a single performance value (objective), this approach results in a single optimal design. Otherwise, multiobjective cases will result in the identification of a Pareto frontier representing the trade-offs between the worst case performance measures.

3. *Collect the objectives for each scenario into a single multiobjective problem:* This approach formulates a single MOP, where the objectives of this MOP are the collection of all of the identified objectives for each scenario [60, 67, 69]. The result of this approach is a multiobjective optimization that returns a Pareto frontier/surface.

Research Needs: It should be observed that for the first two multi-scenario optimization approaches described above, the optimization problem is typically for a single objective or function. Consequently, these approaches do not identify sets of Pareto designs, and the performance trade-offs between different scenarios are therefore difficult to observe (i.e., the aggregate or worst case performance does not readily present decision-makers the performance information of the product/system during individual scenarios). In addition, the third multi-scenario approach seeks to preserve the performance information for the different scenarios by obtaining a Pareto frontier representing the performance trade-offs between the identified scenarios, but does not capture how the product compares to the Pareto frontiers that could be obtained for the individual design scenarios. As such, none of these approaches effectively observes the trade-off between the multi-scenario optimization and the equivalent single scenario optimizations. In part, this is due to the form of the traditional MOP (see Problema 2.1 and 2.2 above), and the inherent inability to easily evaluate multiple scenarios both individually, and simultaneously, without requiring the formulation of multiple MOP's (one MOP for each scenario, and one that uses the resulting Pareto frontiers to simultaneously optimize for all the scenarios). Therefore, a new MOP formulation that efficiently evaluates multiple scenarios is needed.

In reference to the method presented in this dissertation, it is also important to remember that, like most areas of engineering, research in the area of multiobjective optimization has experienced stages of evolution [70]. The first generation of research in multiobjective optimization focused on the development of theory and algorithms [71–73]. The second generation focused on the development of methods of using these algorithms to support general engineering [37, 59, 74]. The third (current) generation is using/combining/expanding these methods and algorithms in ways that

improve design identification, selection, and/or exploration [2, 11, 12, 75–88] (e.g. making products more difficult to reverse engineer). Therefore, this work does not develop a new algorithm for multiobjective optimization, but instead shows how a series of optimization routines can be used in a novel way to develop a *single* product that is capable of traversing a changing (dynamic) s-Pareto frontier through the addition of modules.

2.3 Optimization of Modular Products

The literature states that designers are often skeptical regarding the advantages of modularity [89]. This is largely due to the inferior performance commonly obtained by modular designs compared to equivalent custom built optimal alternatives [90, 91]. Attempts to address various issues in modular product design such as planning for commonality, optimizing the degree of commonality and finding the optimum settings for the common modules have been made [7, 92, 93].

In order to implement an optimization routine, the determination and formulation of objectives and constraints representing the performance of the product/system to be optimized is required. The use of a number of methods to address this need when optimizing modular products have been proposed, including: (i) defining rules and metrics for evaluating the effects of modularity [94, 95]; (ii) evaluating the performance in terms of the design requirements and cost [7, 96, 97]; (iii) identifying the trade-offs resulting from shared systems, subsystems, and/or components [69, 98]. Although, it is noted that many of the above mentioned metrics are actually measuring efficiency rather than engineering measures of performance [95].

The literature shows that a desirable product family can be identified from among the designs comprising the Pareto frontier [11, 12, 37] obtained through the evaluation of a multiobjective problem (see Section 2.2). These previous developments evaluate and select product family members from among the set of Pareto designs by considering the design's unique performance *and* common features compared to other designs in the product family (a critical part of product family design). For example, one method of identifying module and platform variables is through the use of Pareto-filtering methods that explore the effects of each variable on the objective space performance [11, 12].

Additional methods that have been used with the intent of optimizing a modular product or product family include the following: (i) genetic algorithms [7, 99]; (ii) compromise decision support problems using goal programming [26, 95, 100–102]; (iii) MOP formulations identifying the Pareto surface based on commonality constraints used to define the common elements of the various product variants [7, 69, 103]; (iv) target cascading [98]; (v) integer-programming optimization formulations [92]; (vi) selection-integrated optimization [30]; (vii) design-under-uncertainty method [104]; (viii) flexible design methodology [105]; (ix) state-feedback-control law [106]; and (x) robust concept exploration methods [100, 101, 107, 108].

Research Needs: While there exists useful elements in the literature on the subjects of multiobjective optimization and product modularity and adaptability, ***a method for finding balance in the context of changing customer needs (preferences), implementation environments, design concepts, and analysis models*** is needed to fulfill the objective of this dissertation identified in Section 1.1. Similar to traditional multiobjective optimization approaches, the method presented in this dissertation seeks non-dominated (optimal) solutions. However, the presented method expands upon traditional approaches to provide the desired adaptability by using a series of strategically constructed MOP formulations to select modular product designs, within anticipated regions of interest, based on two characteristics of the design. The first is the solution's ability to expand/adapt to satisfy known changes in preferences, environments, concepts, and models over time. The second is the solution's ability to minimize the offset of each modular configuration from a set of non-modular Pareto-optimal solutions characterizing the known preference, environment, concept, and model changes (i.e., offset from a changing/dynamic s-Pareto frontier).

2.4 Collaborative-Product Design

As described in Section 1.2, part of the research presented in this dissertation explored alternative modular product design strategies. As a result, *collaborative-products*, a new category of modular products, was defined/identified. The definition of a collaborative-product is one that is created when physical components from two or more products are temporarily recombined to form another product capable of performing additional tasks. As such, collaborative-products have

great potential to increase the *task-per-cost ratio* of a set of products by reducing the number of products required to perform a given number of tasks.

In order to facilitate the identification of optimal products sets capable of being recombined to create a collaborative-product, a seven-step design method was developed (see Figure 2.7). At each step, the method guides the designer in making decisions, gathering needed information, and implementing design practices. The method also incorporates an optimization routine that identifies the optimal set of collaborative products. This optimization matches the component functions of the products in the set to a target product while seeking to minimize both the number of products in the set, and the number of components of the products that are not used to create the collaborative product. For a detailed discussion of each step see Morrise et al 2011 [4].

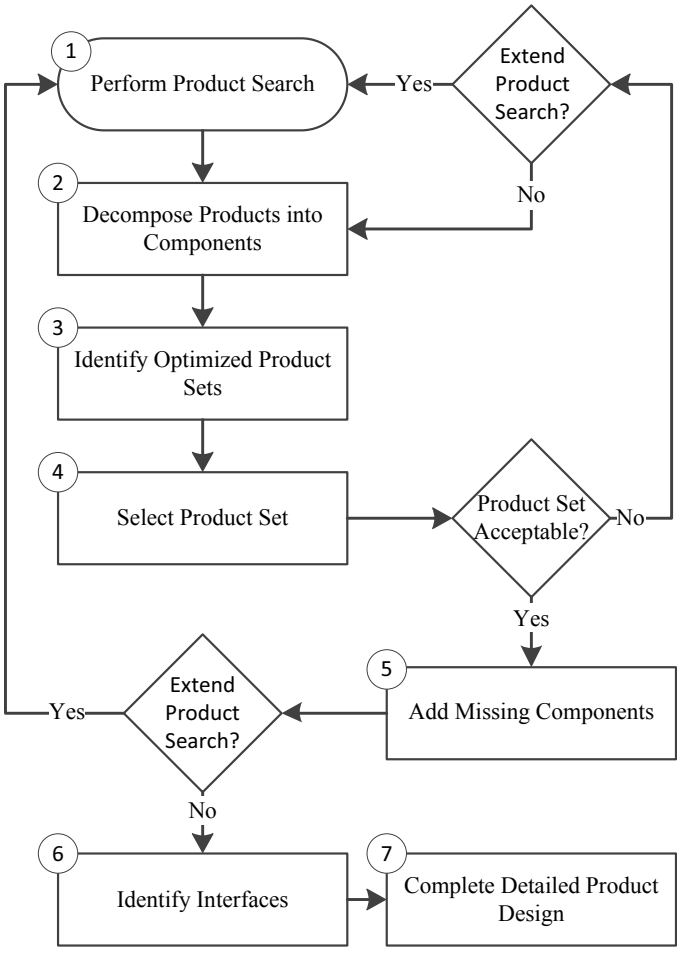

Figure 2.7: Seven-Step method for designing Collaborative products [109].

Some of the industries that could benefit from these types of products are payload conscious industries such as aerospace and backpacking, and income generating products for those in extreme poverty. Though few in number, examples of existing products that fit into this new category of modular products can be found on the market today in kitchen tools (e.g., salad tongs created by joining a serving spoon and serving fork) and carpenter's tools (e.g., a combination square that is created by joining a ruler and small level). An example of a simple collaborative-product developed using this method is a block plane (see Figure 2.8(a)). This block plane is collaboratively created using a chisel (see Figure 2.8(b)) and sanding block (see Figure 2.8(c)). Other theoretical examples of collaborative-products identified through this method include an apple peeler and a brick press.

(a) (b) (c)

Figure 2.8: (a) Collaborative block plane created by combining the components of a (b) chisel and (c) sanding block.

Through these examples the need for an optimization method capable of balancing the performance trade-offs in creating a collaborative-product from a set of products was observed. As a result, a four-step method that replaces the final two steps of the method presented in Figure 2.7 was developed, and is provided in Figure 2.9.

It should be noted that the completed research presented in this section represents the Masters research of Jacob Morrise [4, 109] and Nick Wasley [110]. Due to the emphasis on optimization-based modular product design within this dissertation, research collaboration was focused on the refinement of the method and implemented optimization routines.

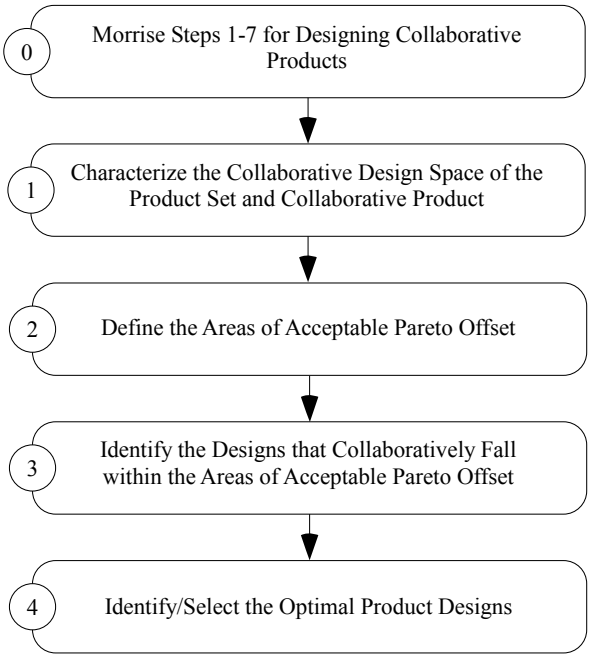

Figure 2.9: Four-Step method for Collaborative product design optimization [110].

2.5 Design Principles Identification

The most successful design methods use design principles that are important to a target market to guide development efforts/decisions [111, 112]. In addition, these principles can be viewed as indicators of the information and customs that are most important to the identified target market. Consequently, the better these principles are understood, the higher the probability that design efforts will result in a successful product.

In situations where these principles are not explicitly known or understood, designers will often focus on principles they have observed in other design experiences [20]. However, when designing products for unfamiliar markets this approach has a higher risk of failure, especially when these markets are unfamiliar due to the geographical locations and cultural differences between the market and the designers [113–116].

In order to facilitate the identification of design principles, the five-step method presented in Figure 2.10 was developed. A complete description of each of the identified steps in Figure 2.10 is presented in Campbell et al 2011 [5], along with two case study method implementations.

The first case study establishes a point of reference by applying the method to best selling products in the US (study identified 19 design principles). The second case study applies the

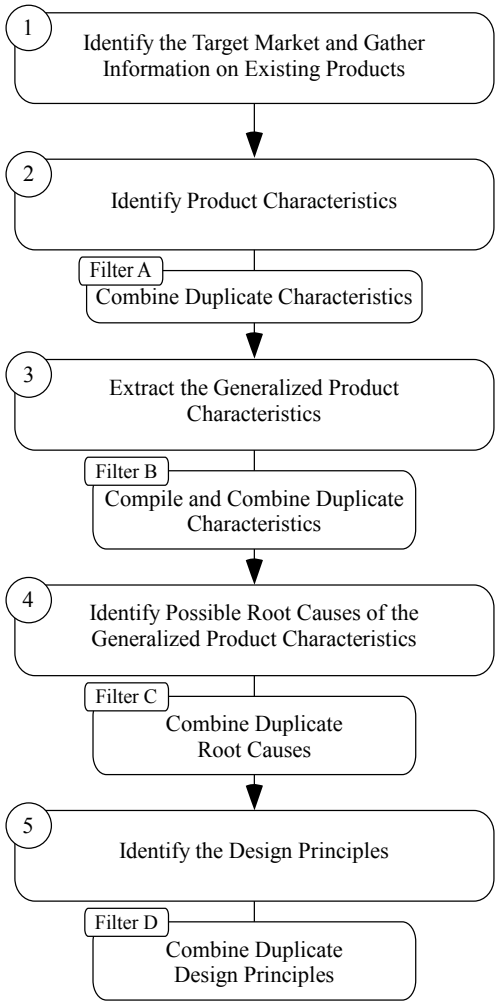

Figure 2.10: Flow chart describing a five-step method for identifying design principles.

method to products created for the developing world (study identified 21 design principles). The resulting principles from the two case studies were analyzed and compared to highlight the similarities and differences between the identified principles. An illustration of how the identified principles compared for the two case studies is shown in Figure 2.11 in the form of a Venn Diagram. The list of principles identified for each case study is presented in Campbell et al 2011 [5].

Through these case studies and subsequent comparisons, it was concluded that the presented method enables designers to successfully identify the principles for specific markets, including the developing world. It should be noted that the research presented in this section represents the Masters research of Robert Campbell [5, 117]. Due to the potential of design principles to enable designers to identify/quantify/incorporate information and customs into optimization models

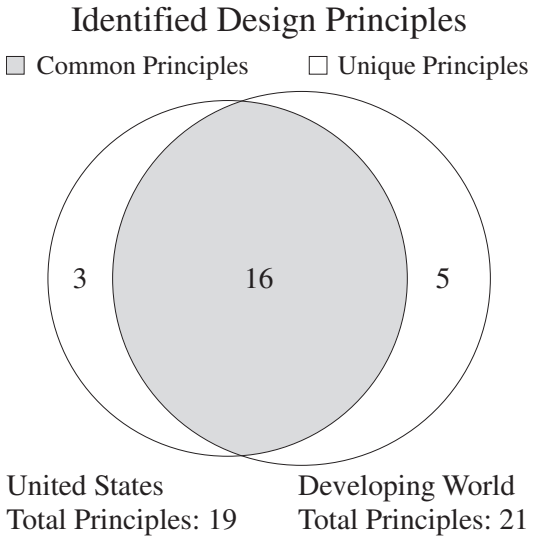

Figure 2.11: Illustration of the number of common and unique design principles identified for two case study implementations of the design principles identification method presented in Figure 2.10.

and decision making, research collaboration was focused on the refinement and implementation of the presented method.

2.6 Summary of Research Needs

From the review of published literature and parallel research developments in collaborative product design and design principle identification provided in this chapter, there are four key research needs that are addressed through the research presented in this dissertation. The first is to enable the identification of product family platforms that facilitate modularity, even if maximum variable commonality is not explicitly obtained. The second is the ability to drive module-enabled performance as close to predicted future performance needs as possible, without regard to the diversity of those future needs. Third is the identification of a new MOP that efficiently evaluates multiple scenarios resulting from changes in preferences, environments, concepts, and models to obtain the dynamic s-Pareto frontier. Finally, the fourth is a method for finding balance in the context of these known changes by expanding traditional/developed approaches to use dynamic s-Pareto frontiers to improve the identification and selection of modular products/systems.

CHAPTER 3. PHASE 1 METHOD DEVELOPMENT: TRAVERSING PARETO FRONTIERS

In this chapter, the first phase in the development of a multiobjective optimization design method providing a Pareto-optimal product and module designs capable of satisfying changes in customer needs over time is described for *single* Pareto frontier design cases [75, 78].

3.1 Optimization-Based Method for the Identification of Platforms and Modules that Account for Changing Needs

By its nature, a Pareto frontier contains many optimal, yet functionally different, designs representing all optimal product candidates. To satisfy changes in customer needs over time through the addition of modules requires the strategic selection of these Pareto-optimal designs based on their ability to facilitate adaptability. Figure 3.1 illustrates the intent of the method to satisfy changing customer needs by selecting a Pareto-optimal product platform design which, through the addition of modules, expands to other Pareto-optimal designs. The first (μ_1) and second (μ_2) objectives are represented along the horizontal and vertical axis, respectively.

Through further examination of Figure 3.1, it is seen that the platform design, shown as $\mu^{(1)}$, adapts to become $\mu^{(2)}$ through the addition of Module 1. Through this approach, the platform and subsequent modules, provide the desired product performance resulting from the changing customer needs as represented by $\mu^{(1)}$, $\mu^{(2)}$, $\mu^{(3)}$, and $\mu^{(4)}$. Figure 3.2 provides a flow chart that illustrates the five primary steps of the multiobjective optimization design method developed in this chapter. This method is a first step in meeting the identified research objectives from Section 2.2 of developing a method for finding balance between multiobjective optimization and product modularity and adaptability in the context of changing customer needs. Each of these steps is described in the following sections.

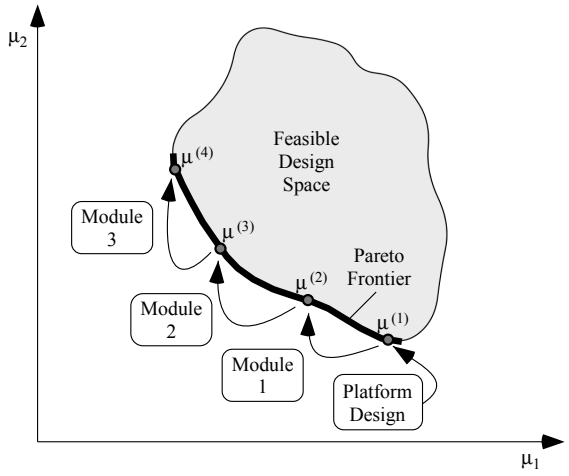

Figure 3.1: Graphical representation of the intent of the method to provide a product that expands from one Pareto-optimal design to another through the addition of modules.

3.2 Step A: Characterize the Multiobjective Design Space

The first step of the method explores the multiobjective design space to evaluate and characterize the effects of each design variable on the objective space performance, and is accomplished through the evaluation of an MOP as described in Section 2.2. Recalling that the result of the evaluation of an MOP as presented in Section 2.2 is a Pareto frontier, it should be noted that it is the responsibility of the designer to identify an appropriate Pareto frontier generation method based on the specifics of the design problem being addressed.

It should also be noted that the Pareto frontier identified at this stage of the method does not represent optimal modular-product designs, but is the characterization of a non-modular product. The purpose of this Pareto frontier is to inform the designer what the best possible solutions are, and will be used to guide and inform the optimization of the modular-product in Step E.

3.3 Step B: Define Anticipated Regions of Interest

The second step of the method captures the predicted changes in customer needs over time and enhances the ability of an optimizer to select the designs that are optimal for adaptation, as illustrated in Figure 3.1, by identifying designs within *Anticipated Regions of Interest*. Although one of the assumptions used in developing this method is that these anticipated regions of interest

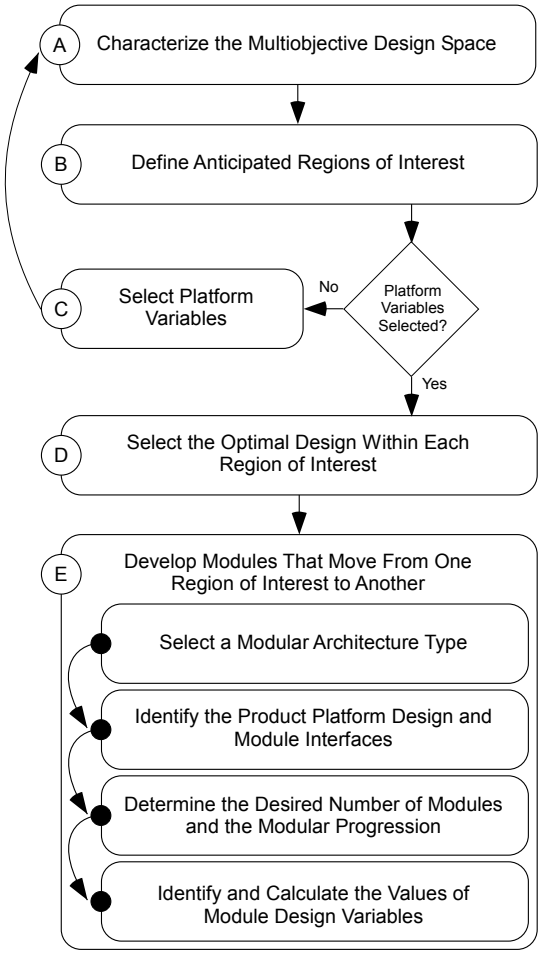

Figure 3.2: Flow chart describing the five-step multiobjective optimization design method developed in this chapter.

are known, potential methods of identifying these regions could include the use of focus groups, surveys, market observation (i.e. identification of a series of current benchmark products), etc.

For each anticipated region of interest presented in Figure 3.3, a new MOP, with a reduced design space, is defined by additional objective constraints based on known changes in customer needs. For example, for the left most region of interest in Figure 3.3(b) the objective μ_1 is constrained by $\mu_{1,l}^{(1)} \leq \mu_1^{(1)} \leq \mu_{1,u}^{(1)}$, where $\mu_{1,l}^{(1)}$ and $\mu_{1,u}^{(1)}$ are prescribed. The result is the bounding of the MOP to search the design space within the geometric shape of the anticipated region of interest. Further definition of the anticipated region of interest is unnecessary due to the function of a MOP of finding solutions along the Pareto frontier. For the examples presented in Figure 3.3, the information capturing the changes in customer needs over time for each design in the set would be

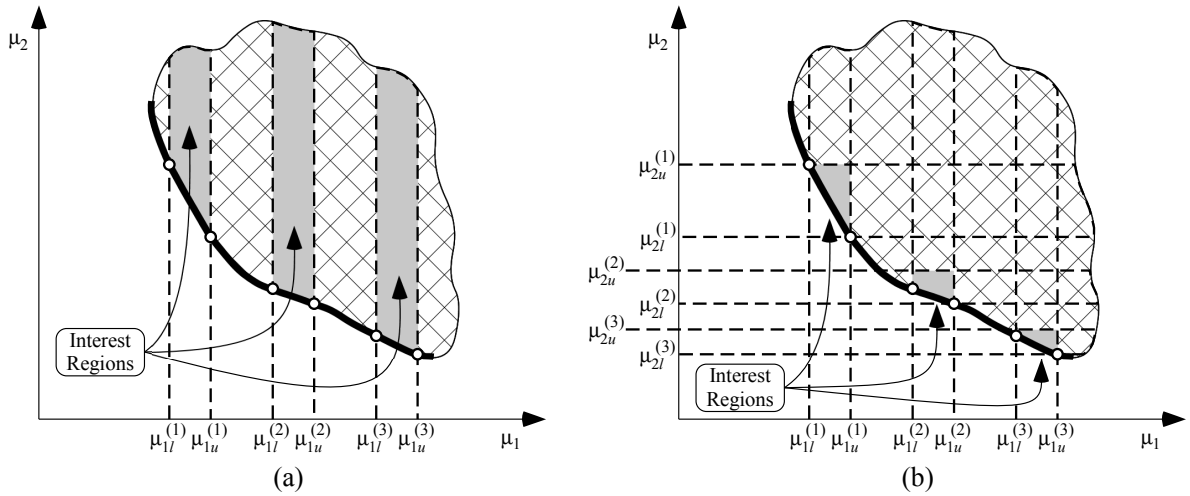

Figure 3.3: Representation of the construction of Anticipated Regions of Interest for known changes in customer needs for three intervals. The anticipated regions of interest in (a) provide inequality constraints for μ_1. The anticipated regions of interest in (b) provide inequality constraints for μ_1, and μ_2.

expressed as additional boundary constraints for the acceptable values of μ_1 and μ_2. In the event that the anticipated region of interest restricts the optimizer to an infeasible space, a compromise in the acceptable range of the objectives for the infeasible region of interest is required, or a new non-modular design concept/model must be considered which provides feasible solutions within the desired region of interest.

It should be noted that there are inherent uncertainties related to the identification of the anticipated regions of interest. For this phase of the research these uncertainties are ignored. The incorporation of uncertainty analysis and mitigation methods is provided in the fourth phase of the research developments presented in Chapter 9 of this dissertation.

3.4 Step C: Select Platform Variables

The third step of the method uses the Pareto frontier *within* the regions of interest identified previously to identify those variables which are best suited as platform variables (x_p). This may be accomplished through the use of Pareto-filtering methods as described in Section 2.1 or any other suitable method. In cases where a concept of how the product is intended to expand through module addition has previously been identified (i.e., variables which are best suited as platform variables are already known), this step simplifies to the providing of that information for the remaining steps

of the method. In addition, as is illustrated in Figure 3.4, by selecting platform variables, it is likely that the Pareto frontier will shift. This shift represents a loss in the best possible performance due to the restricting of design variable values. To ensure that the resulting shift in the Pareto frontier has not produced a shift that places an anticipated region of interest in what is now infeasible space, Steps A and B of the method must be repeated as shown in Figure 3.2.

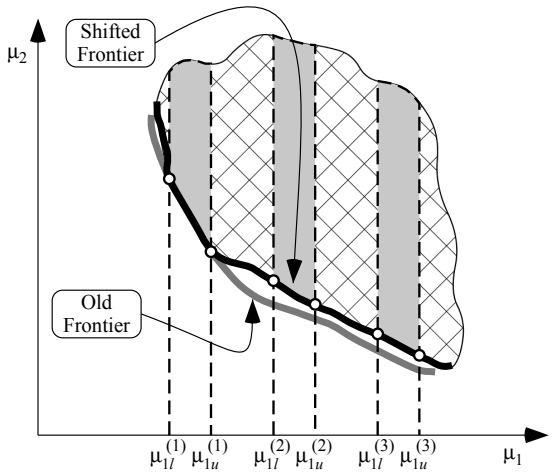

Figure 3.4: Illustration of the expected shift in the Pareto frontier from Figure 3.3 due to the selection of platform variables. The anticipated regions of interest presented in Figure 3.3(a) are also shown.

3.5 Step D: Select the Optimal Design Within Each Region of Interest

The fourth step of the method is to develop the n-dimensional optimization routine used to select the optimal design in each anticipated region of interest and identify the accompanying design variable values. The resulting optimal design set (D_a) containing all variable values is obtained through the following single-objective optimization formulation:

Problem 3.1: Optimization Formulation for Optimal Adaptive Product Identification

$$D_\mathrm{a} := \{(x^*_{\mathrm{p},1}, x^*_{\mathrm{p},2}, ..., x^*_{\mathrm{p},n_{x_\mathrm{p}}}, x^{*(i)}_{\mathrm{a},1}, x^{*(i)}_{\mathrm{a},2}, ..., x^{*(i)}_{\mathrm{a},n_{x_\mathrm{a}}}) \mid \forall i \in \{1,2,...,n_t\}\} \tag{3.1}$$

$x_{\mathrm{p}}^{*}, x_{\mathrm{a}}^{*(i)}$ defined by:

$$\min_{x_{\mathrm{p}}, x_{\mathrm{a}}^{(i)}} \left\{ \frac{1}{n_t} \sum_{i=1}^{n_t} J^{(i)}(x_{\mathrm{a}}^{(i)}, x_{\mathrm{p}}, p^{(i)}) \right\} \tag{3.2}$$

where:

$$J^{(i)} = w_1^{(i)} \cdot \mu_1(x_{\mathrm{a}}^{(i)}, x_{\mathrm{p}}, p^{(i)})^m + , ..., + w_{n_\mu}^{(i)} \cdot \mu_{n_\mu}(x_{\mathrm{a}}^{(i)}, x_{\mathrm{p}}, p^{(i)})^m \quad (n_\mu \geq 2) \tag{3.3}$$

subject to:

$$g_q^{(i)}(x_{\mathrm{a}}^{(i)}, x_{\mathrm{p}}, p^{(i)}) \leq 0 \quad \forall q \in \{1, ..., n_g^{(i)}\} \tag{3.4}$$

$$h_v^{(i)}(x_{\mathrm{a}}^{(i)}, x_{\mathrm{p}}, p^{(i)}) = 0 \quad \forall v \in \{1, ..., n_h^{(i)}\} \tag{3.5}$$

$$x_{\mathrm{a},j,l} \leq x_{\mathrm{a},j}^{(i)} \leq x_{\mathrm{a},j,u} \quad \forall j \in \{1, ..., n_{x_{\mathrm{a}}}\} \tag{3.6}$$

$$x_{\mathrm{p},r,l} \leq x_{\mathrm{p},r} \leq x_{\mathrm{p},r,u} \quad \forall r \in \{1, ..., n_{x_{\mathrm{p}}}\} \tag{3.7}$$

$$\mu_{y,l}^{(i)} \leq \mu_y^{(i)} \leq \mu_{y,u}^{(i)} \quad \forall y \in \{1, ..., n_{\tilde{\mu}}^{(i)}\} \tag{3.8}$$

where the adjustable variables (x_{a}) represent all non-platform design variables (variables that are either scaled or discretely adjusted); x_{p} is the vector of platform design variables; n_t is the anticipated number of time-steps, scenarios, or changes in preferences and/or environments; m is a compromise programming power [51]; $w_1^{(i)}, w_2^{(i)}, ..., w_{n_\mu}^{(i)}$ are weights associated with the local preference within each region of interest; the set D_{a} represents the set of all design variable values of x_{a}^{*} and x_{p}^{*} obtained through the evaluation of the MOP; the subscript $n_{\tilde{\mu}}$ in Equation 3.8 indicates the additional objective constraints needed to define the anticipated regions of interest; and the superscript (i) on p, g, and h indicates the possibility that parameters and constraints are different (non-constant) for each design in the set D_{a}. It is important to note that Problem 3.1 will result in a single solution within each region of interest.

From the optimization formulation presented in Problem 3.1, it is seen that for each design – indicated by the superscript (i) – in the set D_{a}, the values of x_{p}^{*} are required to be the same for all $D_{\mathrm{a}}^{(i)}$, while the values of $x_{\mathrm{a}}^{*(i)}$ are not. In addition, the solution of Problem 3.1 will result in a set of designs that are located along the Pareto frontier within each region of interest.

Figure 3.5 is a representation of how the solution to Problem 3.1 for the set of anticipated regions of interest and the shifted Pareto frontier are used to identify the values of x_{p}^{*} and

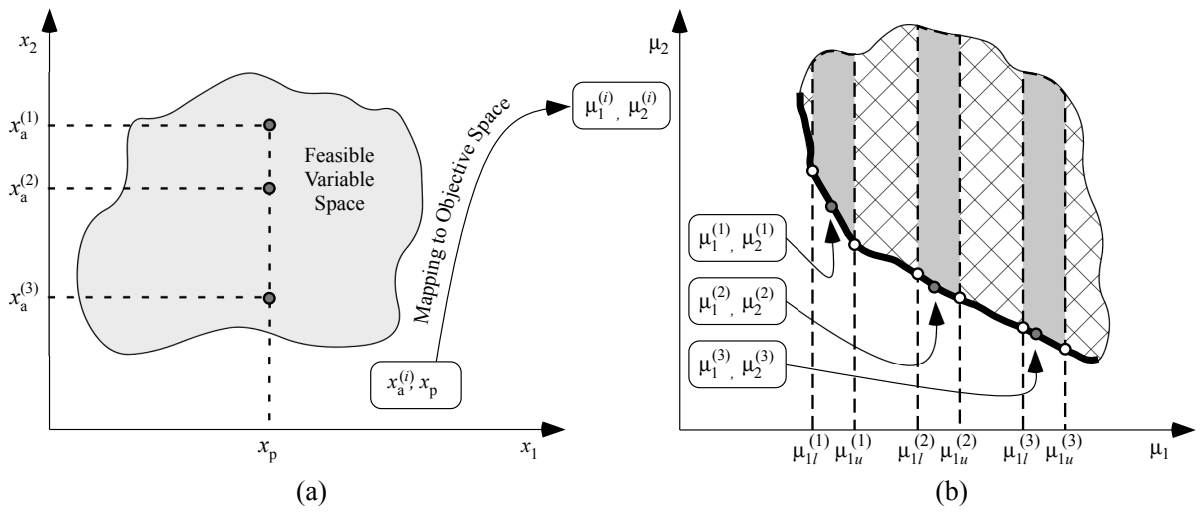

Figure 3.5: Theoretical selection of (a) the values of x_p and $x_a^{(i)}$ that result in (b) Pareto-optimal solutions within the set of anticipated regions of interest and shifted Pareto frontier from Figure 3.4 and the optimization problem formulation presented in Problem 3.1.

$x_a^{*(i)}$. In addition, Figure 3.5 shows how the intent of the proposed method to strategically select Pareto-optimal designs based on their ability to facilitate adaptability is satisfied through the implementation of Problem 3.1.

3.6 Step E: Develop Modules That Move From One Region of Interest to Another

By this step in the process, the set D_a now contains all variable values that can be used to develop the module designs. Developing these designs is now a matter of constrained module design – modules are designed in a manner that constrains them to provide a specified progression in product performance when added to a specific embodiment of the product while only using the variable values from set D_a. It should be noted that in order to do this, the designer must develop predictive design models for each of the modules that will be designed. As such, to complete this final step of the method, and obtain the module designs requires the following: (i) *Select a modular architecture type*, (ii) *Identify the platform design and module interfaces*, (iii) *Determine the desired number of modules and modular progression*, and (iv) *Identify and calculate the values of module design variables*. Each of these four parts is briefly discussed.

Select a modular architecture type: Of the four types of modularity identified in the literature (see Section 2.1), *Slot-modular architecture* and *Bus-modular architecture* are best suited for

implementation in the present method due to the use of platform designs. The decision of which architecture type to be used depends on the desired functionality of the product and modules as a whole.

Identify the product platform design and module interfaces: Prior to the identification of modules, one of the designs in set D_{a} must be identified as the product platform design. In order to facilitate adaptability, the platform design is generally identified as the design contained in D_{a} with the most commonality. In addition, the module interfaces must be specified according to the modular architecture type selected previously, and any other related interfacing design activities must be performed (i.e. begin defining the design model(s) describing the module(s)).

Determine the desired number of modules and the modular progression: With a knowledge of the modular architecture type that is desired, it is now possible to determine the number of modules (n_m) that are desired. The identification of n_m requires a knowledge of the manner in which the product is intended to expand. For the slot/bus-modular cases the maximum and minimum values for n_m obtained for all possible module progression sequences are identified as follows.

$$n_{m,\max} = \sum_{n=1}^{n_t-1} n \tag{3.9}$$

$$n_{m,\min} = n_t - 1 \tag{3.10}$$

it follows that the selected value of n_m is an integer satisfying the condition:

$$n_{m,\min} \leq n_m \leq n_{m,\max}$$

Using the integer value of n_m that is desired, it is now possible to create an n_m-by-2 matrix (δ) dictating the desired progression from one design contained in set D_{a} to another. As a note,

the first entry of the δ matrix ($\delta_{1,1}$) is generally the platform design from set D_{a} identified in the previous section. A generic construction of a δ matrix is presented as follows:

$$\delta = \begin{bmatrix} \alpha_1 & \beta_1 \\ \alpha_2 & \beta_2 \\ \vdots & \vdots \\ \alpha_{n_m} & \beta_{n_m} \end{bmatrix} \tag{3.11}$$

where α and β respectively refer to the starting and the ending designs of the set D_{a} that each module is bridging. This information is used in the final step to refer to the values of x_{a} needed to design each module.

Identify and calculate the values of module design variables: The identification of module designs first requires that the development of the design model(s) describing the module(s) be completed, and those variables that are best suited to characterize the modules be identified – module variables (x_{m}). This identification of module variables can be performed using the same methods described previously for identifying platform variables (i.e., Pareto filtering, concept generation, or any other suitable method). In cases where a designer knows which variables are best suited as module variables for manufacturing a modular product, this process of variable identification simplifies to the providing of that information for the module design routine presented below. Using this information, and the information provided in δ and D_{a}, a generic n-dimensional constrained module design routine is presented below.

Problem 3.2: Optimization Problem Formulation for Constrained Module Design

$$D_{\mathrm{m}} := \{(x^*_{\mathrm{p},1}, x^*_{\mathrm{p},2}, ..., x^*_{\mathrm{p},n_{x_{\mathrm{p}}}}, x^{*(i)}_{\mathrm{m},1}, x^{*(i)}_{\mathrm{m},2}, ..., x^{*(i)}_{\mathrm{m},n_{x_{\mathrm{m}}}}) \mid \forall i \in \{1, 2, ..., n_m\}\} \tag{3.12}$$

x^*_{m} is defined by:

$$\min_{x_{\mathrm{m}}} J^{(i)} = \left|\left| \mu^{(\beta)} - \hat{\mu}^{(i)} \right|\right| \tag{3.13}$$

where:

$$\alpha \;=\; \delta_{i,1} \tag{3.14}$$

$$\beta = \delta_{i,2} \tag{3.15}$$

$$\hat{\mu}^{(i)} = \mu^{(\alpha)} + \Delta\hat{\mu}^{(i)} \tag{3.16}$$

defined by:

$$\mu^{(\alpha)} = \left(\mu_1|_{x_a^{*(\alpha)}, x_p^*, p^{(\alpha)}},\ \mu_2|_{x_a^{*(\alpha)}, x_p^*, p^{(\alpha)}}, ...,\ \mu_{n_\mu}|_{x_a^{*(\alpha)}, x_p^*, p^{(\alpha)}} \right) \quad (n_\mu \geq 2) \tag{3.17}$$

$$\mu^{(\beta)} = \left(\mu_1|_{x_a^{*(\beta)}, x_p^*, p^{(\beta)}},\ \mu_2|_{x_a^{*(\beta)}, x_p^*, p^{(\beta)}}, ...,\ \mu_{n_\mu}|_{x_a^{*(\beta)}, x_p^*, p^{(\beta)}} \right) \quad (n_\mu \geq 2) \tag{3.18}$$

$$\Delta\hat{\mu}^{(i)} = \left(\Delta\hat{\mu}_1(x_m^{(i)}, x_p^*, \hat{p}^{(i)}),\ \Delta\hat{\mu}_2(x_m^{(i)}, x_p^*, \hat{p}^{(i)}), ...,\ \Delta\hat{\mu}_{n_\mu}(x_m^{(i)}, x_p^*, \hat{p}^{(i)}) \right) \quad (n_{\hat{\mu}} = n_\mu) \tag{3.19}$$

where D_m is the set of values and variables of x_p^* and x_m^* for each module design; $\mu^{(\alpha)}$ and $\mu^{(\beta)}$ characterize the objective space performance of the base (α) and target (β) designs; $\hat{\mu}^{(i)}$ represents the objective space performance of design α when used in conjunction with the i-th module; $\Delta\hat{\mu}^{(i)}$ represents the change in objective space performance from design α to $\hat{\mu}^{(i)}$; and x_m^* represents the value(s) and variable(s) that characterize $\Delta\hat{\mu}$.

In examining Problem 3.2 it is seen that for each design in the set D_m, the values of x_p^* are the same as those contained in set D_a. Also, if the variables contained in x_a^* are geometric (i.e., lengths, widths, heights), x_m^* represents the change of the geometric values of the variables that produce the desired $\Delta\mu^{(i)}$. If the variables contained in x_a^* are non-geometric (i.e., technology selection, hardware selection, software selection), x_m^* provides the information needed to create the bridge between x_a^* from design α to design β and provide the desired $\Delta\mu^{(i)}$.

With completion of the constrained module design process, a product capable of adapting to changes in customer needs over time through the addition of modules is achieved. In addition, each configuration of the product obtained through the addition of modules provides the optimal performance according to the objectives provided in Problem 3.1 (see Section 3.5).

In the following chapter, the development of a modular unmanned air vehicle is provided as an example of the implementation of the method described in this chapter.

CHAPTER 4. PHASE 1 EXAMPLE: UNMANNED AIR VEHICLE (UAV) DESIGN

The example that follows shows the application of the multiobjective optimization design method presented in Chapter 3 in the creation of a small (wingspan (b) $\leq$ 2.5 meters) modular UAV. In addition, the ability of the method developed in the previous section to provide platform and module designs capable of satisfying three different operating conditions and parameters representing changing customer needs over time is shown.

4.1 UAV Design & Multiobjective Optimization

Others have shown the benefits of using multiobjective optimization based methods in UAV design. For example, in Gonzalez et al. [118], a framework in which optimization problems can be analyzed along with the use of evolution strategies incorporating concepts of multiobjective optimization, hierarchical topology, asynchronous evaluation of candidate solutions, and parallel computing is implemented in bi-objective (drag and weight) UAV wing plan-form optimization examples. In Jun et al. [119] a new method of collaborative optimization (multi-level decomposed methodology for a large-scale multidisciplinary design optimization) is presented and implemented in the design of an aircraft wing. Rajagopal and Ganguli [120] demonstrate the use of a Multiobjective Genetic Algorithm (MOGA) in the bi-objective (endurance and wing weight) optimization of a low speed, long endurance UAV. In Viswamurthy and Ganguli [121, 122] optimization techniques are used to obtain the Pareto frontier for a bi-objective (hub vibration and flap control power) optimization of the location of trailing-edge flaps on a helicopter.

In each case, as seen in these articles, multiobjective optimization has extended the designers capabilities and made newer and better designs achievable. The developments presented in this dissertation also extend the capabilities of the designer and make newer and better designs achievable. Specifically, the method enables the designer to anticipate and plan for changing needs,

and to subsequently design modular UAVs capable of being optimally adjustable to the needs of differing mission profiles.

Chapter Nomenclature:

D_{turn}	Distance traveled in a complete 360° UAV turn (m)
$\hat{D}_{\text{turn}}$	Distance traveled per degree of turn (m/°)
E	Surveillance elevation of a UAV mission profile (m)
$\hat{g}$	Acceleration due to gravity (m/s^2)
η_{max}	Maximum load factor
θ	Degree of UAV turn (°)
L	Temperature lapse rate (K/m)
L_{m}	Module wing extension lengths (m)
M	Molar mass of dry air (kg/mol)
m_{t}	Total mass of the UAV (kg)
m_{e}	Mass of onboard equipment like cameras, batteries, computers, etc. (kg)
m_{f}	Mass of the UAV fuselage (kg)
m_{w}	Mass of the UAV wings (kg)
$\grave{p}_0$	Sea level standard atmospheric pressure (Pa)
$\grave{p}$	Atmospheric pressure at E (Pa)
ρ	Density of air at E (kg/m^3)
R	Universal gas constant (J/(mol·K))
R_{turn}	Minimum radius of turn of the UAV (m)
S_{ref}	Reference wing area (m^2)
T	Temperature of air at E (K)
T_0	Sea level standard temperature (K)
T_{lost}	Time lost in a 180° UAV turn (s)
$\hat{T}_{\text{lost}}$	Time lost per degree of turn (s/°)
$\hat{T}_{\text{lost,max}}$	Maximum time lost allowed per degree of turn (s/°)
t_{w}	Equivalent thickness of a rectangular cross-section wing (m)
V	Mission cruise velocity (m/s)

4.2 Modular UAV Concept & Mission Profile Definitions

For the scale of aircraft addressed in this example, design traditionally involves the optimization of performance objectives for a set of operating conditions and mission parameters, traditionally expressed through a mission profile. Drive for the development of this modular UAV stems from the need to have a fleet of aircraft that meet the needs of a diverse range of mission profiles, or accept losses in performance of the aircraft due to changes in operating conditions and parameters when the aircraft is used for missions other then it was designed for. To overcome this disparity, a concept wing design for a modular UAV is developed (see Figure 4.1) to provide the ability to optimally expand the design of the aircraft (see Figure 4.2) between missions through the addition of modules. The intent of this concept is not to provide details on the manner or mechanics of how these modules would be attached, but to simply provide an idea of how a UAV could be optimally expanded through modules.

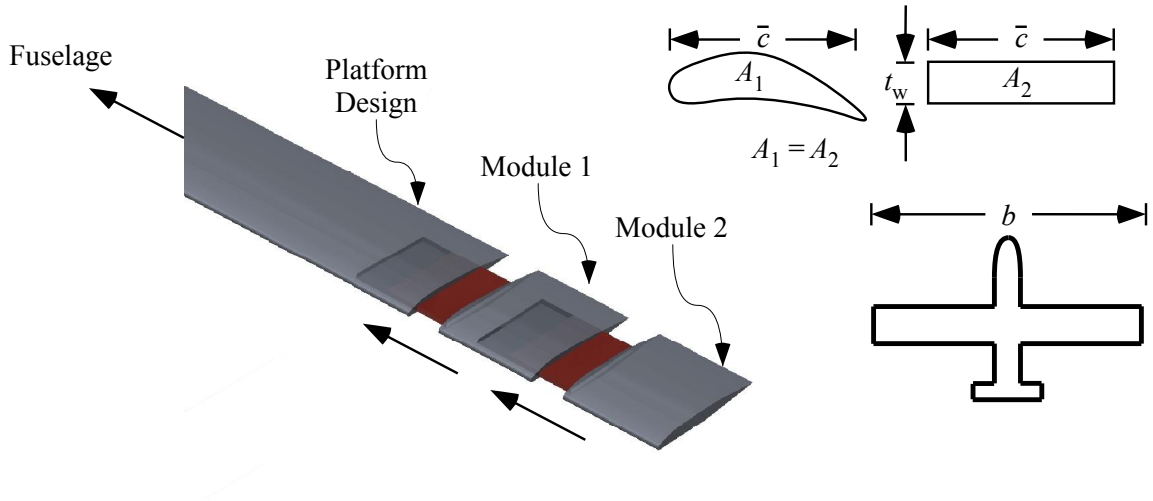

Figure 4.1: Schematic of a concept modular UAV wing design that provides the ability to optimally satisfy different mission profiles.

Figure 4.2 provides an illustration of the three mission profiles considered in this example. The first profile corresponds to a low altitude mission with relatively open terrain that reduces the need to quickly turn the aircraft. The second profile also represents a lower altitude mission, but needs to be able to execute turns more quickly due to increased numbers of visibility obstructions

(bushes, trees, boulders, etc.). The third profile corresponds to high altitude, mountain terrain surveillance that requires more maneuverability (quicker turns) to avoid elements of the mountain terrain.

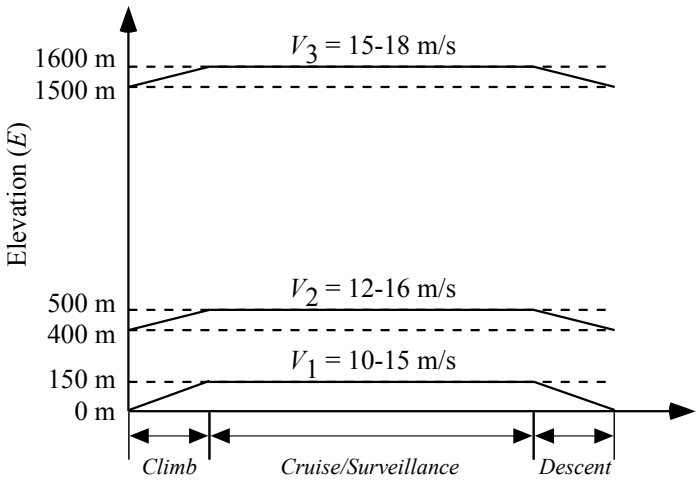

Mission	180^{o} Min Turn Time Allowable	180^{o} Max Turn Time Allowable
1	1.85 sec	2.0 sec
2	2.25 sec	2.5 sec
3	2.85 sec	3.0 sec

Figure 4.2: Schematic of the three mission profiles used in the UAV example.

4.3 Method Implementation

Inspection of Figures 4.1 and 4.2 reveal the platform variable best suited for manufacturing this concept design as the average cord length ($\bar{c}$). Assumptions made in this example are as follows: (1) The numbers assigned to the mission profiles do not correspond to a desired sequence of missions (i.e., the mission profiles can be executed in any order). (2) During surveillance operations of the mission profiles, the UAV flies at constant altitude. (3) The aircraft has sufficient thrust for a sustained turn [123]. (4) The coefficients of lift ($C_{\mathrm{L}_{\max}}$) and thrust ($C_{\mathrm{T}_{\max}}$) are constant and equal 1.2 and 0.1 respectively [123]. (5) The UAV is being designed for remote location surveillance operations where useful data is not captured when the aircraft executes a turn. Additionally, the operator must carry all needed equipment. Therefore, the design objectives for this problem are to minimize the surveillance time lost per degree of UAV turn ($\hat{T}_{\mathrm{lost}}$) and the total mass of the UAV (m_{t}). (6) Density (ρ_{w}) of the wing material does not change with changes in b. As a note, the wing material is assumed to be 1.9 lb EPP foam. Current design approaches increase wing density where the wing connects to the fuselage as the wings lengthen to provide more strength [124].

In the concept presented in Figure 4.1, this final assumption requires that the connection between the fuselage and wings be designed for the maximum wing span possible. The mass associated with this connection is accounted for in m_{f}. The complete formulation of the single-objective optimization problem and identification of anticipated regions of interest based upon the information provided in Figure 4.2 for this example is as follows.

Problem 4.1: UAV Example – MOP Formulation

$$D_{\mathrm{a}} := \{(x^*_{\mathrm{p},1}, x^*_{\mathrm{p},2}, ..., x^*_{\mathrm{p},n_{x_{\mathrm{p}}}}, x^{(i)*}_{\mathrm{a},1}, x^{(i)*}_{\mathrm{a},2}, ..., x^{(i)*}_{\mathrm{a},n_{x_{\mathrm{a}}}}) \mid \forall i \in \{1,2,3\}\} \tag{4.1}$$

$x^*_{\mathrm{p}}, x^*_{\mathrm{a}}$ defined by:

$$\min_{x^{(i)}_{\mathrm{a}}\ x_{\mathrm{p}}} \left(\frac{1}{3}\right) \sum_{i=1}^{3} \left(\hat{T}_{\mathrm{lost}}(x^{(i)}_{\mathrm{a}}, x_{\mathrm{p}}, p^{(i)}) + m_{\mathrm{t}}(x^{(i)}_{\mathrm{a}}, x_{\mathrm{p}}, p^{(i)}) \right) \tag{4.2}$$

where:

$$x_{\mathrm{p}} = \{\bar{c}\} \tag{4.3}$$

$$x^{(i)}_{\mathrm{a}} = \left\{ \begin{array}{cc} V^{(i)} & b^{(i)} \end{array} \right\} \tag{4.4}$$

$$p^{(i)} = \left\{ \begin{array}{ccccccccccc} m_{\mathrm{e}} & m_{\mathrm{f}} & \rho_{\mathrm{w}} & t_{\mathrm{w}} & T_0 & L & \grave{p}_0 & R & M & E^{(i)} \end{array} \right\} \tag{4.5}$$

subject to:

$$\hat{T}^{(i)}_{\mathrm{lost}} - \hat{T}^{(i)}_{\mathrm{lost,\ max}} \leq 0 \tag{4.6}$$

$$\hat{T}^{(i)}_{\mathrm{lost,\ min}} - \hat{T}^{(i)}_{\mathrm{lost}} \leq 0 \tag{4.7}$$

$$V^{(i)}_l \leq V^{(i)} \leq V_u \tag{4.8}$$

$$1.1\mathrm{m} \leq b^{(i)} \leq 2.5\mathrm{m} \tag{4.9}$$

$$0.09\mathrm{m} \leq \bar{c} \leq 0.17\mathrm{m} \tag{4.10}$$

where:

$$\hat{T}^{(i)}_{\mathrm{lost}} = \frac{\hat{D}^{(i)}_{\mathrm{turn}}}{V^{(i)}} \tag{4.11}$$

$$m^{(i)}_{\mathrm{t}} = m_{\mathrm{e}} + m_{\mathrm{f}} + m^{(i)}_{\mathrm{w}} \tag{4.12}$$

Table 4.1: Values of the constant parameters of $p^{(i)}$ needed to evaluate Problem 4.1.

Constant Parameters								
m_e (kg)	m_f (kg)	ρ_w (kg/m^3)	t_w (m)	T_0 (K)	L (K/m)	$\grave{p}_0$ (Pa)	R (J/(mol·K))	M (kg/mol)
0.25	1.5	30.435	0.06	288.5	0.0065	101325	8.31447	0.0289644

with supporting equations:

$$m_w^{(i)} = \rho_w S_{ref}^{(i)} t_w \tag{4.13}$$

$$S_{ref}^{(i)} = \bar{c} b^{(i)} \tag{4.14}$$

$$T^{(i)} = T_0 - LE^{(i)} \tag{4.15}$$

$$\grave{p}^{(i)} = \grave{p}_0 \left(1 - \frac{LE^{(i)}}{T_0}\right)^{\left(\frac{\hat{g}M}{RL}\right)} \tag{4.16}$$

$$\rho^{(i)} = \frac{\grave{p}^{(i)} M}{RT^{(i)}} \tag{4.17}$$

$$\eta_{max}^{(i)} = \frac{\rho^{(i)} (V^{(i)})^2 S_{ref}^{(i)} C_{L_{max}}}{2 m_t^{(i)} \hat{g}} \tag{4.18}$$

$$R_{turn}^{(i)} = \frac{(V^{(i)})^2}{\hat{g}\sqrt{(\eta_{max}^{(i)})^2 - 1}} \tag{4.19}$$

$$D_{turn}^{(i)} = \frac{\pi R_{turn}^{(i)} \theta}{180} \tag{4.20}$$

$$\hat{D}_{turn}^{(i)} = \frac{D_{turn}^{(i)}}{\theta} \tag{4.21}$$

$$T_{lost}^{(i)} = \frac{D_{turn}^{(i)}}{V^{(i)}} \tag{4.22}$$

where each of the terms in the preceding equations are defined in the Nomenclature section of this Chapter.

Values of the elevation (E), $\hat{T}_{\text{lost, max}}$, and $\hat{T}_{\text{lost, min}}$, along with the lower ($V_l$) and upper ($V_u$) limits of the mission cruise velocities for the different designs presented in Tables 4.1 and 4.2 are obtained from the mission profiles presented in Figure 4.2. Values of T_0, L, $\grave{p}_0$, R, and M presented

Table 4.2: Values of the non-constant objective limits, adjustable variable limits, and parameters of $p^{(i)}$ needed in Problem 4.1 to obtain the i-th design of set D_a.

	Adjustable Variable Limits		Objective Limits		Parameters
i	V_l (m/s)	V_u (m/s)	$\hat{T}_{\text{lost, min}}$ (s/°)	$\hat{T}_{\text{lost, max}}$ (s/°)	E (m)
1	10	15	1.85/180	2.0/180	150
2	12	16	2.25/180	2.5/180	500
3	15	18	2.85/180	3.0/180	1600

Table 4.3: Variable and objective values obtained through evaluation of Problem 4.1 for the i-th design of set D_a.

	Variables			Objectives			
i	$\bar{c}^*$ (m)	V^* (m/s)	b^* (m)	m_t^* (kg)	$\hat{T}^*_{\text{lost}}$ (s/°)	$\Rightarrow$	T_{lost} (s)
1	0.17	15	2.4635	2.5147	0.0103	$\Rightarrow$	1.8617
2	0.17	16	1.8259	2.3168	0.0127	$\Rightarrow$	2.2923
3	0.17	18	1.3857	2.1802	0.0159	$\Rightarrow$	2.8708

in Table 4.1 come from the 1976 International Standard Atmosphere document [125]. The variable t_w represents an equivalent thickness of the wings – approximates the wing cross sectional area as a rectangle (See Figure 4.1). Equations used to evaluate the unmanned air vehicle's objective space performance (see Eqs. 4.11 and 4.12) are derived from equations presented in Nigam et al (see Eqs. 4.18 and 4.19) [123]. Equations used to calculate the density of air (see Eqs. 4.16–4.18 above) as a function of E are obtained using the ideal gas law assumption [126]. Evaluation of Problem 4.1 was performed using a multiobjective genetic algorithm, and complete results indicating the variable and objective values of each design are presented in Table 4.3.

Through the evaluation of Problem 4.1 above, the set D_a now contains all variable values needed to develop the module designs (see Table 4.3). Prior to developing the module designs, information on the type, number, and desired progression of modules that are to be used to obtain the Pareto-optimal designs contained within set D_a is needed. Using the information provided in Figure 4.1, it can be seen that a bus-modular approach was selected for this example. Examination of the nature of the x_a variables reveals that the differences in the variable b for each design in D_a is geometric, and therefore the design with the most commonality is the design with the smallest

length of b^* ($D_{\mathrm{a}}^{(3)}$). Using this information, the desired number of modules to be developed (n_m) is chosen to be two, and the δ matrix is constructed in the following equation:

$$\delta = \begin{bmatrix} 3 & 2 \\ 2 & 1 \end{bmatrix} \tag{4.23}$$

Formulation of a constrained module design routine of the form presented in Problem 3.2 is presented as follows.

Problem 4.2: UAV Example – Constrained Module Design

$$D_{\mathrm{m}} := \{(x_{\mathrm{p},1}^*, x_{\mathrm{p},2}^*, ..., x_{\mathrm{p},n_{x_{\mathrm{p}}}}^*, x_{\mathrm{m},1}^{(i)*}, x_{\mathrm{m},2}^{(i)*}, ..., x_{\mathrm{m},n_{\hat{x}_{\mathrm{m}}}}^{(i)*}) \mid \forall i \in \{1,2\}\} \tag{4.24}$$

x_{m}^* is defined by:

$$\min_{x_{\mathrm{m}}} J^{(i)} = \left(\mu^{(\beta)} - \hat{\mu}^{(i)}\right)^2 \tag{4.25}$$

defined by:

$$\begin{aligned}
\hat{\mu}^{(i)} &= \mu^{(\alpha)} + \Delta\hat{\mu}^{(i)} && (4.26)\\
\mu^{(\alpha)} &= \left(\hat{T}_{\mathrm{lost}}^{(\alpha)}\big|_{x_{\mathrm{a}}^{(\alpha)*}, x_{\mathrm{p}}^*, p^{(\alpha)}},\ m_{\mathrm{t}}^{(\alpha)}\big|_{x_{\mathrm{a}}^{(\alpha)*}, x_{\mathrm{p}}^*, p^{(\alpha)}}\right) && (4.27)\\
\mu^{(\beta)} &= \left(\hat{T}_{\mathrm{lost}}^{(\beta)}\big|_{x_{\mathrm{a}}^{(\beta)*}, x_{\mathrm{p}}^*, p^{(\beta)}},\ m_{\mathrm{t}}(\beta)\big|_{x_{\mathrm{a}}^{(\beta)*}, x_{\mathrm{p}}^*, p^{(\beta)}}\right) && (4.28)\\
\Delta\hat{\mu}^{(i)} &= \left(\Delta\hat{T}_{\mathrm{lost}}^{(i)},\ \Delta m_{\mathrm{t}}^{(i)}\right) && (4.29)
\end{aligned}$$

where:

$$\begin{aligned}
x_{\mathrm{m}}^{(i)} &= \{L_{\mathrm{m}}^{(i)}, V^{(\beta)*}\} && (4.30)\\
x_{\mathrm{p}}^* &= \{\bar{c}^*\} && (4.31)\\
\alpha &= \delta_{i,1} && (4.32)\\
\beta &= \delta_{i,2} && (4.33)
\end{aligned}$$

Table 4.4: Variable values of the platform and module designs obtained through evaluation of Problem 4.2.

Platform Design			Module Designs			
Variables	Values	Units	Variables	Module # 1	Module # 2	Units
$\bar{c}$	0.17	(m)	L_{m}	0.2201	0.3188	(m)
b	1.3857	(m)	V	16	15	(m/s)
V	18	(m/s)				

$$\Delta\hat{T}_{\mathrm{lost}}^{(i)} = \hat{T}_{\mathrm{lost}}\left((b^{(\alpha)*}+2L_{\mathrm{m}}^{(i)}),V^{(\beta)*},\bar{c}^{*},p^{(\beta)}\right)-\hat{T}_{\mathrm{lost}}\left(b^{(\alpha)*},V^{(\alpha)*},\bar{c}^{*},p^{(\alpha)}\right) \quad (4.34)$$

$$\Delta m_{\mathrm{t}}^{(i)} = m_{\mathrm{t}}\left((b^{(\alpha)*}+2L_{\mathrm{m}}^{(i)}),V^{(\beta)*},\bar{c}^{*},p^{(\beta)}\right)-m_{\mathrm{t}}\left(b^{(\alpha)*},V^{(\alpha)*},\bar{c}^{*},p^{(\alpha)}\right) \quad (4.35)$$

$$L_{\mathrm{m}}^{(i)} = 0.5(b^{(\beta)*}-b^{(\alpha)*}) \quad (4.36)$$

where all variables in the preceding equations are defined in the Nomenclature section of this Chapter.

Results of the evaluation of Problem 4.2, as well as the variable values of the platform design are presented in Table 4.4.

4.4 Results & Discussion

Results of the evaluation of Problem 4.2 above (see Table 4.4 for complete summary) provide the variable values needed to describe the module designs. With completion of the constrained module design process, a UAV capable of adapting to three different mission profiles through the addition of modules is achieved. Figure 4.3 provides a graphical representation of the Pareto frontier for the 3 regions of interest defined in Problem 4.1, along with the objective values for the solutions to Problem 4.1 (indicated by the symbol "$\circ$") and Problem 4.2 (indicated by the symbol "$\times$"). Confidence in the representation of the Pareto frontier provided in Figure 4.3 is two-fold: (1) A comparison of the desired boundary points of each region of interest provided in Table 4.2 and the end points of the Pareto frontier within each interest region of Figure 4.3 reveals that the obtained boundary points match those provided in Table 4.2. (2) The solid line approximation of the Pareto frontier in each region of interest was obtained by connecting straight lines to a set of 60 Pareto points within each region of interest which were distributed between the corresponding boundary

points. In addition, Figure 4.3 illustrates the ability of each configuration of the UAV obtained through the addition of modules to provide the desired Pareto-optimal performance according to the objectives, parameters, and constraints provided in Problem 4.1, and thus satisfy the intent of the design method. The side of the Pareto frontier representing feasible solutions is indicated by the direction of the $\wedge$ symbols placed along the frontier.

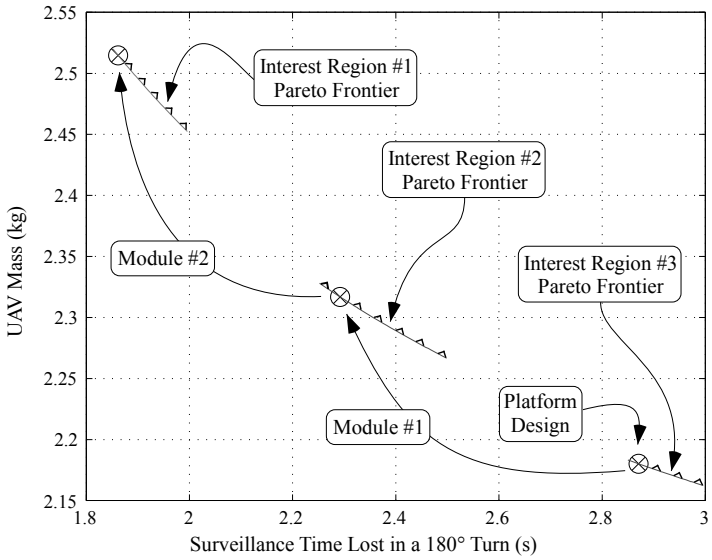

Figure 4.3: Graphical representation of the Pareto frontier for the 3 regions of interest defined in Problem 4.1, along with the plotted solutions to Problem 4.1 (indicated by the symbol "$\circ$") and Problem 4.2 (indicated by the symbol "$\times$"). The plot shows that each configuration of the UAV obtained through the addition of modules provides the desired Pareto-optimal performance from Problem 4.1. The side of the Pareto frontier representing feasible solutions is indicated by the direction of the $\wedge$ symbols placed along the frontier.

CHAPTER 5. PHASE 2 METHOD DEVELOPMENT: TRAVERSING S-PARETO FRONTIERS

In this chapter, the second phase in the development of a multiobjective optimization design method providing a Pareto-optimal product and module designs capable of satisfying changes in customer needs over time is described for s-Pareto frontier design cases [77, 79, 80].

5.1 Accounting for Changing Needs With Multiple Design Concepts

Similar to the Pareto frontier, an s-Pareto frontier contains many optimal, yet functionally different, designs representing all optimal product candidates. However, an s-Pareto frontier represents the optimal product candidates from disparate design concepts – distinct product ideas that have evolved to the point that there are parametric models that represent the performance of the products [37]. Recalling from Chapter 3 that to satisfy changes in customer needs over time through the addition of modules requires the strategic selection of Pareto designs based on their ability to facilitate adaptability, the focus of this chapter is to demonstrate how the method presented in Chapter 3 can be expanded to incorporate the strategic selection of s-Pareto designs.

Figure 5.1(a) illustrates the intent of the expanded method to satisfy changing customer needs by selecting an *s-Pareto-optimal* product platform design which, through the addition of modules, expands to other s-Pareto designs. As was the case in Figure 3.1 (reproduced in this chapter as Figure 5.1(b)), the first (μ_1) and second (μ_2) objectives are represented along the horizontal and vertical axis, respectively. From Figure 5.1(a) it is seen that the platform design, shown as $\mu^{(1)}$, adapts to become $\mu^{(2)}$ through the addition of Module 1. In like manner, the subsequent target designs identified as $\mu^{(3)}$, and $\mu^{(4)}$ are also achieved through Modules 2 and 3 respectively.

In comparing Figures 5.1(a) and (b), it can be seen that the phase 1 method developments presented in Chapter 3 would be represented by $\mu^{(2)}$ being a platform design, and Module 2, which scales of the system design from $\mu^{(2)}$ to $\mu^{(3)}$ on the same frontier. As such, the method extensions

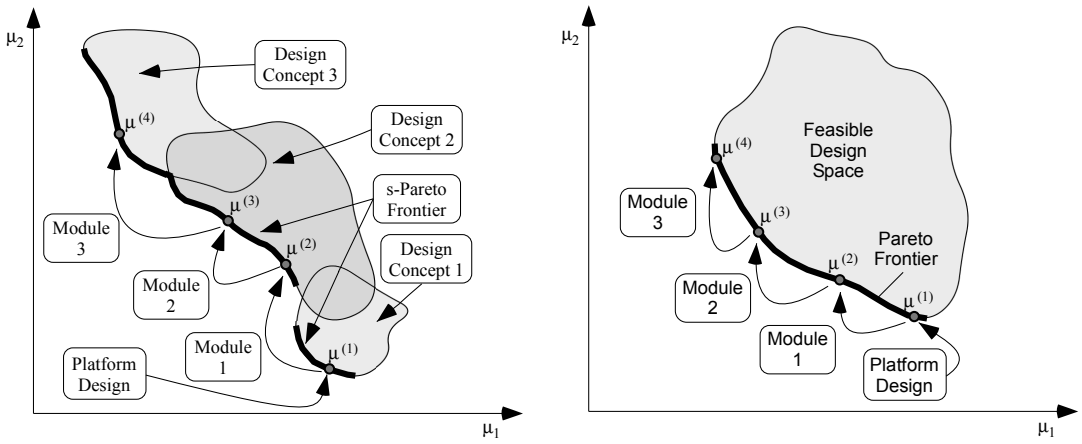

Figure 5.1: (a) Graphical representation of the intent of the expanded method to provide a product that expands from one s-Pareto-optimal design to another through the addition of modules. (b) Repeated illustration from Figure 3.1.

presented in this chapter are to also enable the identification of modules that can span different concepts (Modules 1 and 3 in Figure 3.1).

Figure 5.2(a) provides a flow chart that illustrates the six primary steps of the expanded multiobjective optimization design method developed in this chapter. By comparing Figure 5.2(a) and Figure 3.2 (reproduced in this chapter as Figure 5.2(b)) it can be seen that the major difference between Figures 5.2(a) and (b), is the insertion of an additional step between Steps C and D of Figure 5.2(b) in which the s-Pareto frontier within the anticipated regions of interest is assembled. Although Steps A-C and E-F of Figure 5.2(a) appear to be identical to Steps A-E of Figure 5.2(b), due to the use of multiple design concepts, the MOP formulations, and functions of these steps, must necessarily change. The expanded function of each of these steps is described in the following sections.

5.2 Step A: Characterize the Multiobjective Design Space

The first step of the method explores the multiobjective design space to evaluate and characterize the effects of each design variable on the objective space performance. As presented in Figure 5.3, when multiple design concepts are needed to satisfy the future product needs, this step of the

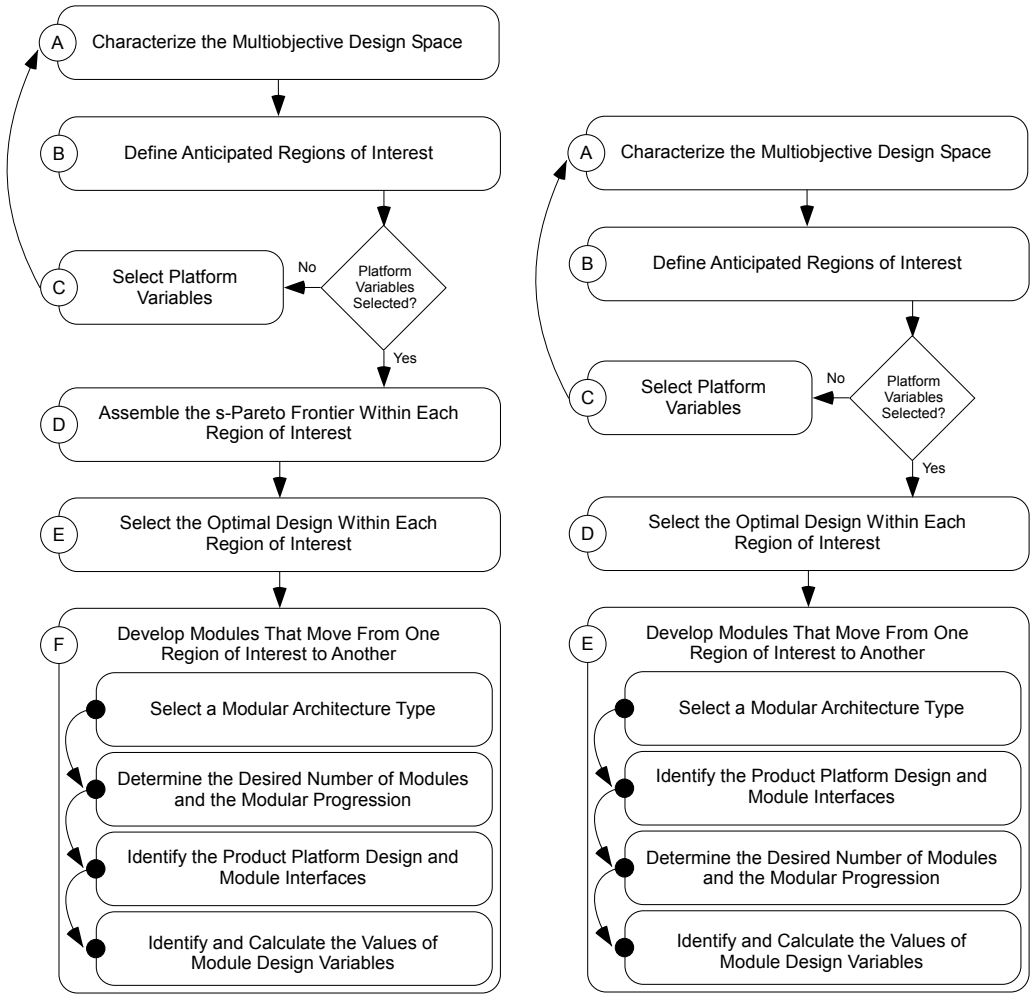

Figure 5.2: (a) Flow chart describing the six-step multiobjective optimization design method developed in this chapter. (b) Repeated illustration from Figure 3.2.

method requires that an MOP for each design concept be evaluated and represented in the same design space (i.e., Pareto frontier of each concept is identified).

5.3 Step B: Define Anticipated Regions of Interest

A key idea of the presented method is that changes in the desired system performance are equivalent to changes in the desired values of one or more design objectives. To that end, the second step of the method captures the predicted changes in product/system needs over time, and repre-

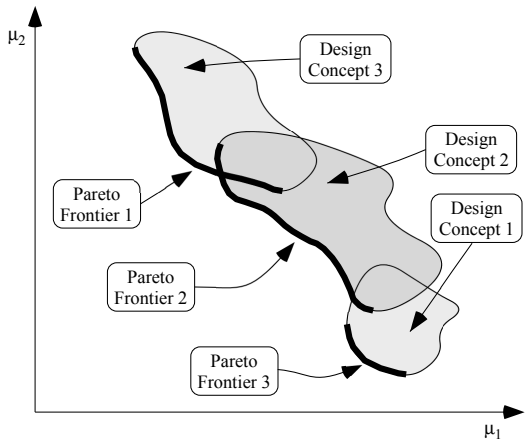

Figure 5.3: Representation of the characterization of three design concepts within the same design space.

sents them as *Anticipated Regions of Interest* of the multiobjective design space, as illustrated in Figure 5.4.

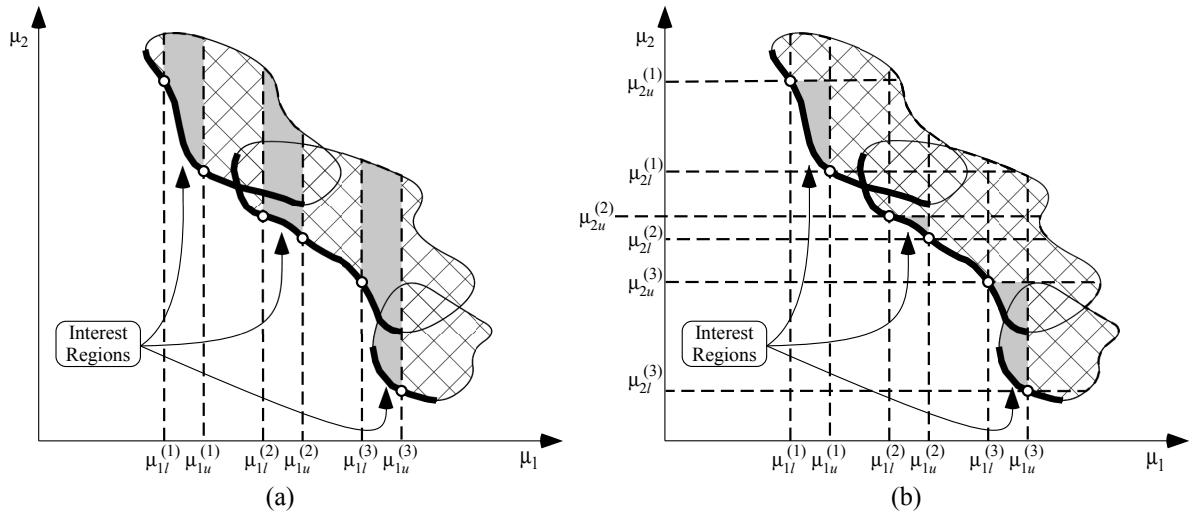

Figure 5.4: Representation of the construction of Anticipated Regions of Interest for known changes in customer needs for three intervals. The anticipated regions of interest in (a) provide inequality constraints for μ_1. The anticipated regions of interest in (b) provide inequality constraints for μ_1, and μ_2.

For each anticipated region of interest presented in Figure 5.4, a new MOP, with a reduced design space, for the corresponding design concepts is defined by additional objective constraints based on known changes in customer needs. Further definition of the anticipated region of interest is unnecessary due to the function of a MOP of finding solutions along the s-Pareto frontier. For

the examples presented in Figure 5.4, as was the case for the examples provided in Figure 3.3, the information capturing the changes in customer needs over time for each design in the set is expressed as additional boundary constraints for the acceptable values of μ_1 and μ_2.

In considering the identification and characterization of future needs, it is observed that such needs fall into two classes. The first class involves needs that are known or reasonably predicted (e.g., cost reductions over time, availability of increased CPU speeds, better gas mileage). The second class involves needs that are not yet known or not reasonably predicted. Note that this chapter does not attempt to address the complexities of identifying this second class of unknown needs. However, some potential methods that could be used in identifying/characterizing future needs are: (i) to identify external drivers of change and then identify components that are likely to change in response [93], and (ii) to gather information by adapting common methods for identifying current needs (e.g. focus groups, surveys, observation). In terms of the method presented in this chapter, once again it will be assumed that future needs are known or can be reliably characterized as anticipated regions of interest.

5.4 Step C: Select Platform Variables

The third step of the method uses the disparate Pareto frontiers *within the anticipated regions of interest* identified previously to identify those variables that are best suited as platform variables (x_p). As is illustrated in Figure 5.5, by selecting platform variables, it is likely that the Pareto frontier of the different design concepts will shift. To insure that the resulting shift in the Pareto frontiers has not placed an anticipated region of interest in what is now infeasible space, Steps A and B of the method must be repeated as shown in Figure 5.2(a).

Identifying platform variables across multiple concepts can be noticeably more difficult than doing the same for a single concept model. The following guidelines for selection can ease this difficulty: (i) platform variables should be common across all concept analysis models, (ii) platform variables should be related to concept features that do not need to change over time, and (iii) platform variables should cause minimal variation along the Pareto frontiers within many (if not all) anticipated regions of interest. As described in Yearsley and Mattson [12], one approach to identify minimal variation is to calculate the standard deviation of each common design variable

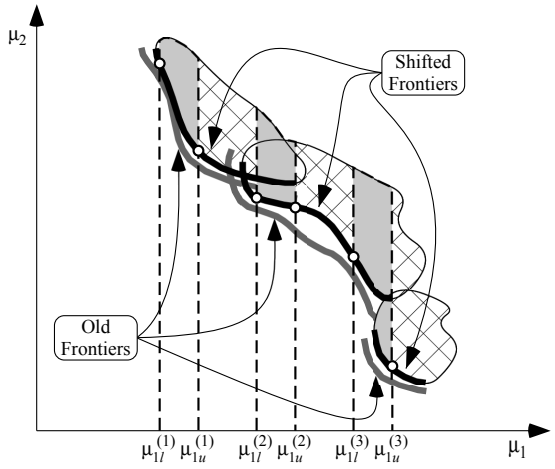

Figure 5.5: Illustration of the expected shift in the Pareto frontiers from Figure 5.4 due to the selection of platform variables. The anticipated regions of interest presented in Figure 5.4(a) are also shown.

for all concept-specific Pareto points within the regions of interest. However, any other suitable method may be used.

It is observed that as the number of concepts and regions of interest increases, the likelihood of identifying a suitable platform decreases. This is due to the reduced likelihood of identifying system concepts that all lend themselves to facilitating modularity across the identified regions of interest. As such, the ability of the method to provide good solutions is dependent on: (i) the designers selection of concepts; and (ii) the level to which the concepts lend themselves to modularity. In situations where a good platform cannot be identified for a given set of system concepts and regions of interest, the designer should ask the following question: In order to progress the design, is there a subset of concepts that a platform can be identified for?

If the answer to this question is yes, then the designer has two options: (i) Use the identified subset of concepts and continue with the method (subset must contain solutions in all identified regions of interest); or (ii) Alter/replace any concept(s) to incorporate the identified platform or a different platform. If the answer to this question is no, then there is no modular design that can satisfy the identified needs. As such, the designer has two options: (i) Refine the regions of interest; and/or (ii) Alter/replace the considered concepts to enable the identification of a common platform.

5.5 Step D: Assemble the s-Pareto Frontier Within Each Region of Interest

The fourth step of the method identifies the platform-constrained solutions from the various system concepts *within each region of interest* that are best suited as s-Pareto – globally optimal – solutions. Notice that because the platform-constrained Pareto frontier of each system concept was obtained in the previous step of the method, the current step may be easily accomplished through the use of Pareto-filtering methods as described in Section 2.2. Alternatively, the s-Pareto frontier can be generated directly based on the chosen platform variables and regions of interest using Problem 2.2. or any other suitable method. Figure 5.6 illustrates the result of this step of the method.

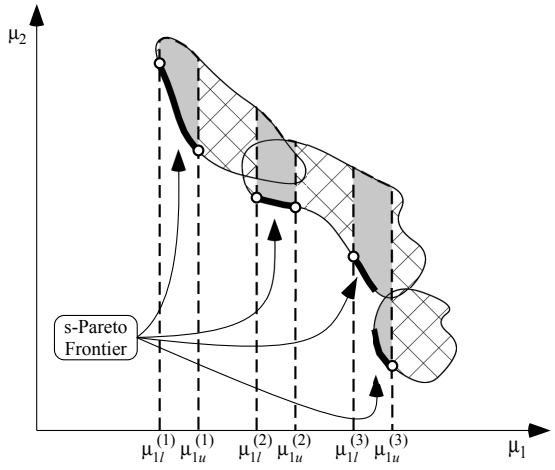

Figure 5.6: Illustration of the resulting s-Pareto frontier within the anticipated regions of interest from Figure 5.4(a).

5.6 Step E: Select the Optimal Design Within Each Region of Interest

The fifth step of the method implements an optimization routine to select one design within each region of interest that will be used in the final step of the method as targets for the platform and module combinations developed. The resulting optimal design set D_{a}, containing all variable values of x_{p}^{*} and $x_{\mathrm{a}}^{*(i)}$, is obtained through the following optimization formulation:

Problem 5.1: s-Pareto MOP Formulation for Optimal Adaptive Product Identification

$$D_{\mathrm{a}} := \{(x^*_{\mathrm{p},1}, x^*_{\mathrm{p},2}, ..., x^*_{\mathrm{p},n_{x_{\mathrm{p}}}}, x^{*(i)}_{\mathrm{a},1}, x^{*(i)}_{\mathrm{a},2}, ..., x^{*(i)}_{\mathrm{a},n^{(i)}_{x_{\mathrm{a}}}}) \mid \forall i \in \{1,2,...,n_t\}\} \tag{5.1}$$

$x^*_{\mathrm{p}}, x^{*(i)}_{\mathrm{a}}$, and $n^{(i)}_{x_{\mathrm{a}}}$ defined by:

$$\min_{x_{\mathrm{p}}, x^{(i)}_{\mathrm{a}}} \left\{ \sum_{n=1}^{n_t} w^{(i)} J^{(i)}(x^{(i)}_{\mathrm{a}}, x_{\mathrm{p}}) \right\} \tag{5.2}$$

where:

$$J^{(i)}(x^{(i)}_{\mathrm{a}}, x_{\mathrm{p}}) \;=\; \min_{k} \left\{ \min_{x^{(k)}_{\mathrm{a}},\, x_{\mathrm{p}}} J^{(k)}(x^{(k)}_{\mathrm{a}}, x_{\mathrm{p}}) \right\} \tag{5.3}$$

subject to:

$$g^{(k)}_q(x^{(k)}_{\mathrm{a}}, x_{\mathrm{p}}, p^{(k)}) \leq 0 \quad \forall q \in \{1,...,n^{(k)}_g\} \tag{5.4}$$

$$h^{(k)}_v(x^{(k)}_{\mathrm{a}}, x_{\mathrm{p}}, p^{(k)}) = 0 \quad \forall v \in \{1,...,n^{(k)}_h\} \tag{5.5}$$

$$x_{\mathrm{a},j,l} \leq x^{(k)}_{\mathrm{a},j} \leq x_{\mathrm{a},j,u} \quad \forall j \in \{1,...,n^{(k)}_{x_{\mathrm{a}}}\} \tag{5.6}$$

$$x_{\mathrm{p},r,l} \leq x_{\mathrm{p},r} \leq x_{\mathrm{p},r,u} \quad \forall r \in \{1,...,n_{x_{\mathrm{p}}}\} \tag{5.7}$$

$$\mu^{(k)}_{y,l} \leq \mu^{(k)}_y \leq \mu^{(k)}_{y,u} \quad \forall y \in \{1,...,n^{(k)}_{\vec{\mu}}\} \tag{5.8}$$

where the adjustable variables (x_{a}) represent all non-platform design variables (variables that are either scaled or discretely adjusted) for each design concept; k, $1 \leq k \leq n_{\mathrm{dm}}$, denotes the k-th design concept; $w^{(i)}$ are weights associated with the local preference within the i-th region of interest; $J^{(i)}$ and $J^{(k)}$ are aggregate objective functions for the i-th region of interest and k-th concept respectively; and the superscript (k) on p, g, and h indicate that parameters and constraints can be different (non-constant) for each system concept. It should be noted that the introduction of the superscript k in Problem 5.1 captures the extension of the presented method from a single system concept to multiple concepts. As such, if $n_{\mathrm{c}} = 1$, Problem 5.1 reduces to the original formulation presented in Problem 3.1.

Figure 5.7 is a representation of how the solution to Problem 5.1 for a set of three anticipated regions of interest and the corresponding s-Pareto frontiers are used to identify the values

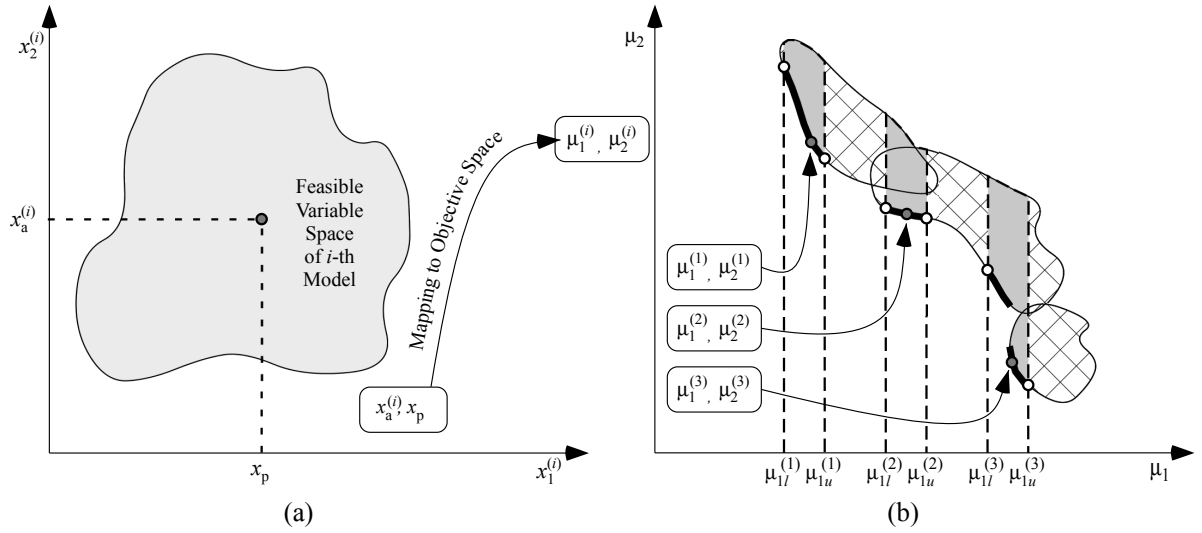

Figure 5.7: Theoretical identification of the values of x_p and $x_a^{(i)}$ for a set of three anticipated regions of interest and s-Pareto frontier from the MOP formulation presented in Problem 5.1.

of x_p^* and $x_a^{*(i)}$. In addition, Figure 5.7 illustrates the outcome of evaluating Problem 5.1, which is the identification of a single system design $(\mu_1^{(i)}, \mu_2^{(i)})$ within each region of interest defined by Equation 5.8.

Considering the design objective space performance of each design identified through Problem 5.1, the final step of the method identifies the variables and values of the module specific design variables (x_m) that target the performance of the identified designs in D_a.

5.7 Step F: Develop Modules That Move From One Region of Interest to Another

By this step in the process, the set D_a now contains all variable values that can be used to develop the module designs. Developing these designs is now, as was described in Section 3.6, a matter of constrained module design. To complete this final step of the method and obtain the module designs requires the following:

1. *Select a modular architecture type* – Identify the desired functionality of the platform and modules as a whole, and select an applicable modular architecture [20, 127].

2. *Identify the system platform design and module interfaces* – The target system identified through Problem 5.1 with the most commonality to the other target designs is selected as the

platform. Module interfaces are then defined based on the selected architecture type (i.e., begin developing concept module designs).

3. *Determine the desired number of modules and modular progression* – Identify the number of modules to be developed, and the corresponding module progression matrix (δ) defining the intended module progression sequences (i.e., a module connecting $\mu^{(1)}$ and $\mu^{(2)}$ in Figure 5.1(a) would correspond to a row entry of [1 2] in δ). Additional information on the form and definition of δ is provided in Section 3.6. It should be noted that in situations where the desired modular progression bridges two or more different concepts, modular system/product concepts must now be developed that are capable of creating the needed connections between concepts.

4. *Identify and calculate the values of module design variables* – Complete the development of all module concepts, and determine the optimal values of the module specific design variables ($x_{\mathrm{m}}^{*(i)}$) that will enable the combined platform and modules to obtain the target system performances identified in Problem 5.1.

For more detailed information on each of these four parts, see Section 3.6. The expanded n-dimensional optimization problem formulation for constrained module design is presented as follows:

Problem 5.2: s-Pareto Optimization Problem Formulation for Constrained Module Design

$$D_{\mathrm{m}} := \{(x_{\mathrm{p},1}^{*}, x_{\mathrm{p},2}^{*}, ..., x_{\mathrm{p},n_{x_{\mathrm{p}}}}^{*}, x_{\mathrm{m},1}^{*(i)}, x_{\mathrm{m},2}^{*(i)}, ..., x_{\mathrm{m},n_{x_{\mathrm{m}}}^{(i)}}^{*(i)}) \mid \forall i \in \{1, 2, ..., n_m\}\} \tag{5.9}$$

x_{m}^{*} is defined by:

$$\min_{x_{\mathrm{m}}} J^{(i)} = \left|\left| \mu^{(\beta)} - \hat{\mu}^{(i)} \right|\right| \tag{5.10}$$

where:

$$\alpha = \delta_{i,1} \tag{5.11}$$

$$\beta = \delta_{i,2} \tag{5.12}$$

$$\hat{\mu}^{(i)} = \mu^{(\alpha)} + \Delta\hat{\mu}^{(i)} \tag{5.13}$$

defined by:

$$\mu^{(\alpha)} = \left(\mu_1\big|_{x_a^{*(\alpha)}, x_p^*, p^{(\alpha)}},\ \mu_2\big|_{x_a^{*(\alpha)}, x_p^*, p^{(\alpha)}}, \ldots,\ \mu_{n_\mu}\big|_{x_a^{*(\alpha)}, x_p^*, p^{(\alpha)}} \right) \quad (n_\mu \geq 2) \tag{5.14}$$

$$\mu^{(\beta)} = \left(\mu_1\big|_{x_a^{*(\beta)}, x_p^*, p^{(\beta)}},\ \mu_2\big|_{x_a^{*(\beta)}, x_p^*, p^{(\beta)}}, \ldots,\ \mu_{n_\mu}\big|_{x_a^{*(\beta)}, x_p^*, p^{(\beta)}} \right) \quad (n_\mu \geq 2) \tag{5.15}$$

$$\Delta\hat{\mu}^{(i)} = \left(\Delta\hat{\mu}_1(x_m^{(i)}, x_p^*, \hat{p}^{(i)}),\ \Delta\hat{\mu}_2(x_m^{(i)}, x_p^*, \hat{p}^{(i)}), \ldots,\ \Delta\hat{\mu}_{n_{\hat{\mu}}}(x_m^{(i)}, x_p^*, \hat{p}^{(i)}) \right) \quad (n_{\hat{\mu}} = n_\mu) \tag{5.16}$$

where all variables and functions are as described in Section 3.6. It should also be noted that the current formulation now allows the variables contained in x_m to be different for each module designed (See Equation 5.9).

With completion of the constrained module design process, a product capable of adapting to changes in customer needs over time through the addition of modules is achieved. In addition, each configuration of the product obtained through the addition of modules provides the optimal performance according to the objectives provided in Problem 5.1 (see Section 5.6).

In the following chapter, the development of a hurricane and flood resistant modular residential structure is provided as an example of the implementation of the method described in this chapter.

CHAPTER 6. PHASE 2 EXAMPLE: HURRICANE & FLOOD RESISTANT STRUCTURE

Over the past 30 years, the frequency and intensity of tropical cyclones has steadily increased [128]. In Latin America alone, approximately 2.5 million people were made homeless by cyclones and other natural disasters between 1990 and 1999 due in large part to the quality of local infrastructure [128]. As a result, international entities, including the World Bank, have called for the development of infrastructure solutions capable of withstanding these increasingly occurring disasters [128].

One implemented concept for addressing this challenge within residential markets is to elevate the living space above the expected flood levels [129]. Building on this idea, this section presents a tri-objective implementation of the phase 2 method developments described in Chapter 5, involving four hurricane and flood resistant residential structure design concepts. Representing these concepts as plane frames, a graphical summary of each concept and the assumed loading conditions is provided in Figure 6.1. It is recognized that the concepts presented in Figure 6.1 could be presented as parameterized versions of each other. However, in order to illustrate the ability of the method to account for multiple system concepts, each is analyzed with a distinct concept analysis model.

6.1 Plane Frame Analysis Model Assumptions

In order to analyze the concept plane frame models represented in Figure 6.1, the following assumptions are made:

1. Column sections are selected from among 28 AISC sections ranging from W12X336 to W12X16.

2. Beam sections are selected from among 57 AISC sections ranging from W33X169 to W18X35, all with width between 0.1524 and 0.3048 meters.

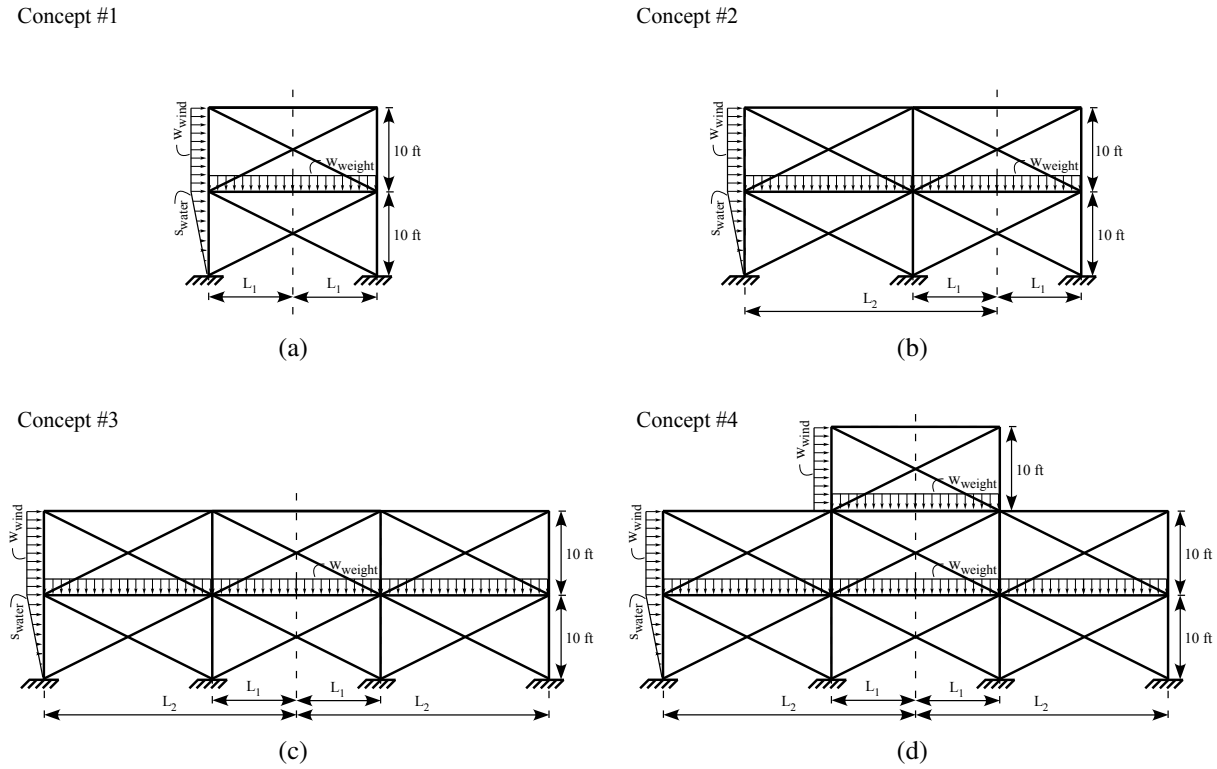

Figure 6.1: Graphical summary of four hurricane and flood resistant residential structure concepts and assumed plane frame loading conditions.

3. Cross brace sections are selected from among 35 AISC hollow square sections ranging from HSS6X6X5/8 to HSS18X6X1/4, all with width of 0.1524 meters.

4. Topology optimization that maintains symmetry in concepts 3 and 4 is performed for all cross braces shown in Figure 6.1.

5. The uniformly distributed wind load (w_{wind}) is 9.46 kN/m.

6. The uniformly distributed weight load (w_{weight}) is 10.95 kN/m.

7. The triangular distributed flood water load (s_{water}) is 6.34 kN/m.

8. The allowable inter-story drift is 0.01016 meters.

9. All joints connected to ground are assumed to be fixed.

10. The connections for shared beam joints are constrained to be the same for displacements and rotations.

11. The safety factor for buckling is 2.

12. The cost to material volume ratio of the structure is 1.

13. The allowable normal stress (σ_{allow}) is 206842.72 kN/m^2 for column and beam sections, and 190295.3 kN/m^2 for cross brace sections.

14. The allowable shear stress (τ_{allow}) is 137895.15 kN/m^2 for column and beam sections, and 126863.53 kN/m^2 for cross brace sections.

15. Half of the width of the first bay (L_1) can be values in 0.1524 meter increments between 2.286 and 4.572 meters.

16. The width of the second bay plus half of the width of the first bay (L_2) can be values in 0.1524 meter increments between 6.858 and 13.716 meters.

17. Columns and beams on the same level all have the same respective cross section.

18. Cross braces in the same bay and level have the same cross section.

19. The structures are assumed to extend 9.144 meter out of plane (used to calculate livable area).

6.2 Method Implementation

Prior to implementing the method described in Chapter 5, the objectives are identified as (1) *minimize* cost (C); (2) *minimize* the max stress to allowable stress ratio ($\hat{\sigma}_{\text{max}} = \sigma_{\text{max}}/\sigma_{\text{allow}}$); and (3) *maximize* the livable area of the building (A in m^2) . Using these objectives, the bounds of four anticipated regions of interest in terms of these objectives are provided in Table 6.1.

Figure 6.2 provides a graphical illustration of the candidate s-Pareto target designs identified within each region of interest through Step D of the method. These results were obtained using a custom multiobjective genetic algorithm (population = 500, blend crossover rate = 0.4, mutation rate = 0.2, and number of generations = 1200) tailored to search all regions of interest simultaneously. Analysis of the optimization objectives (C, $\hat{\sigma}_{\text{max}}$, and A) for the plane frame structures were performed using a matrix stiffness computer program developed in Balling 2009 [68].

Table 6.1: Objective limits for the i-th anticipated region of interest.

i	Objective Limits					
	$C_l^{(i)}$	$C_u^{(i)}$	$\hat{\sigma}_{\max_l}^{(i)}$	$\hat{\sigma}_{\max_u}^{(i)}$	$A_l^{(i)}$	$A_u^{(i)}$
1	6500	9000	0	1	41.81	55.74
2	9600	12500	0	1	139.35	153.29
3	13000	17000	0	1	236.90	250.84
4	18000	25000	0	1	278.71	306.58

Results of the objective values for the optimal design set proceeding from Step E of the method are presented in Table 6.2. It should be noted that the selected designs do not represent platform and module designs. Instead, they represent the non-modular system designs chosen by the method to be the best suited for conversion into platform and module designs in the remaining steps of the method. To obtain these results, the regional weights required by Equation 5.2 of Problem 5.1 are $w^{(i)} = \{0.6, 0.5, 0.2, 0.1\}$. These weights were selected based on the assumption that aggregate objective function values for designs selected in the first two regions of interest are more highly emphasized then in the last two regions. Although, it is noted that for this example the sensitivity of the resulting target designs to the values of $w^{(i)}$ is very low. In addition, the aggregate objective function required by Equation 5.3 is identified in Equation 6.1 as a Substitute Objective Function [130, 131].

$$J^{(k)} = \prod_{j=1}^{n_\mu} \left(\frac{\mu_{j,\max}^{(i)} - \mu_i^{(k)}}{\mu_{j,\max}^{(i)} - \mu_{j,\min}^{(i)}} \right) \tag{6.1}$$

where $\mu_{j,\text{max/min}}^{(i)}$ is the maximum/minimum non-shifted s-Pareto value of the j-th objective within the i-th region of interest.

The cross-brace topology, along with the values of L_1, L_2 (See Figure 6.1), and the selected cross sections is presented in Figure 6.3. Since the design selected in the fourth region of interest also represents the designs from the other regions, this design is the only one represented in Figure 6.3.

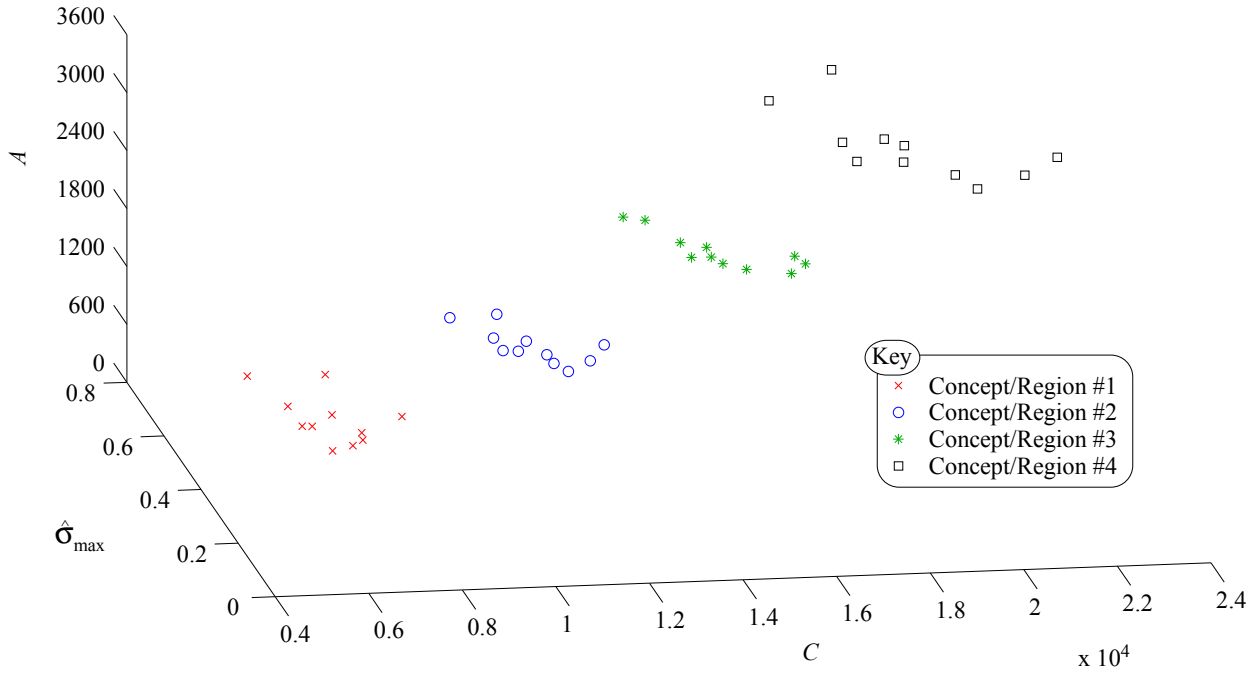

Figure 6.2: The candidate s-Pareto target designs within each region of interest identified through Step D of the method.

Table 6.2: Objective values of the optimal design selected within the i-th region of interest (column 1) obtained through Step E of the method. The design concept (k) corresponding to the design selected within each region is equal to the i-th region (see column 1).

	Optimal Objective Values		
i,k	$C^{*(i)}$	$\hat{\sigma}_{\max}^{*(i)}$	$A^{*(i)}$
1	5969	0.6483	41.81
2	9489	0.4440	144.93
3	13009	0.3975	256.41
4	17102	0.6433	298.22

Prior to developing the module designs, information on the type, number, and desired progression of modules that are to be used to obtain the s-Pareto designs contained identified in Table 6.2 is needed. For this example, a slot-modular approach was selected for the modular architecture [20, 78]. By examining the concepts presented in Figure 6.1, it is observed that the design that is common to all other concepts will correspond to concept/region one (i.e., $D_{\text{a}}^{(1)}$). Using this information, and the assumption that the customer preference is to progress sequentially from one

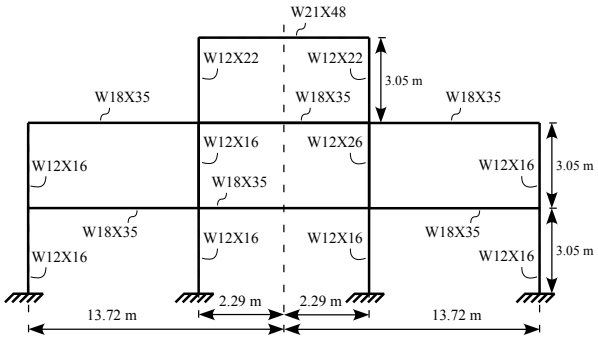

Figure 6.3: Graphical representation of the optimal topology, along with the values of L_1, L_2, and the selected cross sections corresponding to the fourth region of interest.

region to the next, the desired number of modules to be developed (n_m) is chosen to be three. In addition, the matrix δ (see Section 5.7), defining the desired modular progression, is constructed in Equation 6.2. Columns 1 and 2 in δ respectively refer to the starting and target design in D_{a} for each module (rows in δ). Note that although this example presents a modular progression that is sequential (modules move sequentially through the regions of interest), the method is not constrained to do this (i.e., a module could be identified to result in a jump from interest region 1 to interest region 3).

$$\delta = \begin{bmatrix} 1 & 2 \\ 2 & 3 \\ 3 & 4 \end{bmatrix} \tag{6.2}$$

Results from evaluating a constrained module design routine of the form presented in Problem 5.2 are presented in Table 6.3. The modular variables identified in Table 6.3 are: (i) the length of the beam sections for module 1 (L_1), (ii) the length of the beam sections for module 2 (L_2), (iii) the AISC cross-section of the top level columns (S_{c}), and (iv) the AISC cross-section of the top level beam (S_{b}). All other variables defining the module designs are identified within the selected platform design.

Table 6.3: Variable values of the module designs (i) obtained through evaluation of a constrained module design routine of the form presented in Problem 5.2.

	Module Variables			
i	L_1^* (m)	L_2^* (m)	S_c	S_b
1	11.2776	–	–	–
2	–	11.2776	–	–
3	–	–	W12X22	W21X48

6.3 Discussion of Results

With completion of the constrained module design process, a modular residential structure capable of expanding through the addition of three different modules is achieved. To illustrate the selected platform and three module designs identified in Table 6.3, Figure 6.4 is provided.

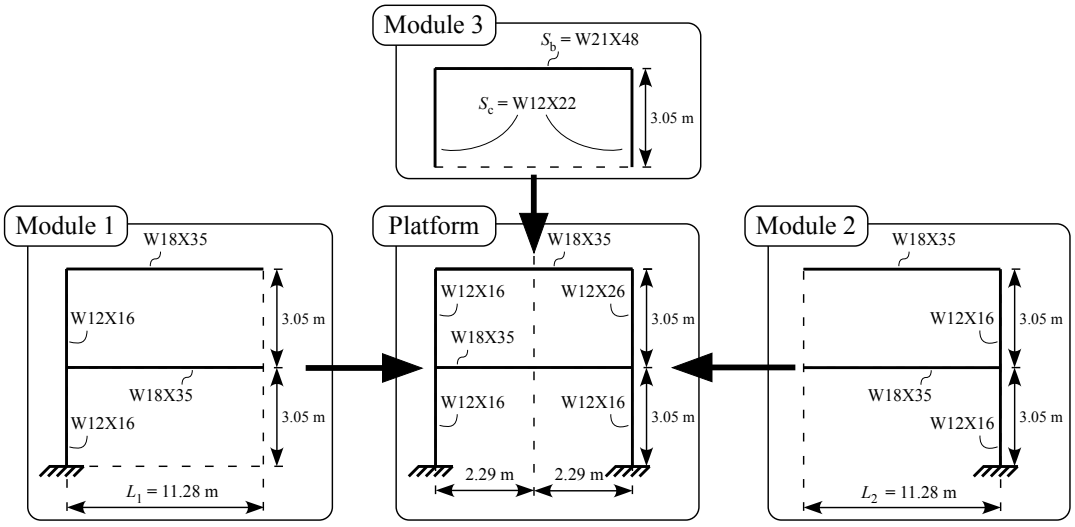

Figure 6.4: Graphical representation of the selected platform and three module designs identified in Table 12.4.

It should be remembered that the anticipated regions of interest identified in Step B of the method (see Table 6.1) represent what the customer/designer wishes to achieve over time. As such, the identified solutions are deemed to be good for three reasons: (i) the designs identified in Step E of the method (see Table 6.2) are within the designer-defined regions of interest; (ii) the selected platform variables enabled the identified solutions to be located on the original Pareto frontiers of

each concept (shift from s-Pareto frontier to accommodate modularity was minimized); and (iii) modules that enable the system to traverse the identified s-Pareto solution set using the selected platform were identified.

Due to the optimization formulations found in Steps E and F, these results are not surprising. The formulation in Step E serves to ensure that identified designs are within the regions of interest, while the formulation of Step F ensures that the modules developed are as close to the s-Pareto designs selected in Step E as possible.

CHAPTER 7. PHASE 3 METHOD DEVELOPMENT: IDENTIFYING DYNAMIC S-PARETO FRONTIERS

As described in Chapter 2, engineering design is a multifaceted decision making process that often involves several conflicting design objectives. One facet that is not commonly considered is how the resolution of conflicts changes over time. That is, how to consider changes in both the preferences that dictate the selection of Pareto designs, and changes in the Pareto or s-Pareto frontier itself over time. When developing a single product for multiple scenarios, a common approach in multiobjective optimization is to combine the product performance in each scenario into a single aggregate performance [131]. As a result, valuable information about the design space for individual scenarios is lost, and the effect of design decisions on the performance of a product in a given scenario is difficult to interpret.

In terms of individual design scenarios, the idea of changing design selection due to changes in preference is illustrated is Figure 7.1(a) where the points $\mu^{(1)}$, $\mu^{(2)}$, and $\mu^{(3)}$ represent the designs selected along the Pareto frontier (bold line) at times 1, 2, and 3 respectively. Recognizing that Pareto/s-Pareto frontiers, and the resulting design space, may be dynamic due to model, concept, or environmental changes, Figure 7.1(b) demonstrates the concept of both dynamic s-Pareto frontiers and preferences. From these figures it is observed that in situations where these changes can be predicted, these dynamic s-Pareto frontiers and preferences can and should be considered when making design decisions in the present. Examples of situations where these changes could be predicted include changes in manufacturing cost models due to economies of scale, planned implementation of new technologies, ranges of known operating environments, and governmental performance regulation changes (i.e., gas mileage requirements of vehicles).

This phase of the research explores the idea of dynamic s-Pareto frontiers and preferences. Specifically, what they are (see Figure 7.1), how they are obtained (see Section 7.2), and how they can be used to make better decisions in the present (See Chapter 8). In order to facilitate this exploration, in Section 7.1 a discussion of the types of changes that existing methods could address

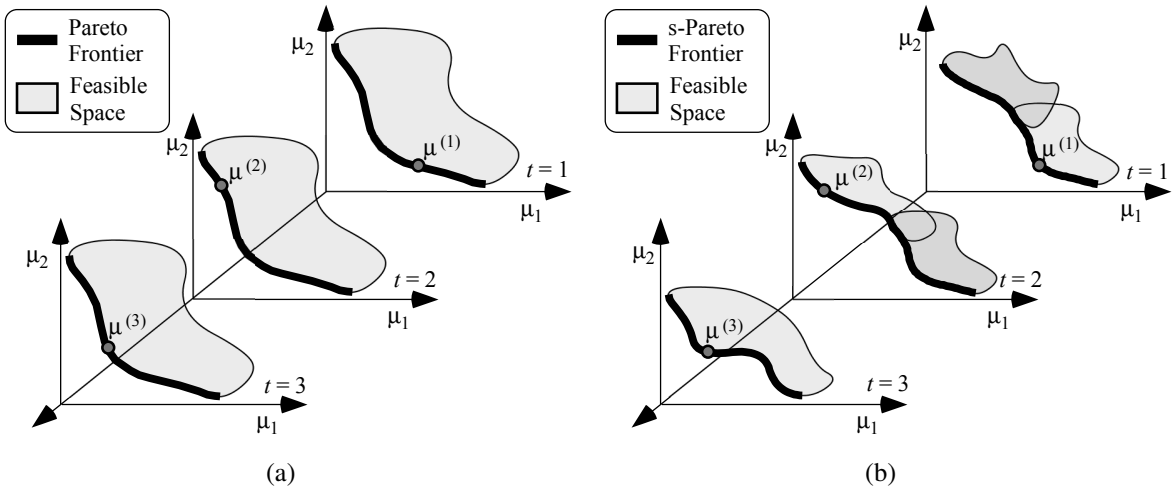

Figure 7.1: (a) Design selections over time due to changing preference. (b) Design selections due to both changing preference and changing models, concepts, and/or environment.

is provided. Section 7.2 presents a new optimization formulation capable of constructing dynamic Pareto frontiers in the presence of known/predicted changes in preferences, models, concepts, and operating environment.

7.1 Sources of Change & Existing Methods

As described in Section 2.2, the selection of a Pareto-optimal solution typically involves the construction of an aggregate objective function that implements knowledge of the objective function parameters and sometimes constraints to capture customer needs or preferences [131, 132]. Within the context of this dissertation, changes in Pareto solutions and preferences over time introduce unique challenges in selecting Pareto-optimal solutions. These changes can result from preference, model, concept, or environmental changes, where in this dissertation we assume the following descriptions of these sources of change:

(i) *Preferences* refer to the customer desires/needs that dictate the selection of Pareto designs;

(ii) *Models* refer to the design models used to analyze a design;

(iii) *Concepts* refer to the design concepts that the design models analyze; and

(iv) *Environment* refers to the operating environment of the design concept;

In order to illustrate what combinations of changes have received attention in multiobjective optimization literature Table 7.1 is provided. Table 7.1 presents every possible combination of these potential sources of change, along with references to chapters of this dissertation, and other publications, presenting methods capable of allowing for the identified combination.

Table 7.1: Presentation of potential sources of change (columns 1-4), along with references (column 5) to chapters of this dissertation, and other publications, that allow for the indicated sources of change. For each combination, only sources of change with an "x" in the corresponding column are considered to change.

Sources of Change				Publications	
Preference	Model	Concept	Environment	Y/N	Citations
x	x	x	x	N	–
x	x	x		N	–
x	x		x	N	–
x		x	x	Y	Chapter 5, [24, 80, 133]
	x	x	x	N	–
x	x			N	–
x		x		Y	Chapter 5, [24, 80, 133]
x			x	Y	Chapters 3 & 5, [24, 30–32, 78, 80, 133]
	x	x		N	–
	x		x	N	–
		x	x	Y	Chapter 5, [24, 80, 133]
x				Y	Chapters 3 & 5, [24, 30–32, 78, 80, 133]
	x			N	–
		x		Y	[24, 133]
			x	Y	[30, 30, 31, 31, 32, 32, 134–136]
				Y	Traditional MOP

It should be observed from Table 7.1 that publications exist that have the potential to allow for changes in concept, preference, and environment, but are for specific design approaches (e.g., modular products [78, 80], families of products [24, 133], and reconfigurable/adaptable/flexible systems [30–32]). In addition, it should be observed that no publications/methods exist for combinations that contain changes in design models. This gap in publications is in part due to the form of the traditional MOP (see Section 2.2), and the inherent difficulty this formulation has in adapting to an evolving design problem [83, 84]. As such, a new MOP formulation that efficiently

identifies a dynamic s-Pareto frontier resulting from changes in preference, model, concept, and environment is needed.

7.2 Generic Dynamic s-Pareto Frontier Formulation

The purpose of the dynamic MOP presented in this section is to overcome the inefficiencies of tradition MOP formulations in adapting to changes in preferences, concepts, models, and environments by identifying the dynamic s-Pareto frontier for a series of known sources of change combinations. The efficient identification of this dynamic s-Pareto frontier will then enable and encourage the use of this information to guide and improve design decisions.

As MOP formulations change, what was a design parameter in one formulation could be an inequality constraint in the next formulation. Thus to avoid confusion, any variable, parameter, constraint, or objective associated with a design is termed a *design object* [83, 84]. With this understanding, we present a generic dynamic multiobjective optimization problem capable of identifying the s-Pareto frontier for each time step:

Problem 7: Dynamic s-Pareto MOP Formulation

$$D_{\mathrm{x}} := \{(x_1^{*(k^{(t)})}, ..., x^{*(k^{(t)})}_{n_x^{(k^{(t)})}}) | \forall t \in (1, 2, ..., n_t)\} \tag{7.1}$$

$x^{*(k^{(t)})}$ is defined by:

$$\min_{k^{(t)}} \left\{ \min_{y^{(k^{(t)})}} \left\{ \mu_1^{(k^{(t)})}(x^{(k^{(t)})}),\ ...,\ \mu^{(k^{(t)})}_{n_\mu^{(k^{(t)})}}(x^{(k^{(t)})}) \right\}\ (n_\mu^{(k^{(t)})} \geq 2) \right\} \left\{ k = 1, ..., n_k^{(t)} \right\} \tag{7.2}$$

subject to:

$$x_{l,i}^{(k^{(t)})} \leq x_i^{(k^{(t)})} \leq x_{u,i}^{(k^{(t)})} \quad \{i = 1, ..., n_x^{(k^{(t)})}\} \tag{7.3}$$

where:

$$\mu^{(k^{(t)})} \ = \ \chi^{(k^{(t)})} \cdot x^{(k^{(t)})} \tag{7.4}$$

Table 7.2: Conditions for specifying design objects and object limits.

Design Object x_i	**Condition**
Minimized Objective	$\chi_{i,i}^{(k^{(t)})} = 1$
Maximized Objective	$\chi_{i,i}^{(k^{(t)})} = -1$
Non-Objective	$\chi_{i,i}^{(k^{(t)})} = 0$
Inequality Constraint	$x_{l,i}^{(k^{(t)})} \neq x_{u,i}^{(k^{(t)})}$ AND $i > n_y^{(k^{(t)})}$
Equality Constraint	$x_{l,i}^{(k^{(t)})} = x_{u,i}^{(k^{(t)})}$ AND $i > n_y^{(k^{(t)})}$
Design Variable	$x_{l,i}^{(k^{(t)})} \neq x_{u,i}^{(k^{(t)})}$ AND $i \leq n_y^{(k^{(t)})}$
Design Parameter	$x_{l,i}^{(k^{(t)})} = x_{u,i}^{(k^{(t)})}$ AND $i \leq n_y^{(k^{(t)})}$

$$\chi^{(k^{(t)})} = \begin{bmatrix} \chi_{1,1}^{(k^{(t)})} & \cdots & 0 \\ \vdots & \ddots & \vdots \\ 0 & \cdots & \chi_{n_x^{(k^{(t)})},n_x^{(k^{(t)})}}^{(k^{(t)})} \end{bmatrix} \tag{7.5}$$

$$x^{(k^{(t)})} = \left[y_1^{(k^{(t)})}, ..., y_{n_y^{(k^{(t)})}}^{(k^{(t)})}, z_1^{(k^{(t)})}(y^{(k^{(t)})}), ..., z_{n_z^{(k^{(t)})}}^{(k^{(t)})}(y^{(k^{(t)})}) \right]^T \tag{7.6}$$

$$n_x^{(k^{(t)})} = n_y^{(k^{(t)})} + n_z^{(k^{(t)})} \tag{7.7}$$

where $x^{(t)}$ is a vector composed of independent ($y^{(k^{(t)})}$) and dependent ($z^{(k^{(t)})}$) design objects at time step t; and the objectives identifier matrix, $\chi^{(k^{(t)})}$, is a diagonal matrix for time step t, where $\chi_{i,i}^{(k^{(t)})} \in \{-1, 0, 1\}$.

It should be noted that, with a few exceptions, Problem 7 is very similar to the generic s-Pareto MOP formulation (Problem 2.2) presented in Section 2.2. For instance, the nature of x has changed to include independent and dependent design *objects*, while in Problem 2.2, x only contained independent design *variables*. The role of each design object is determined by Equations 7.3–7.5, and the conditions determining a design object's behavior are summarized in Table 7.2 [83, 84]. Additionally, we note that Problem 7 is minimized over $y^{(k^{(t)})}$ rather than $x^{(k^{(t)})}$ to ensure that the problem is mathematically valid.

It should be noted that Problem 2.2 and Problem 7 will yield the same s-Pareto frontier for a given t. However, the benefit of the formulation of Problem 7, is that the MOP is established to

be able to quickly and efficiently identify the dynamic s-Pareto frontier for all selected values of t. As such, the ability to use this information to guide and improve design decisions is provided. In the next chapter, implementation of the presented dynamic formulation and the ability of the resulting dynamic s-Pareto frontier to improve design decisions is illustrated through a simple aircraft example with three design scenarios.

CHAPTER 8. PHASE 3 EXAMPLE: SIMPLE AIRCRAFT DESIGN PROBLEM

This chapter implements the formulation presented in Problem 7 (see Section 7.2) for an example based on numerical aircraft performance models presented in Heintz (2002) [137] and Nigam and Kroo (2008) [123]. Motivation for this example comes from the Lockheed C-130 Hercules, which was designed in 1951 to meet the needs of the Korean War [138]. Initial design requirements of the C-130 specified cargo capacity, the ability to take off from short airstrips, and the ability to fly slow enough for paradrops. Though different from the missions considered in the design, the C-130 has also successfully operated as a cargo transport, a refueling aircraft, a weather reconnaissance aircraft, and a combat gunship. To perform these new missions the aircraft was modified to meet these roles after being produced as standard C-130 models, providing a versatility that has made the platform a success [139]. In light of the focus of this dissertation and the various modifications that the C-130 has received over the years, the question arises of how the C-130 might have been designed if the many different missions this aircraft would need to perform were known and considered during the aircraft's development. Building from the concept of this question, the given example sets forth a method of illustrating how an optimization problem can be formulated to account for many different changes.

For this example all identified sources of change described in Section 7.1 are considered. Changes in preference and environment are represented in three scenarios as a series of changes in the aircraft mission profile for each scenario/time-step. Figure 8.1 provides the generic mission profile implemented in this example. The mission parameters shown in Fig. 8.1 are defined with the model descriptions provided in Section 8.1. The three profiles implemented in this example correspond to (1) a bombing mission (high sprint speed and high cargo weight), (2) a cargo transportation/drop mission (both medium sprint speed and cargo weight), and (3) a high altitude surveillance mission (low sprint speed and low cargo weight).

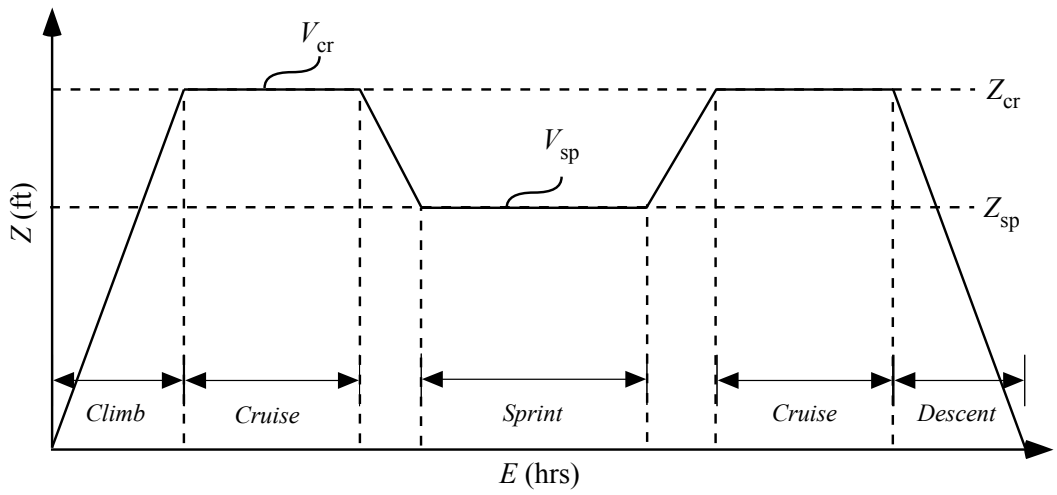

Figure 8.1: Generic mission profile used to define the needed aircraft performance at different time-steps. Parameter definitions are provided in Section 8.1.

A summary of the concepts and objectives considered at each time-step are provided in Table 8.1, where W is the total aircraft weight, P is a measure of the aircraft take-off/climb performance, and $\hat{T}_{\text{lost}}$ is the surveillance time lost per degree of turn. Changes in aircraft concepts are differentiated by the ranges of available engine power (φ) in billion horse power (bhp), maximum flaps down lift coefficient ($C_{\text{L,fd}}$), and the aircraft wing span (b) in feet. Changes in concepts over time are represented in Table 8.1 by the introduction of Concept 3 at time-step two, and the removal of Concept 1 at time-step three. Changes in model are also represented in Table 8.1 by the introduction of a new objective and corresponding analysis model for the final time-step. The introduction of $\hat{T}_{\text{lost}}$ as an objective in the final time-step ($t = 3$) indicates that for this mission the aircraft will be performing surveillance tasks, and consequently needs to be able to turn as quickly as possible, which assumes that no usable surveillance is captured while executing a turn.

Table 8.1: Summary of the concepts and objectives considered at each time-step (t).

t	Concepts	Objectives
1	1, 2	min$\{W, P\}$
2	1, 2, 3	min$\{W, P\}$
3	2, 3	min$\{W, P, \hat{T}_{\text{lost}}\}$

8.1 Analysis Model Descriptions

In order to identify the s-Pareto frontiers at each time-step (obtain the dynamic s-Pareto frontier) for the objectives identified in Table 8.1 requires two analysis models. The first model calculates values of P and W, and comes from Heintz (2002) [137]. The needed analysis functions are provided below:

$$W_{\mathrm{f}} = E \cdot r_{\mathrm{f}} \cdot \varphi \tag{8.1}$$

$$W_{\mathrm{u}} = W_{\mathrm{f}} + W_{\mathrm{c}} \tag{8.2}$$

$$W = W_{\mathrm{u}} \cdot (1 + r_{\mathrm{eu}}) \tag{8.3}$$

$$S_{\mathrm{fd}} = \frac{391\,W}{V_{\mathrm{s,fd}}^2 \cdot C_{\mathrm{L,fd}}} \tag{8.4}$$

$$S_{\mathrm{c}} = \frac{391\,W}{V_{\mathrm{s,c}}^2 \cdot C_{\mathrm{L,c}}} \tag{8.5}$$

$$S = \max(S_{\mathrm{fd}}, S_{\mathrm{c}}) \tag{8.6}$$

$$V_{\max} = 180 \sqrt[3]{\frac{\varphi}{S+100}} \tag{8.7}$$

$$P = \left(\frac{W}{S}\right) \cdot \left(\frac{W}{\varphi}\right) \tag{8.8}$$

$$A = \frac{b^2}{S} \tag{8.9}$$

$$V_{\mathrm{z}} = \frac{7000 \cdot \sqrt[4]{A}}{W/\varphi} \tag{8.10}$$

$$Z_{\max} = 16 \cdot V_{\mathrm{z}} \tag{8.11}$$

$$\hat{V}_{\max} = \begin{cases} \max(V_{\mathrm{cr}}, V_{\mathrm{sp}}) & , \text{for } t \neq 2 \\ \max(V_{\mathrm{cr}}, V_{\mathrm{sp}}, V_{\mathrm{turn}}) & , \text{else} \end{cases} \tag{8.12}$$

$$\hat{Z}_{\max} = \max(Z_{\mathrm{cr}}, Z_{\mathrm{sp}}) \tag{8.13}$$

The second model calculates values of $\hat{T}_{\mathrm{turn}}$, and comes from Nigam and Kroo (2008) [123]. The needed analysis functions are provided below:

$$\eta_{\max} = \frac{1.0752\,\rho\,V_{\mathrm{turn}}^2 \cdot S \cdot C_{L,c}}{W - \frac{W_{\mathrm{f}}}{4}} \tag{8.14}$$

$$R_{\text{turn}} = \frac{2.1503\, V_{\text{turn}}^2}{g\sqrt{\eta_{\text{max}}^2 - 1}} \tag{8.15}$$

$$\hat{D}_{\text{turn}} = \frac{\pi\, R_{\text{turn}}}{180} \tag{8.16}$$

$$\hat{T}_{\text{lost}} = \frac{\hat{D}_{\text{turn}}}{V_{\text{turn}}} \tag{8.17}$$

where the variable definitions in the above models, along with any other variables implemented in this example are given as follows.

φ	Engine horse power (bhp)
r_{f}	Fuel consumption rate (lbs/hr-bhp)
E	Required endurance (hrs)
W_{f}	Useful load (lbs)
W_{c}	Weight of cargo and occupants (lbs)
W_{u}	Useable weight (lbs)
r_{eu}	Ratio of empty weight to usable weight (lbs/lbs)
$V_{\text{s,fd}}$	Stall velocity with wing flaps down (mph)
$C_{\text{L,fd}}$	Coefficient of lift with wing flaps down
W	Total Aircraft Weight (lbs)
S_{fd}	Area of flaps down wings (ft^2)
$C_{\text{L,c}}$	Coefficient of lift with clean wings
$V_{\text{s,c}}$	Stall velocity of clean wings (mph)
S_{c}	Area of clean wings (ft^2)
S	Minimum needed wing area (ft^2)
b	Wing span (ft)
P	Maximum takeoff/climb performance (lbs^2/ft^2-bhp)
V_{max}	Maximum possible aircraft velocity (mph)
A	Wing aspect ratio
V_{z}	Maximum possible rate of climb (ft/min)
$\hat{V}_{\text{max}}$	Maximum required mission velocity (mph)

V_{turn} Aircraft Velocity while executing a turn (mph)

V_{cr} Required mission cruise speed (mph)

V_{sp} Required mission sprint speed (mph)

$Z_{\max}$ Service ceiling (maximum possible flight elevation) (ft)

$\hat{Z}_{\max}$ Maximum required mission elevation (ft)

Z_{cr} Mission cruise elevation (ft)

Z_{sp} Mission sprint elevation (ft)

g Gravitational Constant (ft/s^2)

ρ Density of air (lbs/ft^3)

$\eta_{\max}$ Maximum aircraft load factor

R_{turn} Minimum aircraft turn radius (ft)

$\hat{D}_{\text{turn}}$ Distance traveled per degree of turn (ft/deg)

$\hat{T}_{\text{lost}}$ Surveillance time lost per degree of turn (s/deg)

8.2 Optimization Results and Discussion

Using these two models and the information in Table 8.1, a problem of the form of Problem 7 (see Section 7.2) was created and implemented using the FMINCON function in Matlab. Design object limits and $\chi_{i,i}^{(k^{(t)})}$ values implemented in this example for each concept and time-step are summarized in Appendix A. The resulting s-Pareto frontier at each time-step is shown in Figure 8.2.

Identification of the s-Pareto frontier/surface for each time-step was accomplished by executing a simple line/grid search within the changing objective space, followed by the use of a Pareto filter to remove any non-Pareto designs [37]. As such, areas of the s-Pareto surface for the third time-step where the distribution of s-Pareto designs appear to be sparse, are due to the removal of identified designs by the Pareto filter.

From Figure 8.2 it can be observed that the s-Pareto frontier, as anticipated, changes over time due to the changes in preferences, concepts, models, and environments. As described in Chapter 7, the purpose of obtaining these optimal designs within each time-step is to enable better decisions to be made in the present ($t = 1$). One such decision that is required is to determine what

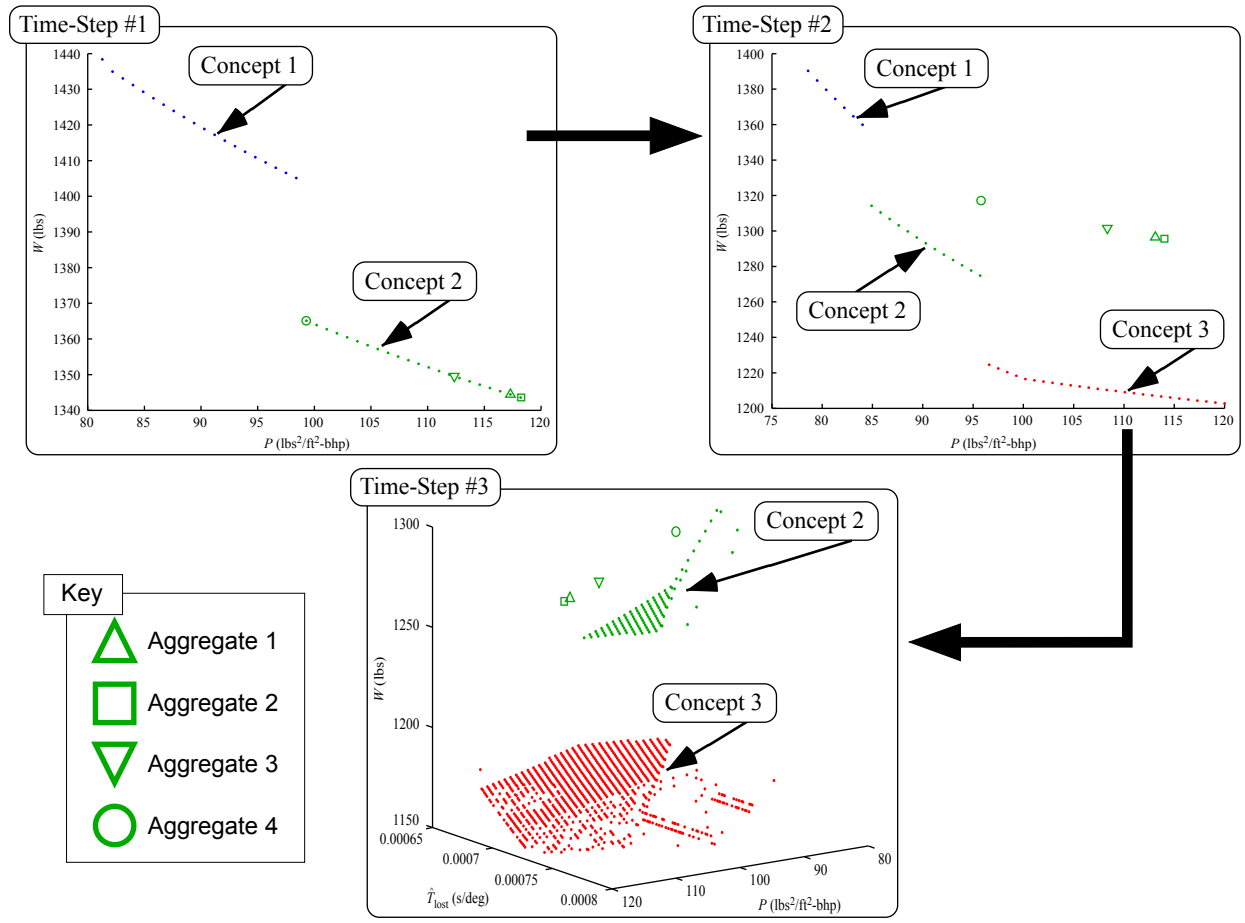

Figure 8.2: Representation of s-Pareto frontier obtained for each time step using Matlab, and aircraft Concept 2 designs (△, □, ∇, and ○) selected using four different aggregate approaches.

type of aircraft will be created to account for the identified changes. Some available options would include: (i) a single non-modular/non-adjustable aircraft designed to operate in every scenario; (ii) a series of related aircraft designs that build on common platforms (product family); (iii) a reconfigurable/adjustable aircraft; or (iv) a modular aircraft that adapts to different scenarios through the addition or subtraction of modules. Recognizing that options (ii)-(iv) require additional design methods and considerations, for this example, option (i) was selected. In addition, due to the selection of option (ii), Concept 2 was selected as the preferred concept since it appears in each time-step, and has a more moderate trade-off between W and P.

In order to select a single aircraft design for Concept 2, four different aggregate approaches were implemented. In each case, the dynamic formulation (of the form of Problem 7) used to

obtain the dynamic s-Pareto frontiers shown in Figure 8.2 was adapted by replacing Equation 7.2 in Problem 7 with the following:

$$\min_{\hat{y}^{(k)}} \left\{ J(\mu^{(k^{(1)})},\ \mu^{(k^{(2)})},\ ...,\ \mu^{(k^{(n_t)})}) \right\} \tag{8.18}$$

where $\hat{y}^{(k)}$ is a vector composed of all common independent design objects ($y^{(k^{(1)})} \cup y^{(k^{(2)})} \cup ... \cup y^{(k^{(n_t)})}$) for the k-th design concept; and J is an aggregate objective that is a function of the objective values at each time-step.

The first aggregate approach used is assumed to be similar to that of the C-130, where the aircraft design was selected based on the specific requirements at one initial time. In this case, the aggregate objective function was a weighted sum of the objective values at $t = 1$ (objective weights for P and W were both 0.5). Selecting a design from the previously identified s-Pareto designs at $t = 1$, the resulting performance at each time-step is represented in Figure 8.2 by the symbol "△". It should be observed that the design selected at $t = 1$ is on the s-Pareto frontier. However, the performance of this design at the other time-steps ($t = 2$ and 3) is highly non-optimal due to the distance/offset of the selected design from the dynamic s-Pareto frontier.

The second aggregate approach used was to combine all objective values of a design at each time-step using a Substitute Objective Function [130, 131] (multiplies the normalized objective values for all t together). The resulting design for this approach is represented in Figure 8.2 by the symbol "□". Once again, it is observed that the design selected at $t = 1$ appears to be on the s-Pareto frontier, but the performance of this design at the other time-steps is even more non-optimal then for the first approach.

The third aggregate approach combined all objective values of a design at each time-step using a weighted sum. The weights used to scale the values of P at each time-step were 0.5. The weights used to scale the values of W at each time-step were 0.5, 0.5, and 0.3 respectively. The weight used to scale the value of $\hat{T}_{\text{lost}}$ for $t = 3$ was 0.2. The resulting design for this approach is represented in Figure 8.2 by the symbol "∇". Again, it is observed that the design selected at $t = 1$ appears to be on the s-Pareto frontier. However, the performance of this design at the other time-steps, although still highly non-optimal, is closer to the s-Pareto frontier then for the first two approaches.

Table 8.2: Summary of the aircraft design offsets from the nearest dynamic s-Pareto point using the four aggregate approaches ($\triangle$, $\square$, ∇, and $\circ$) shown in figure 8.2.

t	Aggregate 1 Offsets	Aggregate 2 Offsets	Aggregate 3 Offsets	Aggregate 4 Offsets
1	0	0.08	0.65	0.03
2	22.89	23.55	19.66	11.28
3	22.83	23.47	19.58	11.29

Note that for each of these three approaches, the design comparisons are focused around the distance/offset of these designs from the identified s-Pareto frontiers, and not simply the objective values, at each time-step. As such, a noted value of using the dynamic s-Pareto formulation is the ability to seek designs that minimize the offset from the dynamic s-Pareto frontier at each time-step. With this in mind, the final aggregate approach combined the offset of a given design at each time-step using a weighted sum. The weights used to scale the offset value at each time-step that resulted in the lowest offsets for $t = 2$ and 3 were 0.1, 0.75, and 0.15 respectively. The resulting design for this approach is represented in Figure 8.2 by the symbol "$\circ$". Note that the design selected at $t = 1$ appears to be on the s-Pareto frontier, and that the offsets of the selected design from the s-Pareto frontier for the remaining time-steps is significantly improved.

It should be noted that the third aggregate approach is capable of selecting the same design as the offset approach (Aggregate 4). However, in order to maintain consistency with the weights used in Aggregate 1, this solution was not shown in Figure 8.2. In addition, it is observed that the selected design for Aggregate 4 at $t = 1$ is at the limits of the s-Pareto points corresponding to Concept 2. Due to this, and the weights of Aggregate 4 required to minimize the design offsets for $t = 2$ and 3, it was concluded that the design requirements for $t = 1$ are what limits the design offset in the other scenarios.

To summarize the results of the four aggregate approaches described above, Table 8.2 presents the offset of each approach.

8.3 Conclusions

In response to the question of how the resolution of conflicts changes over time due to changes in preferences, concepts, models, and environments, the idea of dynamic s-Pareto frontiers and

preferences was presented in Chapter 7. Specifically, changes in both the preferences that dictate design selection, and changes in the s-Pareto frontier over time through the use of a dynamic MOP formulation was explored. The application of the presented dynamic MOP formulation (see Problem 7), and the ability to use the resulting dynamic s-Pareto frontier to guide/improve design decisions, was illustrated in this chapter through a simple aircraft example for three different time-steps.

Through the presented example, the ability to directly explore a changing design space, and identify the resulting dynamic s-Pareto frontier by using the dynamic s-Pareto formulation was demonstrated. In addition, the ability to use the identified dynamic s-Pareto frontier to evaluate design selections based on the offset from the frontier and thus improve design decisions is also shown.

CHAPTER 9. PHASE 4 METHOD DEVELOPMENT: TRAVERSING DYNAMIC S-PARETO FRONTIERS

In this chapter, the fourth phase in the development of a multiobjective optimization design method providing a Pareto-optimal product and module designs capable of satisfying changes in preferences, concepts, environments, and analysis models over time is described [81, 87]. In this section the limitations of the Phase 2 method developments (see Chapter 5) are identified. This discussion is then followed by the presentation of an improved five-step method that incorporates the Phase 3 developments (see Chapter 7), and thus enables the use of the dynamic s-Pareto MOP formulation to overcome the majority of these limitations.

9.1 Phase 2 Method Limitations

The purpose of this section is to describe the limitations of the six-step optimization-based method presented in Chapter 5. This provides the motivation and foundation for the improved method presented in this chapter. Specifically, the notable limitations of this method include the following:

(1) The method is only capable of accounting for changes in preferences and environment. The multiobjective problem formulation implemented in Step E of the method does not allow different sets of concepts or analysis models to be considered within each region of interest (i.e., considered concepts and analysis models cannot change over time).

(2) The method assumes that a useful set of design variables that are common to all concepts considered can be identified as platform variables. This requirement of only considering non-modular concepts that collectively contain a set of common variables predefines the optimization results, and does not allow for concepts with potential improvements in objective space performance to influence the modular-system concepts that are developed.

(3) The optimization of each module is performed separate from the other elements of the modular-system, and assumes that the platform and specified module combinations achieve the desired performance. Consequently, the constrained module optimization formulation in Step F does not account for the possibility that the performance of system configurations achieved through the addition of specific modules do not match the target performances identified in Step E of the method.

(4) Due to the use of predicted changes in preferences and environments, along with the desire to allow changes in analysis models and concepts, uncertainty is an inherent issue that is not incorporated or discussed in the current optimization formulations.

It is generally accepted that uncertainties caused by variations in customer perception, available market data, material properties, manufacturing precision, and other sources can – and should – significantly affect the selection of product designs. In considering the anticipated sources of uncertainty within the context of this research, three general groups that emerge are *parameter/variable uncertainty*, *analysis model output uncertainty*, and *current/future preference uncertainty*.

In the literature are found two broad categories of approaches to determining the level of uncertainty in decision making. The first category are *reliability-based design methods* [140–142] which focus on assessing the probability of design failure, and seek to reduce such probabilities by shifting the mean performance away from constraint limits [142]. The second are *robust design based methods* [51, 143–148] which focus on optimizing the mean performance, and minimizing performance variation, while maintaining feasibility with probabilistic constraints [146, 149, 150].

Some of the common methods of performing uncertainty analysis include: (i) Monte Carlo and Sampling techniques [151–154], (ii) Univariate Dimension Reduction [155, 156], (iii) Deterministic Error by Model Composition [157], (iv) Error Budgets [158, 159], (v) Interval Analysis Methods [160], (vi) Bayesian Inference [161, 162], (vii) Anti-Optimization Techniques [163, 164], and (viii) Taylor Series and Central Moments [150, 165–167].

Note that the analysis of multiple predicted design scenarios inherent in the presented method will often decrease the likelihood of being able to obtain statistical data of the parame-

ters/variables and analysis model outputs for each concept/scenario. As such, to enable the use of either statistical or bounded uncertainty parameter domains, and ensure that designs are selected such that the wost case scenarios will satisfy all design constraints, the optimization formulations developed and presented in this chapter will incorporate Anti-Optimization techniques.

9.2 Improved Five-Step Modular System Optimization Design Method Using Dynamic s-Pareto Frontiers

This section presents an optimization-based method that builds on the presented developments in multiobjective problem formulations of dynamic s-Pareto frontiers (see Chapter 7), and addresses the limitations of the method identified in the previous section. Figure 9.2 illustrates the intent of the method to select an s-Pareto optimal platform design that, through the addition of modules, becomes other designs within anticipated regions of interest along the *dynamic s-Pareto frontier*. For example, the figure shows that the platform design, labeled $\hat{\mu}^{(1)}$, adapts to become $\hat{\mu}^{(2)}$ through the addition of Module 1. In like manner, the subsequent design identified as $\hat{\mu}^{(3)}$ is also achieved through the addition of Module 2.

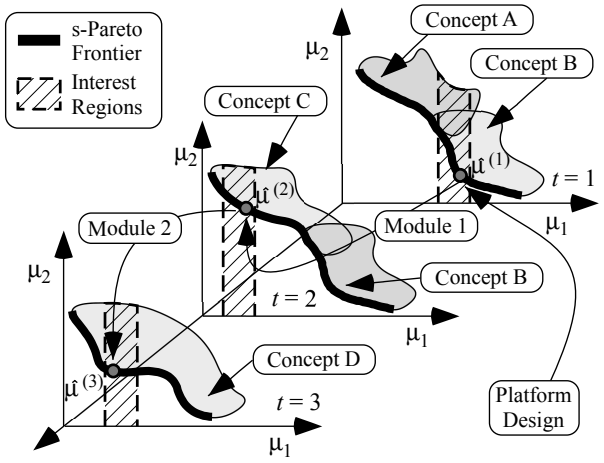

Figure 9.1: Graphical representation of the intent of the improved method to provide a system that expands from one *dynamic s-Pareto design* to another through the addition of modules. Also notice that the designs that it can adapt to are within designer defined regions of interest.

Figure 9.2 provides a flow chart that represents the five primary steps of the multiobjective optimization design method developed herein. Each of these steps is described below. It is im-

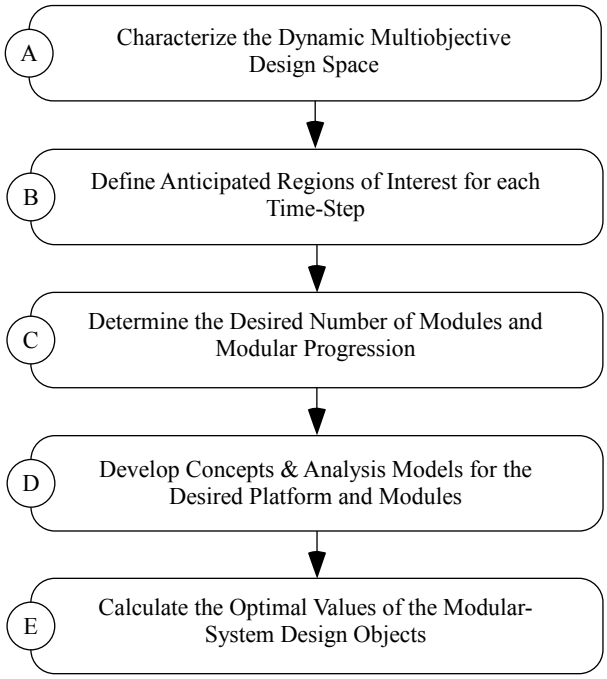

Figure 9.2: Flow chart describing the five-step multiobjective optimization design method developed in this chapter.

portant to note that the titles of some of the steps are similar to the steps/sub-steps of the method presented in Figure 5.2(a). However, each of these steps requires new and essential extensions to enable the method to identify systems capable of traversing a dynamic s-Pareto frontier.

9.3 Step A: Characterize the Dynamic Multiobjective Design Space

The first step of the method is to explore the dynamic multiobjective design space to evaluate and characterize the effects of each design variable on the dynamic objective space performance. In addition, as seen in Figure 9.2, in order to consider multiple system concepts over time to satisfy the future system needs, the expanded function of this step of the method requires the evaluation of a Dynamic s-Pareto Optimization Formulation as presented in Chapter 7. Noting that this dynamic formulation enables design variables, models, concepts, and constraints to change seamlessly, recall that as MOP formulations change, what was a design parameter in one formulation could be an inequality constraint in the next formulation. Thus, to avoid confusion, any variable, parameter, constraint, or objective associated with a design is termed a *design object* (see Section 7.2).

As described in the previous section, there also exists the need to incorporate uncertainty analysis into the method presented in this chapter. With this understanding, a generic dynamic multiobjective optimization problem capable of identifying the s-Pareto frontier for each time step [2], and incorporating anti-optimization is presented below.

Problem 9.1: Dynamic s-Pareto MOP Formulation with Anti-Optimization

$$\min_{k^{(t)}} \left\{ \min_{y^{(k^{(t)})}} \left\{ \mu_1^{(k^{(t)})}(x^{(k^{(t)})}),\ \ldots,\ \mu_{n_\mu^{(k^{(t)})}}^{(k^{(t)})}(x^{(k^{(t)})}) \right\} \ (n_\mu^{(k^{(t)})} \geq 2) \right\} \left\{ k = 1, \ldots, n_k^{(t)} \right\} \tag{9.1}$$

subject to:

$$y_{l,i}^{(k^{(t)})} \leq y_i^{(k^{(t)})} \leq y_{u,i}^{(k^{(t)})} \quad \{i = 1, \ldots, n_y^{(k^{(t)})}\} \tag{9.2}$$

$$g_{\max,j}^{(k^{(t)})} \leq 0 \quad \{j = 1, \ldots, 2n_z^{(k^{(t)})}\} \tag{9.3}$$

where:

$$\mu^{(k^{(t)})} = \chi^{(k^{(t)})} \cdot x^{(k^{(t)})} \tag{9.4}$$

$$\chi^{(k^{(t)})} = \begin{bmatrix} \chi_{1,1}^{(k^{(t)})} & \cdots & 0 \\ \vdots & \ddots & \vdots \\ 0 & \cdots & \chi_{n_x^{(k^{(t)})}, n_x^{(k^{(t)})}}^{(k^{(t)})} \end{bmatrix} \tag{9.5}$$

$$x^{(k^{(t)})} = \begin{bmatrix} y_1^{(k^{(t)})}, \ldots, y_{n_y^{(k^{(t)})}}^{(k^{(t)})}, z_1^{(k^{(t)})}(y^{(k^{(t)})}), \ldots \\ \ldots, z_{n_z^{(k^{(t)})}}^{(k^{(t)})}(y^{(k^{(t)})}) \end{bmatrix}^T \tag{9.6}$$

$$n_x^{(k^{(t)})} = n_y^{(k^{(t)})} + n_z^{(k^{(t)})} \tag{9.7}$$

where $x^{(t)}$ is a vector composed of independent ($y^{(k^{(t)})}$) and dependent ($z^{(k^{(t)})}$) design objects at time step t; and the objectives identifier matrix ($\chi^{(k^{(t)})}$) is a diagonal matrix for time step t satisfying the condition $\chi_{i,i}^{(k^{(t)})} = \{-1, 0, 1\}$; Note that $\mu_i^{(k^{(t)})}$ will be maximized or minimized for values of $\chi_{i,i}^{(k^{(t)})} = -1$ and $\chi_{i,i}^{(k^{(t)})} = 1$ respectively. In addition, the values of $g_{\max,j}^{(k^{(t)})}$ come from the following anti-optimization:

$$\max_{c^{(k^{(t)})}} \left\{ g_j^{(k^{(t)})}(y^{(k^{(t)})}, c^{(k^{(t)})}) \right\} \tag{9.8}$$

subject to:

$$h_v^{(k^{(t)})}(c^{(k^{(t)})}) \leq 0 \quad \{v = 1, ..., n_h^{(k^{(t)})}\} \tag{9.9}$$

where:

$$g_j^{(k^{(t)})} = \begin{cases} z_j^{(k^{(t)})}(y^{(k^{(t)})}, c^{(k^{(t)})}) - z_{u,j}^{(k^{(t)})} & , j \leq n_z^{(k^{(t)})} \\ -z_{j-n_z^{(k^{(t)})}}^{(k^{(t)})}(y^{(k^{(t)})}, c^{(k^{(t)})}) + z_{l,j-n_z^{(k^{(t)})}}^{(k^{(t)})} & , \text{else} \end{cases} \tag{9.10}$$

where $c^{(k^{(t)})}$ is a vector of uncertain parameters which reside in the domain defined by Equation 9.9. Note that for discrete representations of the s-Pareto frontier at each time step, the corresponding $x^{*(k^{(t)})}$ vector and corresponding $k^{(t)}$ for each discrete point are collected in the sets D_{x} and D_{k}. The mathematical definitions of these sets are: $D_{\mathrm{x}} := \{(x_1^{*(t)}, ..., x_{n_p^{(t)}}^{*(t)}) | \forall t \in (1, 2, ..., n_t)\}$ and $D_{\mathrm{k}} := \{(k_1^{*(t)}, ..., k_{n_p^{(t)}}^{*(t)}) | \forall t \in (1, 2, ..., n_t)\}$, where $n_p^{(t)}$ is the number of discrete s-Pareto points identified for the t-th time-step.

As described in Chapter 7, the bi-objective graphical result of Problem 9.1 (identification of the dynamic s-Pareto frontier) is illustrated in Figure 9.3.

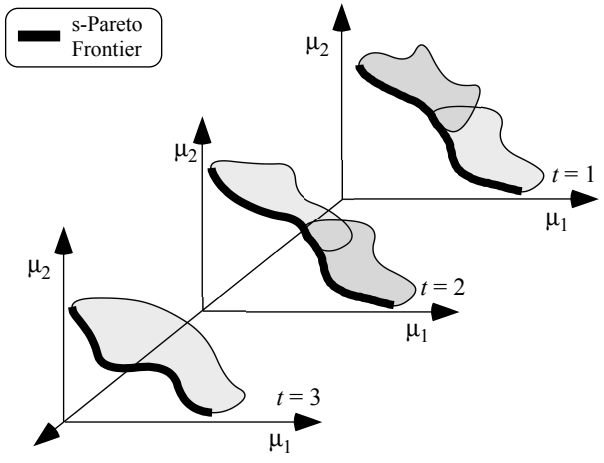

Figure 9.3: Graphical representation of a bi-objective dynamic s-Pareto frontier resulting from the evaluation of Problem 9.1 in Step A of the presented method

9.4 Step B: Define Anticipated Regions of Interest for each Time-Step

As with the method presented in Chapter 5 [80], a key idea of the method presented in this section is that changes in the desired system performance are equivalent to changes in the desired values of one or more design objectives. To that end, the second step of the method captures the predicted changes in system needs over time, and represents them as *Anticipated Regions of Interest* of the dynamic multiobjective design space, as illustrated in Figure 9.4. It is important to note that these regions represent predicted future needs regarding objective performance. To maintain simplicity in the graphical presentation of Figure 9.4, regions of interest involving only one objective (μ_1) are shown. However, as in Chapter 5, it is expected that regions of interested would be specified for as many of the objectives as desired.

As described in Section 9.1, the identification/use of current and predicted future preferences naturally introduces uncertainty in the bounds of the regions of interest identified in this step of the method. Whether statistical data or simple uncertainty bounds are known, it is suggested that at this stage in the method the bounds of the regions of interest be set to provide the largest possible regions. As a result, the upper bounds of each region of interest will be increased and the lower bounds decreased. The mitigation of the uncertainty in the bounds of the regions of interest will be addressed in the final step of the method where the designs of the modular product configurations are selected.

Although not represented in Figure 9.2, it should be observed that in some situations this step of the method may occur before the method begins. One situation where this could occur is when available products on the market have predefined the acceptable ranges of system performance that is desired. In these situations the anticipated regions of interest should be incorporated into the upper and lower design object limits ($x_u^{(k^{(t)})}$ and $x_l^{(k^{(t)})}$ respectively) implemented in the dynamic s-Pareto frontier formulation presented in Problem 9.1. In situations where this step occurs after the evaluation of Problem 9.1, all identified dynamic s-Pareto designs outside of the anticipated regions of interest and that do not satisfy Equation 9.3 are filtered out of D_{x} and D_{k} as shown in Figure 9.4.

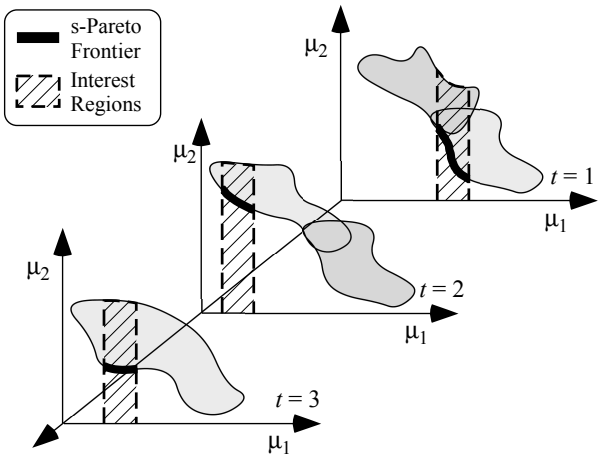

Figure 9.4: Graphical representation of theoretical anticipated regions of interest identified in Step B of the presented method

9.5 Step C: Determine the Desired Number of Modules and Modular Progression

The purpose of this step is to leverage the knowledge gained through the characterization of the dynamic multiobjective design space in Step A in determining the number of modules to be developed, and the desired modular progression of the system. In order to determine this progression requires that a *modular architecture type* [20,29] enabling the desired functionality of the platform and modules as a whole and *platform design target region of interest* be identified. In general, it is assumed that the platform target region corresponds to $t = 1$. However, the constrained module optimization formulation presented and evaluated in Step E is written to enable any region of interest to be selected as the platform target region.

The target result of this step of the method is the corresponding module progression matrix (δ) defining the intended module progression sequences. The definition and expected form of δ is provided below.

$$\delta = \begin{bmatrix} \alpha_0 & \beta_0 \\ \alpha_1 & \beta_1 \\ \vdots & \vdots \\ \alpha_{n_m} & \beta_{n_m} \end{bmatrix} \tag{9.11}$$

where the platform target region is identified by the values of α_0 and β_0 satisfying the condition $\beta_0 = \alpha_0$; and the values of α_i and β_i ($i > 0$) respectively refer to the starting and the ending regions

of interest that the i-th module is bridging (i.e., a module connecting regions of interest at times one and two in Figure 9.2 would correspond to a row entry of [1 2] in δ). It is noted that for the constrained module optimization formulation presented and evaluated in Step E (see Section 9.7), it is assumed that the values of β_i corresponding to each region of interest only appear once in the second column of δ.

9.6 Step D: Develop Concepts & Analysis Models for the Desired Platform and Modules

In the fourth step of the method, concepts and analysis models are developed for the platform and module designs that incorporate the selected modular architecture and facilitate the desired modular progression. An important aspect of these analysis models that is essential to the final step of the method is the characterization of the change in the overall system objective space performance obtained through the addition of each module. Another important goal of this step is to identify the set of modular-system design objects ($\hat{x}$) that define the platform ($\hat{x}^{(0)}$) and i-th modular configuration ($\hat{x}^{(i)}$).

9.7 Step E: Calculate the Optimal Values of the Modular-System Design Objects

The fifth step of the method implements an optimization routine to identify the values of the independent modular-system design objects ($\hat{y}$). The goal of this optimization for the system performance of the combined platform and modules is two-fold. The first is to minimize the distance/offset from the dynamic s-Pareto designs within each region of interest identified in the sets D_{x} and D_{k} ($\hat{\Theta}$). The second is to minimize functions that calculate a penalty value for configurations of the product that are within areas of the regions of interest where preference uncertainties exist ($\hat{\Lambda}$). Graphical illustrations of $\hat{\Theta}$ and $\hat{\Lambda}$ are provided in Figure 9.5.

Building on the dynamic formulation presented in Step A (see Section 9.3), the generic multiobjective optimization formulation identifying the optimal values of the modular-system design objects ($D_{\mathrm{m}} := \{(\hat{x}_1^{*(i)}, ..., \hat{x}_{n_x^{(i)}}^{*(i)}) | \forall i \in (0, 1, ..., n_{\mathrm{m}})\}$) is presented as below.

Problem 9.2: Dynamic s-Pareto Constrained Module MOP Formulation with Anti-Optimization

$$\min_{\hat{y}} \left\{ \hat{\Lambda}^{(i)}(\hat{\mu}^{(i)}, \hat{\mu}_l^{(i)}, \hat{\mu}_u^{(i)}, \hat{\mu}_{l,\mathrm{unc}}^{(i)}, \hat{\mu}_{u,\mathrm{unc}}^{(i)}), \hat{\Theta}^{(i)}(\hat{x}^{(i)}) \mid \forall i \in (0, 1, ..., n_{\mathrm{m}}) \right\} \tag{9.12}$$

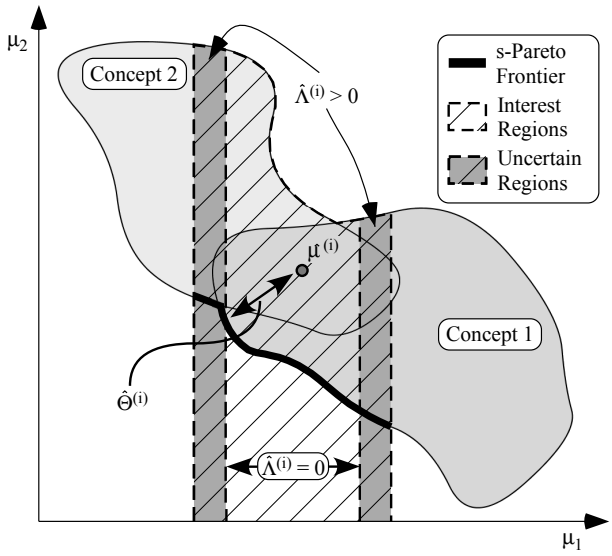

Figure 9.5: Graphical representation of the distance/offset from the dynamic s-Pareto designs within a region of interest ($\hat{\Theta}$), and the penalty function for configurations of the product that are within areas of the regions of interest where preference uncertainties exist ($\hat{\Lambda}$).

subject to:

$$\hat{y}_{l,q}^{(i)} \leq \hat{y}_{q}^{(i)} \leq \hat{y}_{u,q}^{(i)} \quad \{q = 1,...,n_{\hat{y}}^{(i)}\} \tag{9.13}$$

$$\hat{g}_{\max,j}^{(i)} \leq 0 \quad \{j = 1,...,2n_{\hat{z}}^{(i)}\} \tag{9.14}$$

where:

$$\hat{y} = \hat{y}^{(0)} \cup \hat{y}^{(1)} \cup ... \cup \hat{y}^{(n_{\mathrm{m}})} \tag{9.15}$$

$$\hat{\Theta}^{(i)} = \min\left(\left|\left|\mu_{v}^{*(\beta)} - \hat{\mu}^{(i)}\right|\right| \forall v \in \left\{1,...,n_{\mathrm{p}}^{(\beta)}\right\}\right) \tag{9.16}$$

$$\hat{\mu}^{(i)} = \hat{\chi}^{(i)} \cdot \hat{x}^{(i)} \tag{9.17}$$

$$\hat{x}^{(i)} = \left[\hat{y}_{1}^{(i)},...,\hat{y}_{n_{\hat{y}}^{(i)}}^{(i)},\hat{z}_{1}^{(i)}(\hat{y}^{(i)}),...,\hat{z}_{n_{\hat{z}}^{(i)}}^{(i)}(\hat{y}^{(i)})\right]^{T} \tag{9.18}$$

$$n_{\hat{x}}^{(i)} = n_{\hat{y}}^{(i)} + n_{\hat{z}}^{(i)} \tag{9.19}$$

$$\hat{\chi}^{(i)} = \begin{bmatrix} \hat{\chi}_{1,1}^{(i)} & \cdots & 0 \\ \vdots & \ddots & \vdots \\ 0 & \cdots & \hat{\chi}_{n_{\hat{\chi}}^{(i)},n_{\hat{x}}^{(i)}}^{(i)} \end{bmatrix} \tag{9.20}$$

$$\mu_v^{*(\beta)} = \left\{ \chi^{(k_v^{(\beta)})} \cdot x_v^{*(\beta)} \right\} \rightarrow \hat{\mu}^{(i)} \tag{9.21}$$

$$\alpha = \delta_{i,1} \tag{9.22}$$

$$\beta = \delta_{i,2} \tag{9.23}$$

where the values of $\hat{g}_{\max,j}^{(i)}$ come from the following anti-optimization:

$$\max_{\hat{c}^{(i)}} \left\{ \hat{g}_j^{(i)}(\hat{y}^{(i)}, \hat{c}^{(i)}) \right\} \tag{9.24}$$

subject to:

$$\hat{h}_v^{(i)}(\hat{c}^{(i)}) \leq 0 \quad \{v = 1, ..., n_{\hat{h}}^{(i)}\} \tag{9.25}$$

where:

$$\hat{g}_j^{(i)} = \begin{cases} \hat{z}_j^{(i)}(\hat{y}^{(i)}, \hat{c}^{(i)}) - \hat{z}_{u,j}^{(i)} & , \ j \leq n_{\hat{z}}^{(i)} \\ \hat{z}_{l,j-n_{\hat{z}}^{(i)}}^{(i)} - \hat{z}_{j-n_{\hat{z}}^{(i)}}^{(i)}(\hat{y}^{(i)}, \hat{c}^{(i)}) & , \text{ else} \end{cases} \tag{9.26}$$

where $\hat{c}^{(i)}$ is a vector of the i-th modular system configuration uncertain parameters which reside in the domain defined by Equation 9.25; D_{m} is the set of modular-system design object values ($\hat{x}^*$) for the platform ($i = 0$) and modular configurations ($i > 0$); the vector $\hat{\mu}^{(i)}$ represents the objective space performance of the i-th system configuration; $\hat{y}^{(i)}$ represents the values of independent design objects that characterize $\hat{\mu}^{(i)}$; $\hat{\mu}_{l/u}^{(i)}$ are the upper/lower bounds that characterize $\hat{\mu}^{(i)}$; $\hat{\mu}_{l/u,\text{unc}}^{(i)}$ are the upper/lower bounds within the regions of interest where the desirability of designs outside of these bounds is uncertain; $\hat{x}$ is a vector composed of independent ($\hat{y}^{(i)}$) and dependent ($\hat{z}^{(i)}$) design objects for the i-th system configuration; $\hat{\chi}^{(i)}$ is a diagonal matrix of objective identifiers for the i-th system configuration satisfying the condition $\hat{\chi}_{q,q}^{(i)} = \{-1, 0, 1\}$; the vector $\mu^{*(\beta)}$ characterizes the objective space performance of the target designs within the region of interest for time-step β mapped to ($\rightarrow$) $\hat{\mu}^{(i)}$; $\chi^{(k_v^{(\beta)})}$ is the diagonal, objective identifier matrix for concept k identified in Equation 9.5 of Problem 9.1 for the v-th s-Pareto design of time-step β; and $x_v^{*(\beta)}$ is the design object vector for the v-th s-Pareto design of time-step β contained in D_{x}. Note that the i-th module transitions the system from the system configuration in time-step α to time-step β.

It should be observed that Equation 9.12 will result in the identification of many modular-system candidates with varying values of $\hat{\Theta}$, $\hat{\Lambda}$, and the corresponding $\hat{\mu}$. Since the desired result

of this final step of the method is typically a single modular-system, Equation 9.12 will generally be replaced with an aggregate objective function similar in form to:

$$\min_{\hat{y}} J(\hat{\Theta}, \hat{\Lambda}, \hat{\mu}) \tag{9.27}$$

It should also be observed that Problem 9.2 does not provide a suggested form of the penalty function ($\hat{\Lambda}$) used in Equation 9.12. The form of the penalty function is not provided so as to allow a suitable penalty to be determined by the designer. An example form of $\hat{\Lambda}$ is provided in the following chapter through the presented example implementation of the method. The graphical results if this final step of the method are illustrated in Figure 9.6.

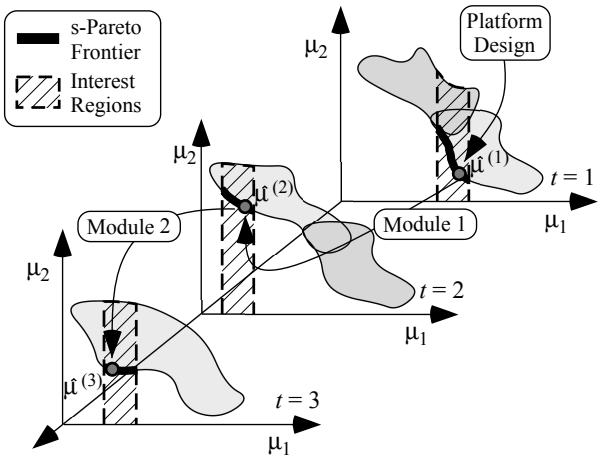

Figure 9.6: Graphical representation of the selection of a modular system with a minimized offset ($\hat{\Theta}^{(i)}$), and uncertain regions of interest penalty function ($\hat{\Lambda}$) for each system configuration.

With completion of the method, a product capable of adapting to changes in preferences, environments, concepts, and models through the addition of modules is achieved. In addition, each configuration of the product obtained through the addition of modules provides the optimal performance according to the objectives provided in Problems 9.1 and 9.2.

In the following chapter, a modular truss design problem is provided as an example of the implementation of the method described in this chapter.

CHAPTER 10. PHASE 4 EXAMPLE: MODULAR TRUSS DESIGN PROBLEM

This section implements the method presented in Section 9.2 using a simple truss example where it is assumed that the sources of change include material volume preferences, analysis models, concepts, and the operation environment. For this example the objectives being considered are to minimize the material volume (V) and the maximum stress ratio ($\bar{\sigma}_{\max} = \max(\sigma_{\max}/\sigma_{\text{allow}}, \sigma_{\max,\text{compression}}/\sigma_{\text{cr}})$.

10.1 Sources of Change & Model/Concept Descriptions

The source of the changing environment comes from the identification of three different loading conditions. These loading conditions, along with the concepts considered for each case are presented in Figure 10.1. Notice that for the first two loading conditions the concepts considered are the same, but due to changes in the directions of the applied loads the analysis models will be different. For all of the concepts presented in Figure 10.1, it is assumed that the truss members are circular tubes, and that the nominal diameter (d) of the truss members and base width (B) of the structures will be fixed values. In addition, the wall thickness (t_{w}) and structure height (H) will be treated as the independent design objects ($y^{(k^{(t)})}$) for all k and t.

A summary of each concept's design objects for $t = \{1,2,3\}$, along with the corresponding values of $\chi^{(k^{(t)})}$, $x_l^{(k^{(t)})}$, and $x_u^{(k^{(t)})}$ needed to evaluate Problem 9.2 are provided in Table 10.1. It should be noted that the bounds of the anticipated regions of interest as defined in Section 9.4 (Step B) are presented in Table 10.1 as the listed values of $V_l^{(k^{(t)})}$ and $V_u^{(k^{(t)})}$. In addition, for this example it is assumed the values of $y^{(k^{(t)})}$ have bounded uncertainties that result in the domain (h) of the uncertain parameters (c) being defined as $c_l^{(k^{(t)})} \leq c^{(k^{(t)})} \leq c_u^{(k^{(t)})}$. The values of $c_l^{(k^{(t)})}$ and $c_u^{(k^{(t)})}$ needed to evaluate Problem 9.1 are also provided in Table 10.1.

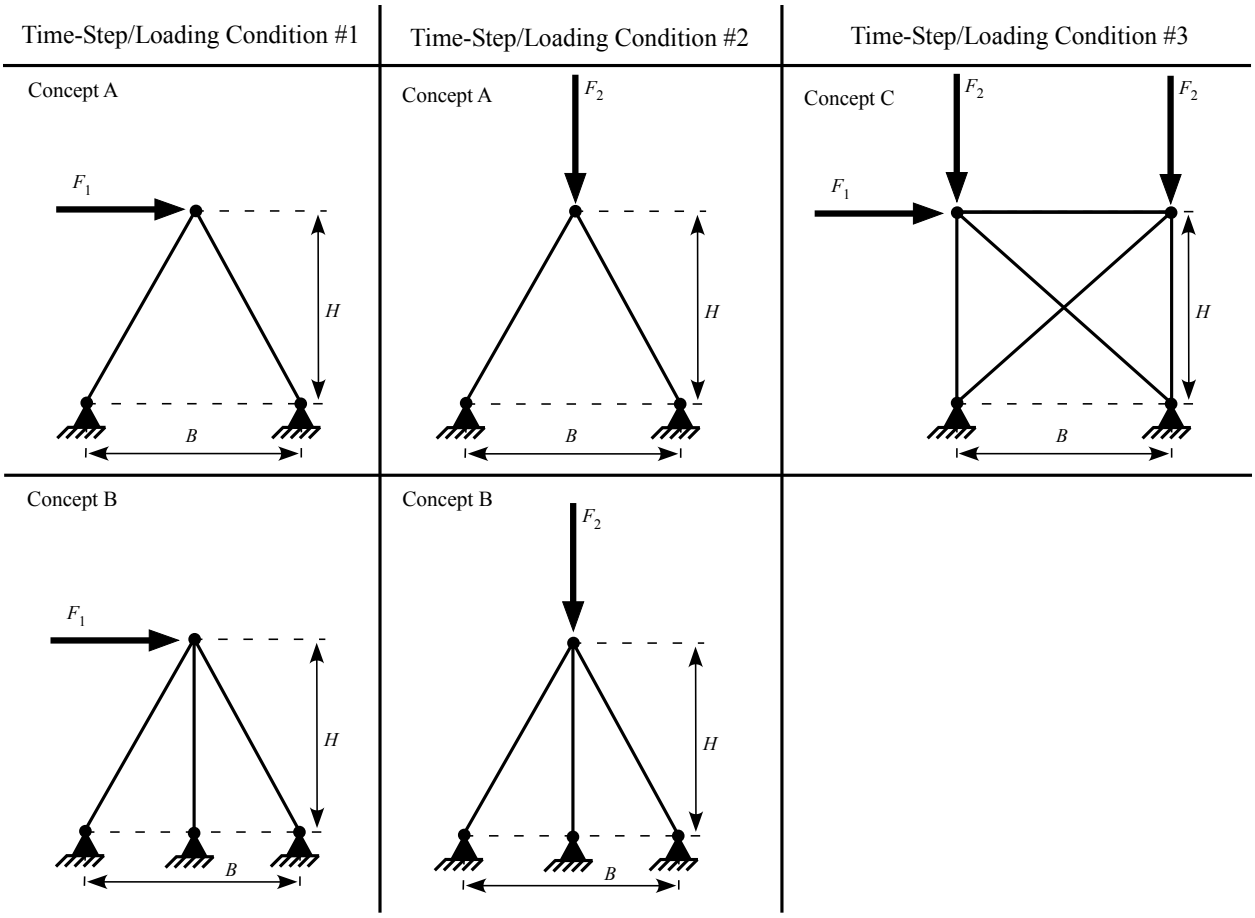

Figure 10.1: Summary of the loading conditions and considered concepts at each time-step

10.2 Method Implementation

Using a Plane Truss analysis program presented in Balling 2009 [68] and MATLAB's fmincon function, the dynamic s-Pareto frontier for each time step within the identified regions of interest was identified (see Figure 10.2). From Figure 10.2, it can be seen that due to the changes in loading conditions, concepts, and required analysis models, the s-Pareto frontier does indeed change over time.

At this point Steps A and B of the method are complete. In Step C, a Type II modular architecture [29] approach is selected, and the definitions of n_{m} and δ are as follows:

$$n_{\mathrm{m}} = 2 \tag{10.1}$$

Table 10.1: Values of the objective identifiers, design object, and uncertain parameter domain limits for the truss example

$k = 1,2$ and $t = 1$										
	H (in)	t_w (in)	B (in)	d (in)	E (kpsi)	σ_{allow} (kpsi)	F_1 (kips)	F_2 (kips)	$\bar{\sigma}_{max}$ (kpsi)	V (in^3)
χ	0	0	0	0	0	0	0	–	1	1
x_l	10	0.125	20	2	30000	90	50	–	0	25
x_u	100	0.5	20	2	30000	90	50	–	1	75
c_l	-0.1	-0.005	-0.1	-0.005	-20	-10	-2	–	–	–
c_u	0.1	0.005	0.1	0.01	20	10	3	–	–	–
$k = 1,2$ and $t = 2$										
	H (in)	t_w (in)	B (in)	d (in)	E (kpsi)	σ_{allow} (kpsi)	F_1 (kips)	F_2 (kips)	$\bar{\sigma}_{max}$ (kpsi)	V (in^3)
χ	0	0	0	0	0	0	–	0	1	1
x_l	10	0.125	20	2	30000	90	–	-80	0	100
x_u	100	0.5	20	2	30000	90	–	-80	1	175
c_l	-0.1	-0.005	-0.1	-0.005	-20	-10	–	3	–	–
c_u	0.1	0.005	0.1	0.01	20	10	–	-2	–	–
$k = 1$ and $t = 3$										
	H (in)	t_w (in)	B (in)	d (in)	E (kpsi)	σ_{allow} (kpsi)	F_1 (kips)	F_2 (kips)	$\bar{\sigma}_{max}$ (kpsi)	V (in^3)
χ	0	0	0	0	0	0	0	0	1	1
x_l	10	0.125	20	2	30000	90	50	-80	0	200
x_u	100	0.5	20	2	30000	90	50	-80	1	250
c_l	-0.1	-0.005	-0.1	-0.005	-20	-10	-2	3	–	–
c_u	0.1	0.005	0.1	0.01	20	10	3	-2	–	–

$$\delta = \begin{bmatrix} 1 & 1 \\ 1 & 2 \\ 2 & 3 \end{bmatrix} \tag{10.2}$$

Using this knowledge of the desired modular progression, the two modular-system concepts shown in Figure 10.3 were developed in Step D. The first concept (Figure 10.3(a)) uses a two-bar truss as the platform design, and then adds modules that convert the two-bar truss into the three-bar truss at $t = 2$, and the five-bar truss at $t = 3$ (referred to hereafter as the 2-3-5 concept). The second concept (Figure 10.3(b)) also uses the two-bar truss as the platform, but only adds modules

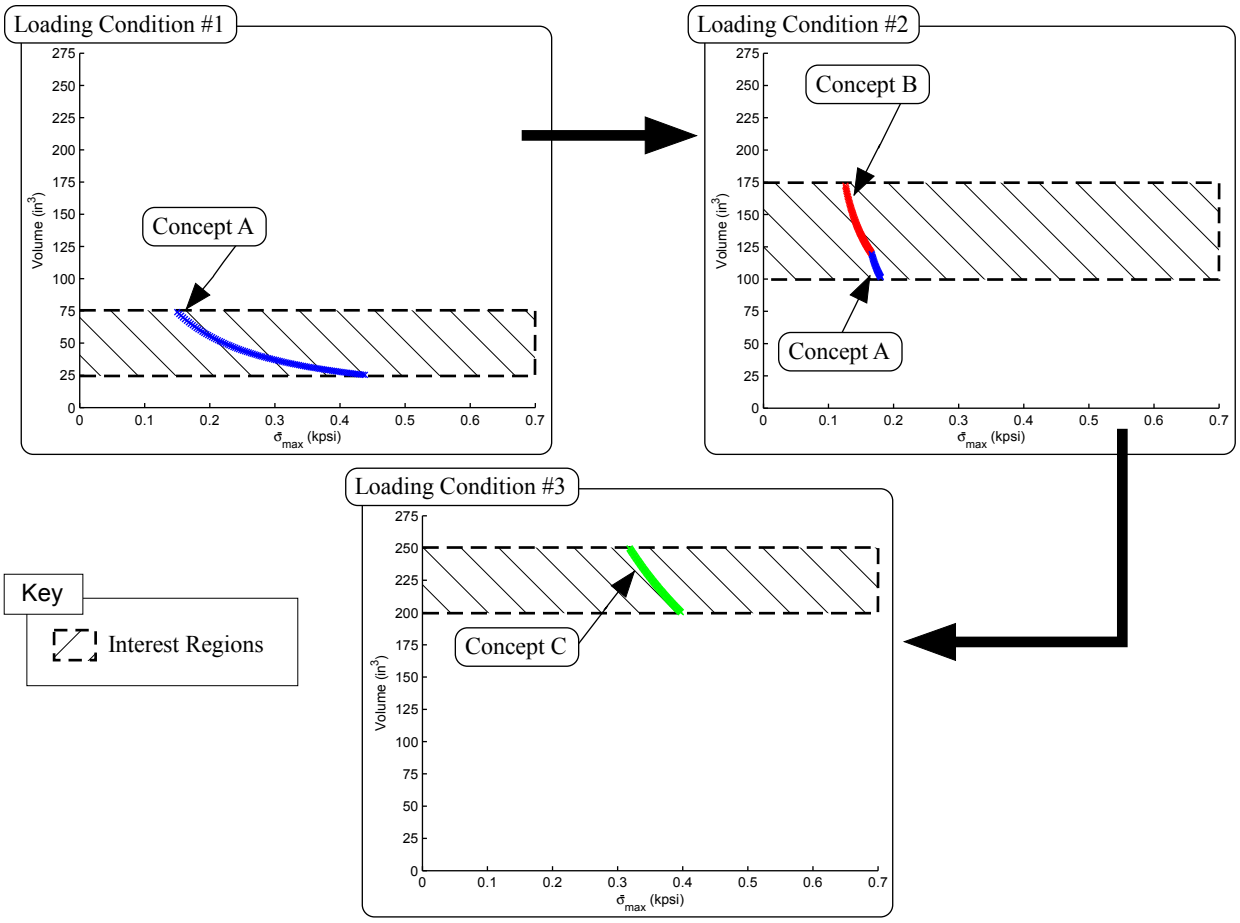

Figure 10.2: Representation of s-pareto frontier obtained for each time-step (loading condition) using MATLAB

to extend the lengths of the two-bar truss members at $t = 2$, and then converts the two-bar truss into the five-bar truss at $t = 3$ (referred to hereafter as the 2-2-5 concept).

In order to facilitate the identification of the modular system, and the creation of the needed analysis models of the platform and intended system configurations, the variables $\hat{t}_w$, $\hat{B}$, $\hat{d}$, $\hat{E}$, and $\hat{\bar{\sigma}}_{\text{allow}}$ were selected as the fixed independent module design objects for all product configurations ($\hat{y}$). In addition, the other independent module design objects for the i-th system configuration ($\hat{y}^{(i)}$) for the platform and two modules were identified as the height of the truss platform design (H_0), the additional structure height added by each module ($\Delta\hat{H}_1$ and $\Delta\hat{H}_2$ respectively), and the loads applied to each system configuration ($\hat{F}_1$ for the platform and second module, $\hat{F}_2$ for both modules).

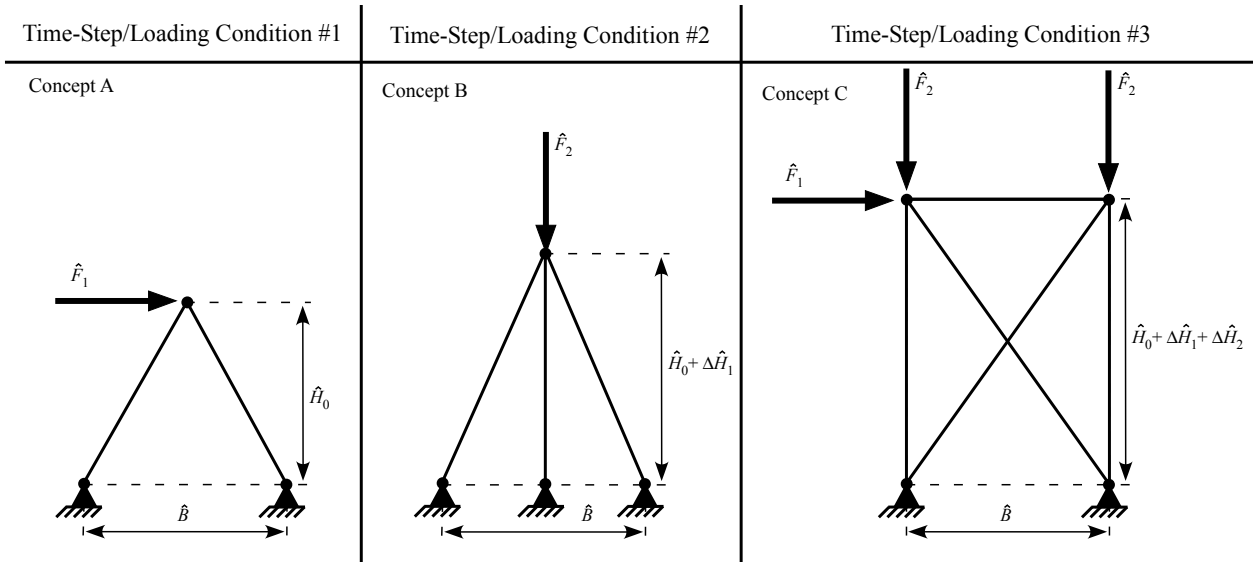

(a)

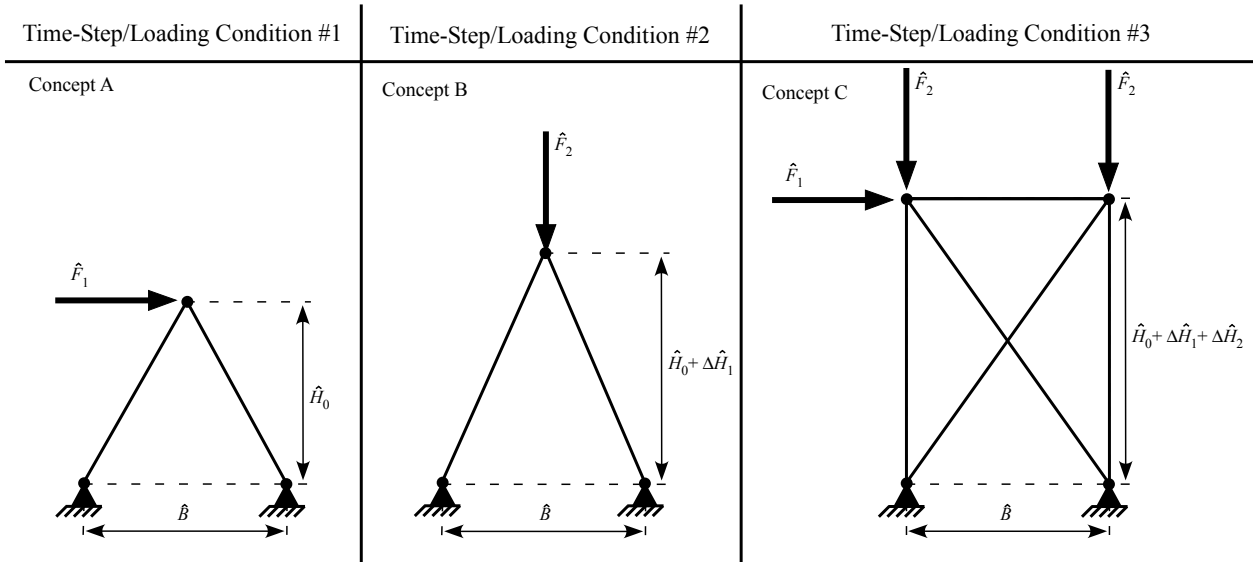

(b)

Figure 10.3: Illustrations of the two modular-system concepts developed in Step D of the method. (a) starts as a two-bar truss, and then becomes a three-bar and five-bar truss through module additions. Concept is referred to as the 2-3-5 concept. (b) starts as a two-bar truss, and then becomes two-bar (with longer members) and five-bar truss through module additions. Concept is referred to as the 2-2-5 concept.

The resulting upper and lower limits of the modular-system independent design objects ($\hat{y}_u$, and $\hat{y}_l$), and the corresponding upper and lower domain limit vectors of the modular-system uncertain parameters ($\hat{c}_u$ and $\hat{c}_l$) needed to evaluate Problem 9.2 are provided in Table 10.2. A summary of the dependent modular-system design objects ($\hat{z}^{(i)}$) for $i = \{0,1,2\}$, along with the values of $\hat{z}_u$,

$\hat{z}_l$, $\hat{\mu}_{l,\text{unc}}$, $\hat{\mu}_{u,\text{unc}}$, and the corresponding diagonal entries in $\hat{\chi}$ needed to evaluate Problem 9.2 are provided in Table 10.3.

Table 10.2: Values of $\hat{y}_l$, $\hat{y}_u$, $\hat{c}_l$, $\hat{c}_u$, and the corresponding diagonal entries in $\hat{\chi}$ for the modular truss concepts

	$\hat{t}_w$ (in)	$\hat{B}$ (in)	$\hat{d}$ (in)	$\hat{E}$ (kpsi)	$\hat{\sigma}_{\text{allow}}$ (kpsi)	$\hat{H}_0$ (in)	$\Delta\hat{H}_1$ (in)	$\Delta\hat{H}_2$ (in)	$\hat{F}_1$ (kips)	$\hat{F}_2$ (kips)
$\hat{\chi}$	0	0	0	0	0	0	0	0	0	0
$\hat{y}_l$	0.125	20	2	30000	90	10	0	0	50	-80
$\hat{y}_u$	0.5	20	2	30000	90	100	50	50	50	-80
$\hat{c}_l$	-0.005	-0.1	-0.005	-20	-10	-0.1	-0.05	-0.05	-2	3
$\hat{c}_u$	0.005	0.1	0.01	20	10	0.1	0.05	0.05	3	-2

Table 10.3: Values of $\hat{z}_u$, $\hat{z}_l$, $\hat{\mu}_{l,\text{unc}}$ (see Figure 10.4), $\hat{\mu}_{u,\text{unc}}$ (see Figure 10.4), and the corresponding diagonal entries in $\hat{\chi}$ for the modular truss concepts.

	System Platform ($i=0$)			Platform/Module 1 ($i=2$)			Platform/Modules 1 & 2 ($i=2$)		
	$\hat{\bar{\sigma}}^{(0)}_{\max}$ (kpsi)	$\hat{V}^{(0)}$ (in^3)	$\hat{\Theta}^{(0)}$	$\hat{\bar{\sigma}}^{(1)}_{\max}$ (kpsi)	$\hat{V}^{(1)}$ (in^3)	$\hat{\Theta}^{(1)}$	$\hat{\bar{\sigma}}^{(2)}_{\max}$ (kpsi)	$\hat{V}^{(2)}$ (in^3)	$\hat{\Theta}^{(2)}$
$\hat{\chi}^{(i)}$	1	1	–	1	1	–	1	1	–
$\hat{z}_l$	0	25	0	0	100	0	0	200	0
$\hat{z}_u$	1	75	∞	1	175	∞	1	250	∞
$\hat{\mu}^{(i)}_{l,\text{unc}}$	–	30	–	–	110	–	–	215	–
$\hat{\mu}^{(i)}_{u,\text{unc}}$	–	65	–	–	150	–	–	235	–

Analysis and optimization of the modular system was also performed using Balling's Plane Truss analysis program [68] and MATLAB's fmincon function. The optimization problem for Step E of the method was evaluated for both of the modular system concepts presented in Figure 10.3, and system concepts were selected using a weighted-sum aggregate objective function ($w_J = \{0.5, 0.5, 1\}$). The definition of this aggregate objective function, along with the penalty

function ($\hat{\Lambda}$) used to evaluate Problem 9.2 are provided below in Equations 10.3 and 10.4, respectively.

$$J(\hat{\Theta},\hat{\Lambda}) = \sum_{i=0}^{n_{\mathrm{m}}} w_J^{(i)} \cdot \left(\hat{\Theta}^{(i)} + \hat{\Lambda}^{(i)}\right) \tag{10.3}$$

$$\hat{\Lambda}^{(i)} = \begin{cases} 2 \cdot \left(1 - \left(\frac{\hat{V}^{(i)} - \hat{\mu}_{u,\mathrm{unc}}^{(i)}}{\hat{V}_u^{(i)} - \hat{\mu}_{u,\mathrm{unc}}^{(i)}} + 1\right)^{-1}\right) & , \hat{V}^{(i)} > \hat{\mu}_{u,\mathrm{unc}}^{(i)} \\ 2 \cdot \left(1 - \left(\frac{\hat{\mu}_{l,\mathrm{unc}}^{(i)} - \hat{V}^{(i)}}{\hat{\mu}_{l,\mathrm{unc}}^{(i)} - \hat{V}_l^{(i)}} + 1\right)^{-1}\right) & , \hat{V}^{(i)} < \hat{\mu}_{l,\mathrm{unc}}^{(i)} \\ 0 & , \text{else} \end{cases} \tag{10.4}$$

10.3 Results & Discussion

The objective space results for the two concepts are presented in Figure 10.4. From this figure it can be observed that although both selected modular-system designs are within the identified regions of interest, their performance in terms of $\hat{\Theta}$ and $\hat{\Lambda}$ are much different. Specifically, the 2-3-5 concept had and average $\hat{\Theta}$ and $\hat{\Lambda}$ of 0.0938 and 0 respectively, while for the 2-2-5 concept these averages were 0.2751 and 0.7302 respectively. From this it is determined that the 2-3-5 concept is the better solution due to the lower average $\hat{\Theta}$, and because none of the system configurations are within the uncertain areas of the regions of interest.

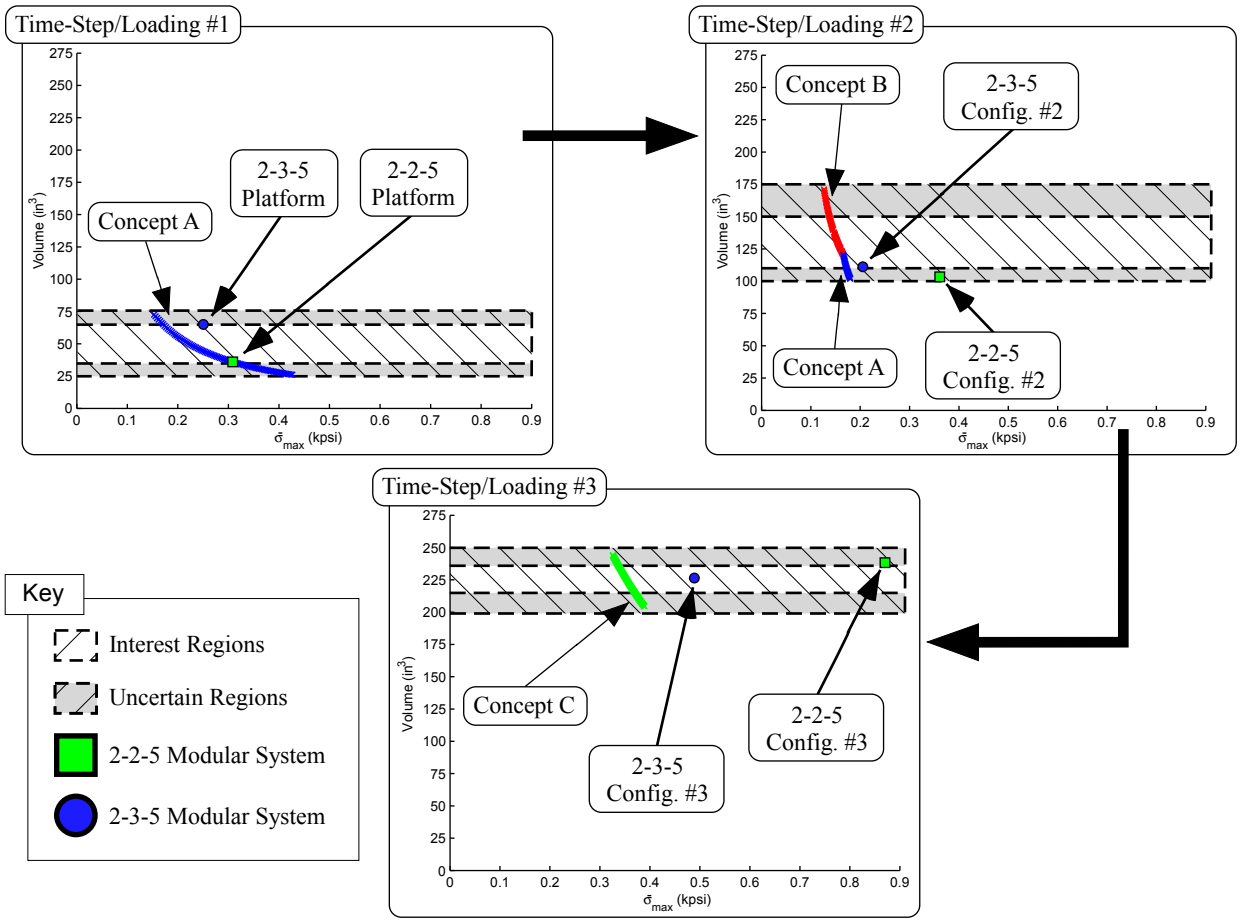

Figure 10.4: Representation of the s-pareto frontier obtained for each time step and the resulting modular systems for the 2-3-5 and 2-2-5 concepts using Matlab.

CHAPTER 11. UNIFYING DESIGN APPROACH

In this chapter, the modular product design method developments described in this dissertation, and the parallel research developments summarized in Chapter 2 are brought together through the identification of a four-step unifying design approach. Motivation for this contribution, as identified in Chapter 1, comes from the recognition that modular/adaptive products only represent one approach for dealing with changes in preferences, environments, models, and/or concepts. As such, this chapter connects the research presented in this dissertation with traditional product development processes, and enables the use of design methods that include, but are not limited to, the development of: (i) single non-modular/non-adjustable products; (ii) a series of related products that build on common platforms (platform-based modular products and product families); (iii) a series of related products that build on each other, with no specified platform (sectional and type II modular products); and (iv) reconfigurable/adjustable products that adapt to new scenarios through reconfiguration of product components, instead of the addition/subtraction of modules.

Figure 11.1 provides a flow chart that represents the four primary steps of the unifying design approach, and each of these steps is described below. Recognizing that the steps identified in Figure 11.1 are similar to steps from traditional product development processes [19, 20], the discussion provided in the following sections will focus on the considerations that are required to incorporate methods accounting for changes in preferences, environments, models, and/or concepts.

11.1 Identify an Opportunity

Product development, as defined by Krishnan and Ulrich [168], can be viewed as the transformation of a market opportunity into a product available for sale. As such, the first step of the approach presented in this chapter is to identify an opportunity. Although the topic of opportunity identification is not commonly discussed in engineering research, there exists a significant body

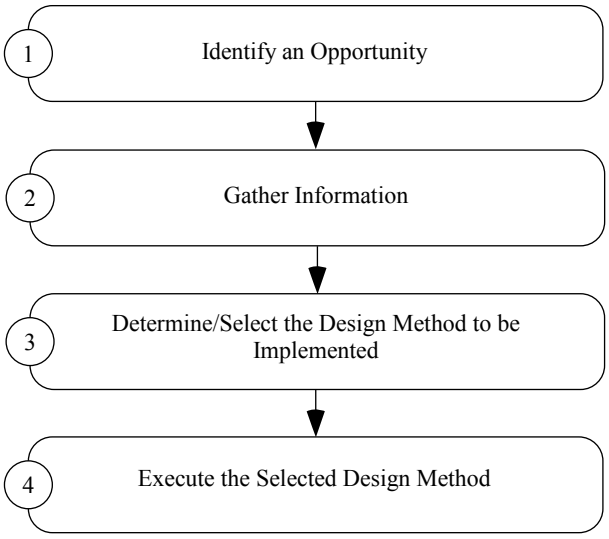

Figure 11.1: Flow chart describing the four-step unifying design approach developed in this chapter.

of research in the fields of technology management, technology innovation, and entrepreneurship focusing on the topic of opportunity recognition [169–175].

In light of the focus of this dissertation, this step is particularly targeting the recognition of opportunities due to changes in customer expectations, available technologies, and/or use environments [172]. The value of recognizing these opportunities is illustrated in the literature by the observed success of firms that were capable of adapting their products as these changes occurred [176]. As such, if it is assumed that these changes can be predicted – a key assumption of the research presented in this dissertation – it would also be assumed that this success could be improved by the ability to strategically plan for these changes instead of reacting to them as they occur.

Due to the use of these predicted changes to identify opportunities, a consideration that is of particular relevance in the context of this dissertation is determining whether pursuing the opportunity will result in a lasting/meaningful impact. Although this is not the research focus of this dissertation, potential methods/approaches that could be used to do this include, but are not limited to: (i) cognitive approaches that look at the stable cognitive qualities that entrepreneurs use to evaluate opportunities [173]; (ii) using past experiences to make connections and observe meaningful patterns [174]; (iii) observe attributes of successful opportunities within a given network [177]; and (iv) evaluation tools testing the assumptions of the identified opportunities [178].

11.2 Gather Information

Prior to the development of most successful products, unmet needs or desires are either observed or identified. Similarly, Ulrich and Eppinger [20] states that the ability to identify and quickly create low cost products that meet the needs of customers is directly related to the economic success of most firms. In terms of the research presented in this dissertation, the identification of needs is particularly focused on situations where the identified needs are predicted/known to be changing over time (i.e., gas mileage efficiency requirements of cars, power requirements of aircraft engines, etc.).

As mentioned in Chapter 3, there are a number of methods that exist for identifying needs (i.e., Interviews, Focus Groups, Observation, Surveys, Ethnography Studies, etc.) [20, 127, 179–181]. Recognizing the increased difficulty of identifying needs that are either predicted or known to change over time, two considerations of particular importance for designers are: (i) determining whether the identified needs are relevant and accurate; and (ii) determining whether sufficient information is gathered to make a decision in the next step of the unifying approach.

In terms of the relevance and accuracy of the needs, one method that could be used is to prioritize the needs with respect to their customer importance [182, 183]. Potential methods that are available for determining these priorities include subjective scoring by the development team, customer rating approaches, and conjoint analysis [184].

In order to determine whether sufficient information has been gathered, the development team should be able to answer "yes" to the following questions:

1. Are the changes in customer needs over the established time-intervals identified?

2. Are the number of desired product iterations/Configurations/variants identified?

It should also be noted that in situations where the identified target customers belong to a market that is unfamiliar to the development team, this step also includes the implementation of the principles identification method [5, 117] described in Section 2.5. The identification of these principles will also assist in interpreting the customer needs identified through this step.

11.3 Determine/Select the Design Method to be Implemented

Using the information related to the list of questions at the end of Step 2 above, the design method that will be implemented is selected. For each of the design method outcomes mentioned at the beginning of this chapter, guidelines/reasons for selecting each of them are provided below:

(i) Single non-modular/non-adjustable products – this method outcome is best suited for situations where the desire is to have one product with zero additional configurations that is designed to operate in multiple scenarios (see the research developments presented in Chapters 7-8);

(ii) Platform-based modular products – this method outcome is best suited for situations where the desire is to have a series of platform related product configurations that differ through the addition/subtraction of modules (see the research developments presented in Chapter 9);

(iii) Sectional and type II modular products (i.e., Collaborative products) – this method outcome is best suited for situations where the desire is to reduce the number of products required to achieve a given number of tasks. This is accomplished by having a set of two or more independently functional products that are capable of being reconfigured/adjusted to enable recombination as an additional product (see collaborative product design method described in Section 2.4).

(iv) Reconfigurable/adjustable products – this method outcome is also best suited for situations where the desire is to reduce the number of products required to achieve a given number of tasks. However, in this case the focus is to reduce the number of products to one. This is accomplished by having a single product that is capable of performing a variety of tasks by reconfiguring specific components of the product, instead of by adding/subtracting modules (i.e., multi-tools). Although each of the reconfigurable components could be considered modules, the idea here is that once the product is purchased, adaptation to different tasks is strictly through the reconfiguration of already present product components.

Although not illustrated in Figure 11.1, prior to moving to the final step of the unifying approach, and implementing the selected design method, the information gathered in the previous

step should be reviewed to verify that all needed information for proper execution of the selected design method has been identified. For example, if the modular product design method presented in Chapter 9 is selected, check that the bounds of the regions of interest have been identified. If any additional information is needed, then the team should return to Step 2 to obtain the needed information.

11.4 Execute the Selected Design Method

In the final step, the gathered information is used to execute the steps of the selected design method. Recognizing the potential that the resulting product(s) may not be successful, an important element of this step is determining if the decision to implement the selected method is a good or bad decision. In order to determine whether the selected method will be likely to result in a successful product, the development team should develop concepts appropriate to the selected method, and then be able to answer ”yes” to the following questions:

1. Do any of the concept solutions have the potential to meet the identified needs?

2. Are the characteristics and attributes of the design in agreement with the principles for the target market?

3. Do the identified needs have sufficient importance to merit the increased complexity of implementing the selected design approach?

In order to demonstrate the implementation of the design approach presented in this chapter, two case studies are presented. The first case study involves the development of a modular irrigation pump for developing countries (Chapter 12). The second case study involves the development of a modular plywood cart that is also intended for developing countries (Chapter 13).

CHAPTER 12. CASE STUDY: MANUAL IRRIGATION PUMP DESIGN

This chapter implements the design approach presented in Chapter 11 in the identification of a modular irrigation pump for developing countries. Background for the motivation and selection of this example is provided in Sections 12.1–12.3, followed by the implementation of the selected design method in Section 12.4. In Section 12.5, the predicted and measured pump performance is compared. Finally, improved optimization results are presented in Section 12.6 based on observations from the physical performance of the pump prototype.

12.1 Step 1: Identify an Opportunity

Over the past thirty years there have been notable advances in using engineering as a resource to address the challenges of poverty alleviation efforts [116]. Published literature has indicated that poverty alleviation approaches with the most measurable, and sustainable effect on poverty possess the following attributes:

- Foster self-sufficiency by increasing income [185–187]
- Create individual opportunities [186, 188]
- Offer choices [185, 186, 188]
- Encourage self-esteem [186, 188]

For example, there are some engineered products on the market today that have helped more than 17 million people to escape poverty by increasing their income [186, 189]. These results have served to strengthen the position of those who advocate that the best way to help people escape poverty is to provide them with a way to make more money [187, 190].

In considering that 75% of those individuals who are in extreme poverty are rural farmers [191], the ability to grow and irrigate additional crops during seasons of the year when there is little or no rain-fall would represent a potential means of increasing their income. As such, one

opportunity for helping these individuals is to enable them to more efficiently irrigate their crops during these seasons of the year.

12.2 Step 2: Gather Information

One of the most commonly implemented ways of irrigating crops during seasons of the year when there is little or no rain-fall is by pumping water from streams, wells, or other water sources [186, 187, 190]. Three successful irrigation pumps that are currently sold on the market today are represented in Figure 12.1 in terms of the measured water flow rate (in L/s) and sales price (in US dollars) of each pump.

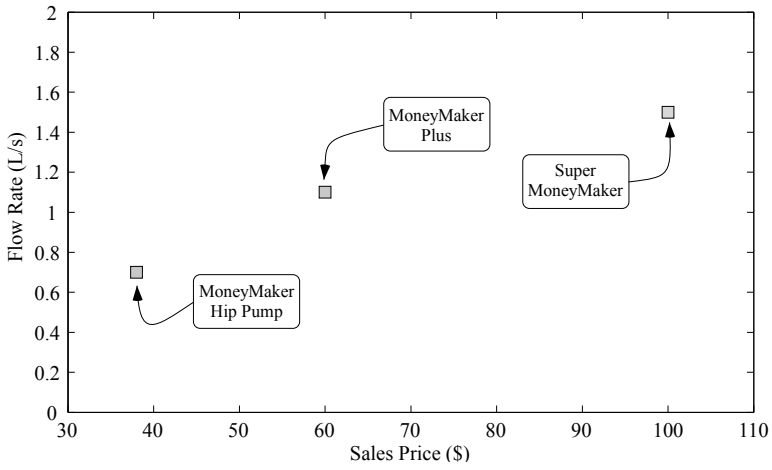

Figure 12.1: Graphical comparison of three non-modular water pumps that are currently sold on the market. The horizontal axis represents the sales price (S) in US dollars, and the vertical axis represents the potential water flow rate (Q) in liters per second [76].

The products represented in Figure 12.1 can be viewed as satisfying a range of what more than 12 million individuals have considered affordable [186]. Despite the measurable impact of these irrigation pumps, the large initial investment required to purchase many such products ($\sim$2-3 months income) has limited their distribution due to the financial risks involved if the product fails to produce additional income [185, 186, 192]. To overcome these financial risks and increase the use and distribution of these products, Lewis et al. 2010 [76] presented the concept of creating low cost modular products. In this situation, one notable advantage of a modular product is the ability to reduce the initial investment required to purchase a product. Furthermore, the income generated

through the initial purchase then serves as a means for financing future upgrades that are made affordable through use of the product.

For example, a modular irrigation pump could be purchased in a series of upgrades. The initial investment of the first platform would be smaller (on the order of the MoneyMaker Hip Pump), yet yield a modest increase in income. This income could then be used to finance the purchase of an add-on or module. This upgrade would then increase the pump performance and subsequently its income generating potential.

12.3 Step 3: Select a Design Method

It is noted that many of the challenges in designing income-generating products for those in extreme poverty could be viewed as conflicting design objectives (i.e., minimize cost, maximize income-generation potential, maximize efficiency, etc.). In addition, increases in income will result in changes in what individuals view as affordable, resulting in changes in the preferences that dictate the acceptable pump sales prices over time. As such, the research presented in this dissertation has direct application.

For this case study, uncertainties in model inputs, model outputs, and changes in preferences are ignored. In addition, there are three types of changes that are identified: (i) preferences; (ii) concepts; and (iii) operating environments. In considering this combination of changes, it can be observed from Table 7.1 that the optimization-based modular-product design method presented in Chapter 5 [80] can be used. In addition to the implementation of the method presented in Chapter 5, this case study will test the feasibility of creating modular income-generating products. This is accomplished by using the method to identify a *theoretical* modular irrigation pump design consisting of a platform and two modules. Using the theoretical results, a physical prototype of the pump was built and tested to validate both the analytical models used to optimize the theoretical design, and the concept of creating a physical product with the desired product configurations.

12.4 Step 4: Method Implementation in Identifying a Modular Irrigation Pump Design

The purpose of this section is to describe the theoretical and physical prototype pump design that resulted from implementing the modular design method presented in Chapter 5. The following

subsections provide analytical models required to evaluate Problems 5.1 and 5.2, followed by the development of a modular pump from the theoretical optimization results to a physical prototype.

12.4.1 Analytical Pump Models

Assuming that suitable objectives for this study are to *minimize* the pump sales price and *maximize* the pump flow rate (see Figure 12.1), this section presents the analytical models needed to evaluate Problems 5.1 and 5.2 and optimize these objectives. First, basic architectures for the analytical models of flow rate (Q) and sales price (S) were developed, and are presented in Figures 12.2 and 12.3 respectively for three pump concepts.

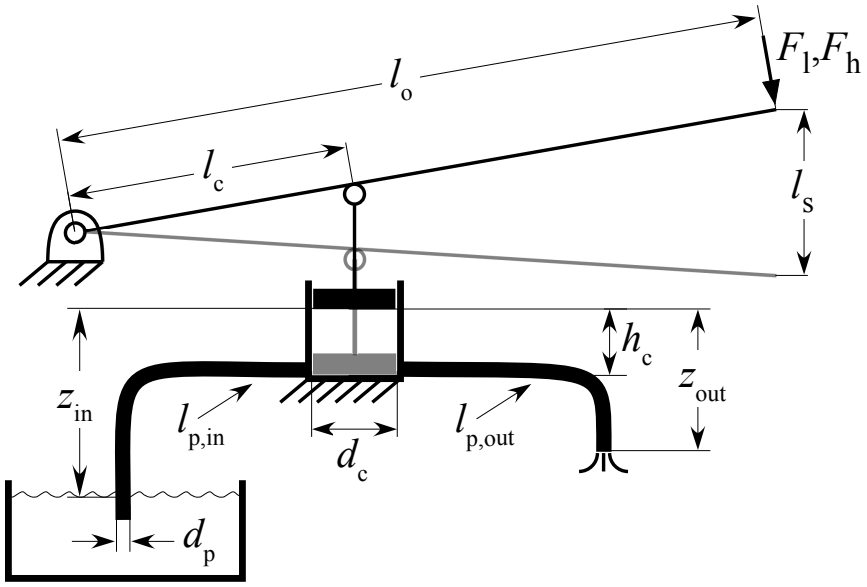

Figure 12.2: Graphical illustration of the basic pump architecture and loading conditions used in the development of the analytical pump fluid models of Q.

Descriptions of the variables and parameters shown in Figure 12.2, along with any other variables implemented in this case study are as follows:

l_o Distance from the pivot to the operator (m)

l_c Distance from the pivot to the pump cylinder (m)

l_c Distance from the pivot to the pump cylinder (m)

d_p Inner diameter of the inlet/outlet pipe (m)

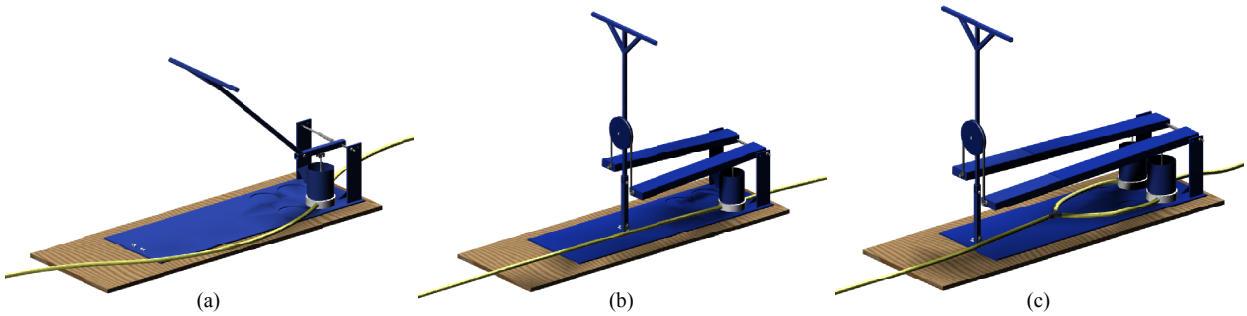

Figure 12.3: Renderings of 3D solid CAD models depicting the basic architectures for the analytical financial models of S described in this section.

d_c	Inner diameter of the piston cylinder (m)
h_c	Distance traveled by the cylinder piston head (m)
l_s	Length of the operator stroke (m)
$l_{p,in}$	Length of the inlet pipe (m)
$l_{p,out}$	Length of the outlet pipe (m)
z_{in}	Vertical distance from the pump to the water source (m)
z_{out}	Vertical distance from the pump to the pipe outlet (m)
F	Force applied by the operator during hand and leg operation of the pump (N)
$n_c^{(k)}$	number of cylinders in the k-th concept
φ	costs scaling factor
A_p	cross sectional flow area of the pipe (m^2)
A_c	cross sectional flow area of the cylinder (m^2)
m_w	mass of the water in the entire pumping system (kg)
ρ	density of water (kg/m^3)
g	gravitational constant (m/s^2)
h_L	head loss in the pump system
$f_{p/c}$	friction coefficients in the pipe (p) and piston cylinders (c) respectively
K_L	minor head loss coefficients from Munson et al [193]
F_{in}	force applied at the cylinder head (N)
V_p	average flow velocity in the pipes (m/s)
V_c	average flow velocity in the cylinders (m/s)

$\hat{Q}$ flow rate in the system assuming a constant flow (L/s)

t_s stroke time of the operator (s)

C_j manufacturing cost of the j-th component of the pump ($)

M_m manufacturing cost margin

M_d distributor cost margin

M_s sales cost margin

The mathematical definitions of Q and S are presented below using the variables identified in Figure 12.2, and the three physical architectures presented in Figure 12.3. Note that for each architecture presented in Figure 12.3, there is a corresponding model of Q and S indicated by the value of k in Equations 12.1-12.23 below, where $k = 1,2,3$ corresponds to Figure 12.3(a), Figure 12.3(b), and Figure 12.3(c) respectively.

Analytical Models of Flow Rate (Q) and Sales Price (S):

$$Q^{(k)} = \begin{cases} 0.5 \cdot \hat{Q} & , n_c = 1 \\ \hat{Q} & , \text{otherwise} \end{cases} \tag{12.1}$$

$$S^{(k)} = \left(\sum_{j=1}^{n_{comp}^{(k)}} C_j^{(k)} \right) \cdot \left(\frac{1 + M_m^{(k)} + M_d^{(k)} + M_s^{(k)}}{\varphi} \right) \tag{12.2}$$

with general fluid model equations:

$$n_c^{(k)} = \begin{cases} 1 & , k \leq 2 \\ 2 & , \text{else} \end{cases} \tag{12.3}$$

$$h_c = \left(\frac{l_c}{l_o} \right) \cdot l_s \tag{12.4}$$

$$A_p = \pi \cdot \frac{(d_p)^2}{4} \tag{12.5}$$

$$A_c = \pi \cdot \frac{(d_c)^2}{4} \tag{12.6}$$

$$m_w^{(k)} = \begin{cases} \rho \cdot (A_c \cdot h_c + A_p \cdot l_{p,in}) & , n_c^{(k)} = 1 \\ \rho \cdot (A_c \cdot h_c + A_p \cdot (l_{p,in} + l_{p,out})) & , \text{else} \end{cases} \tag{12.7}$$

$$h_{\text{L,major}}^{(k)} = \begin{cases} \frac{f_c \cdot h_c \cdot d_p^4}{(d_c)^5} + \frac{f_p \cdot l_{p,in}}{d_p} & , n_c^{(k)} = 1 \\ \frac{f_c \cdot h_c \cdot d_p^4}{(d_c)^5} + \frac{f_p \cdot (l_{p,in} + l_{p,out})}{d_p} & , \text{else} \end{cases} \tag{12.8}$$

$$h_{\text{L,minor}}^{(k)} = \begin{cases} K_{L,1} + K_{L,3} & , n_c^{(k)} = 1 \\ K_{L,1} + K_{L,2} + K_{L,3} & , \text{else} \end{cases} \tag{12.9}$$

$$K_{L,1} = 0.5 \tag{12.10}$$

$$K_{L,2} = 0.45 - 0.625 \cdot \left(\frac{d_p}{d_c}\right) \tag{12.11}$$

$$K_{L,3} = \left(1 - \frac{d_p}{d_c}\right)^2 \tag{12.12}$$

$$\lambda = 1 + h_{\text{L,major}}^{(k)} + h_{\text{L,minor}}^{(k)} \tag{12.13}$$

$$F_{in}^{(k)} = \eta \cdot \left(\frac{l_o}{l_c}\right) \left(\begin{cases} F_h & , k = 1 \\ F_l & , \text{else} \end{cases} \right) \tag{12.14}$$

$$V_p^{(k)} = \begin{cases} \sqrt{2 \cdot \left(\frac{F_{in}^{(k)} \cdot h_c}{\lambda \cdot m_w^{(k)}} + \frac{g}{\lambda} \cdot z_{in} \right)} & , n_c^{(k)} = 1 \\ \sqrt{2 \cdot \left(\frac{F_{in}^{(k)} \cdot h_c}{\lambda \cdot m_w^{(k)}} + \frac{g}{\lambda} \cdot (z_{in} - z_{out}) \right)} & , \text{else} \end{cases} \tag{12.15}$$

$$V_c = V_p^{(k)} \cdot \left(\frac{d_p}{d_c}\right)^2 \tag{12.16}$$

$$t_s = \frac{h_c}{V_c} \tag{12.17}$$

$$\hat{Q} = 1000 \cdot V_p \cdot A_p \tag{12.18}$$

with general financial model supporting equations:

$$C_{\text{pipe}} = (l_{p,in} + l_{p,out}) \cdot \psi_{p,w} \tag{12.19}$$

$$C_{\text{base}} = w_{pa} \cdot (l_o + 1.524) \cdot \psi_{\text{plank}} + w_{pa} \cdot \psi_{p,st} + (w_{pa} \cdot l_o + h_{\text{pivot}} \cdot 0.1524) \cdot \psi_{\text{plate}} \tag{12.20}$$

$$C_{\text{piston}}^{(k)} = \begin{array}{l} n_c^{(k)} \cdot (h_c + 0.03635) \cdot \psi_{\text{cyl}} + n_c^{(k)} \cdot \psi_{\text{valve}} \\ + n_c^{(k)} \cdot (0.8 \cdot A_c \cdot \psi_{\text{plate}} + \pi \cdot d_c \cdot \psi_{\text{seal}}) \end{array} \tag{12.21}$$

$$C_{\text{treadle}}^{(k)} = \begin{cases} 2 \cdot (l_o + 0.1524) \cdot \psi_{\text{tube}} & , k > 1 \\ 0 & , \text{else} \end{cases} \tag{12.22}$$

$$C_{\text{handle}} = \left(\sqrt{(l_o - l_c - 0.0762)^2 + (1.2192 - h_p)^2} + l_c^a + 0.0762 \right) \cdot \psi_{\text{tube}} \tag{12.23}$$

Table 12.1: Limits describing three anticipated regions of interest within the design space of flow rate (Q) and sales proce (S). Limit values, in terms of S and Q, for the i-th region are based on the performance of the MoneyMaker Hip Pump ($i = 1$), MoneyMaker Plus ($i = 2$), and the Super MoneyMaker ($i = 3$).

i	$S_{\min}$ (\$)	$S_{\max}$ (\$)	$Q_{\min}$ (L/s)	$Q_{\max}$ (L/s)
1	20	45	0.25	1.0
2	45	70	0.80	1.3
3	80	110	1.30	2.0

Note that the models of Q presented in Equations 12.1-12.18, were derived from the Energy Equation of the First Law of Thermodynamics as presented in Munson et al [193]. As such, assumptions made in the development of Equations 12.1-12.18 are as follows: (1) Frictional flow losses due to bends in the inlet/outlet pipes are ignored; (2) Water flow is always turbulent; (3) The corresponding friction coefficients for flow in the pump cylinder (f_{c}) and pipes (f_{p}) are approximated by the average friction value for the expected flow speeds and the ratios of the surface roughness (ε) to d_{p} and d_{c} respectively; (4) The force transmission efficiency of the pump (η) is constant and equal to 80%; (5) During *leg* operation of the pump, F_{l} is constant and equal to 889.6 N; (6) During *hand* operation of the pump, F_{h} is constant and equal to 70% of F_{l} (622.72 N); and (7) The design variable best suited as a platform for manufacturing a reconfigurable, modular irrigation pump is the piston cylinder diameter (d_{c}) .

12.4.2 Theoretical Pump Design

In this section the analytical models described above are implemented in the method presented in Chapter 5. Using the information provided in Figure 12.1, three anticipated regions of interest within the design space are developed as required by Step B of the optimization method. The limits describing the i-th anticipated regions of interest within the design space of Q and S are provided in Table 12.1, and are bounded around the indicated performance of the MoneyMaker Hip Pump ($i = 1$), MoneyMaker Plus ($i = 2$), and the Super MoneyMaker ($i = 3$).

It should be noted that some model input variables are naturally discrete – values for d_{c} could be constrained to standard sizes, and it is impossible to have non-integer values of n_{c}. Due

Table 12.2: Values of the limits and step sizes of the selected discrete model inputs.

Variable (units)	Lower Limit	Upper Limit	Step Size
l_o (m)	0.25	0.91	0.01
l_c (m)	0.17	0.25	0.01

Table 12.3: Values of the fixed model inputs.

Parameter (units)	Value	Parameter (units)	Value
g (m/s^2)	9.80665	ρ (kg/m^3)	1000
ε (m)	0.0015	η (%)	80
F_l (N)	889.6	F_h (N)	622.72
l_s (m)	0.3048	d_p (m)	0.0254
$l_{p,in}$ (m)	3.0	$l_{p,out}$ (m)	1.0
z_{in} (m)	-2.0	z_{out} (m)	-1.0
f_c	0.05	f_p	0.075
$t_{s,min}^{(k=1,2,3)}$ (s)	0.3	$t_{s,max}^{(k=1,2,3)}$ (s)	2.5
w_{pa} (m)	0.4064	h_{pivot} (m)	0.4
d_c (\$/m)	0.1023	ψ_{plank} (\$/m^3)	10.63
ψ_{plate} (\$/m^3)	201.50	ψ_{cyl} (\$/m)	105.12
ψ_{tube} (\$/m)	25.59	ψ_{seal} (\$/m)	2.89
$\psi_{p,w}$ (\$/m)	4.36	$\psi_{p,st}$ (\$/m)	6.30
ψ_{valve} (\$)	10	φ	4
$M_d^{(k=1,2,3)}$	5	$M_s^{(k=1,2,3)}$ (%)	3
$M_m^{(k=1,2,3)}$ (%)	25		

to the need to include discrete input variables in the optimization routines executed in the implemented optimization method, a multiobjective genetic algorithm was implemented. Although it is possible to have continuous input variables in genetic algorithms, all other model inputs are defined as either discrete or fixed variables in order to reduce the number of variable value combinations explored. The ranges and value step sizes of l_o and l_p are given in Table 12.2. In addition, the fixed values of the remaining model inputs are provided in Table 12.3.

From the values for $l_{\text{p,in}}$, $l_{\text{p,out}}$, z_{in}, and z_{out} presented in Table 12.3 it should be observed that the pump was being designed to pull water from a water source that is two meters below the pump, and then discharge it into a ditch or furrow one meter below the pump. The modular pump concept that resulted from implementing the method discussed in Chapter 5 is a hand-operated irrigation pump that transforms into a two-cylinder treadle irrigation pump through the addition of two modules. These modules are characterized by the following configuration descriptions: (1) Hand actuated with single cylinder, (2) Foot actuated with a single cylinder, and (3) Foot actuated with two cylinders. The variable values of the platform and module designs identified through the method are presented in Tables 12.4 and 12.5 respectively, where l_{t} is the length of the i-th treadle extension (m) and $\hat{n}_{\text{c}}$ is the number of cylinders added by the i-th module. A representation of the predicted flow rate and sales price for the three configurations of the pump are provided in Figure 12.4, along with the target pump designs from Figure 12.1.

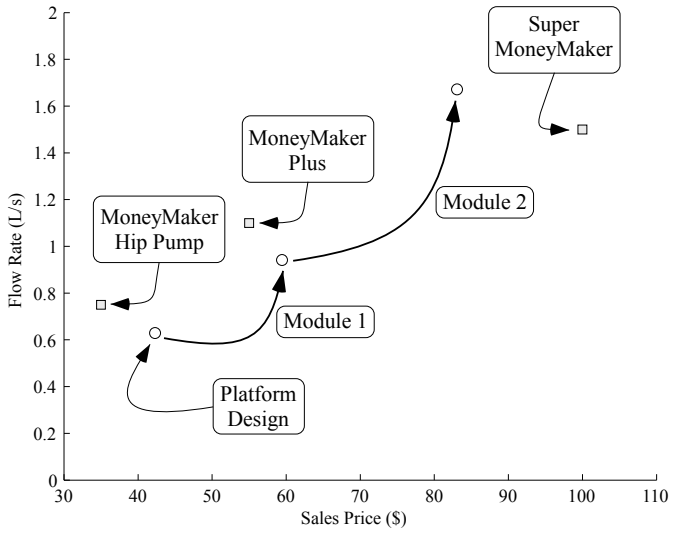

Figure 12.4: Graphical comparison of the predicted modular pump configurations and the three benchmark non-modular water pumps.

12.4.3 Physical Hardware

Using the optimization results presented in Tables 12.4 and 12.5, a physical prototype of the pump was created. The purpose of this subsection is to present the physical modular pump

Table 12.4: Variable and objective values of the platform pump design.

Variables			Objectives	
l_o (m)	l_c (m)	n_c (m)	Q (L/s)	S ($)
0.32	0.17	1	0.63	42.30

Table 12.5: Variable and objective values of the modular pump configurations obtained by adding the i-th module design.

	Variables			Objectives	
i	l_t (m)	l_c (m)	$\hat{n}_c$ (m)	Q (L/s)	S_m ($)
1	0.56	0.17	0	0.94	59.45
2	0.35	0.17	1	1.67	83.07

design and compare the actual dimensions and sales price (in US dollars) of the prototype to the optimization results from Section 12.4.2.

It should be noted that the optimization results from the previous subsection only provided the dimensions for key attributes of the modular pump (cylinder location, length of treadles/treadle extensions, etc.). This is because a conceptual stage model (not a detailed stage model) was used to optimize the design. In order to create a physical prototype of the optimal design, we developed a detailed concept of the pump design. This included defining (i) the shape of the pump support frame; (ii) the material and cross-section of the pump frame members, handle, and treadles; and (iii) the module interfaces for the handle, the single/double cylinder configurations of the pump pistons, and the frame/treadle extensions. Using the optimization results from the previous section, the physical prototype of the detailed pump concept was then built to match the identified key dimensions (see Tables 12.6 and 12.7). Figure 12.5 shows the physical prototype that was developed.

In order to facilitate the discussion of the theoretical and physical prototype pump performance in Section 12.5, the measurements of the key dimensions reported in Tables 12.4 and 12.5, along with the measured values of the operator stroke length (l_s) of each pump configuration are provided in Tables 12.6 and 12.7.

(a) (b) (c)

Figure 12.5: Three configurations of the modular irrigation pump prototype. The first configuration (a) is a hand operated single-cylinder pump indicated in blue. The second configuration (b) is a foot operated single-cylinder pump with the upgrade identified in yellow. The third configuration (c) is a foot operated dual-cylinder pump with the upgrade indicated in red.

Table 12.6: Variable values of the prototype platform pump design.

l_o (m)	l_c (m)	n_c (m)	l_s (m)
0.32	0.17	1	0.305

12.5 Physical & Theoretical Pump Performance Comparison & Observations

The purpose of this section is to describe the performance of the prototype pump. This discussion is divided into the following areas: (i) prototype performance in relation to the identified optimization objectives, and (ii) other observations about the performance of the pump not represented by those objectives.

Table 12.7: Variable values of the prototype modular pump configurations obtained by adding the i-th module design.

i	l_t (m)	l_c (m)	$\hat{n}_c$ (m)	l_s (m)
1	0.56	0.17	0	0.255
2	0.34	0.17	1	0.25

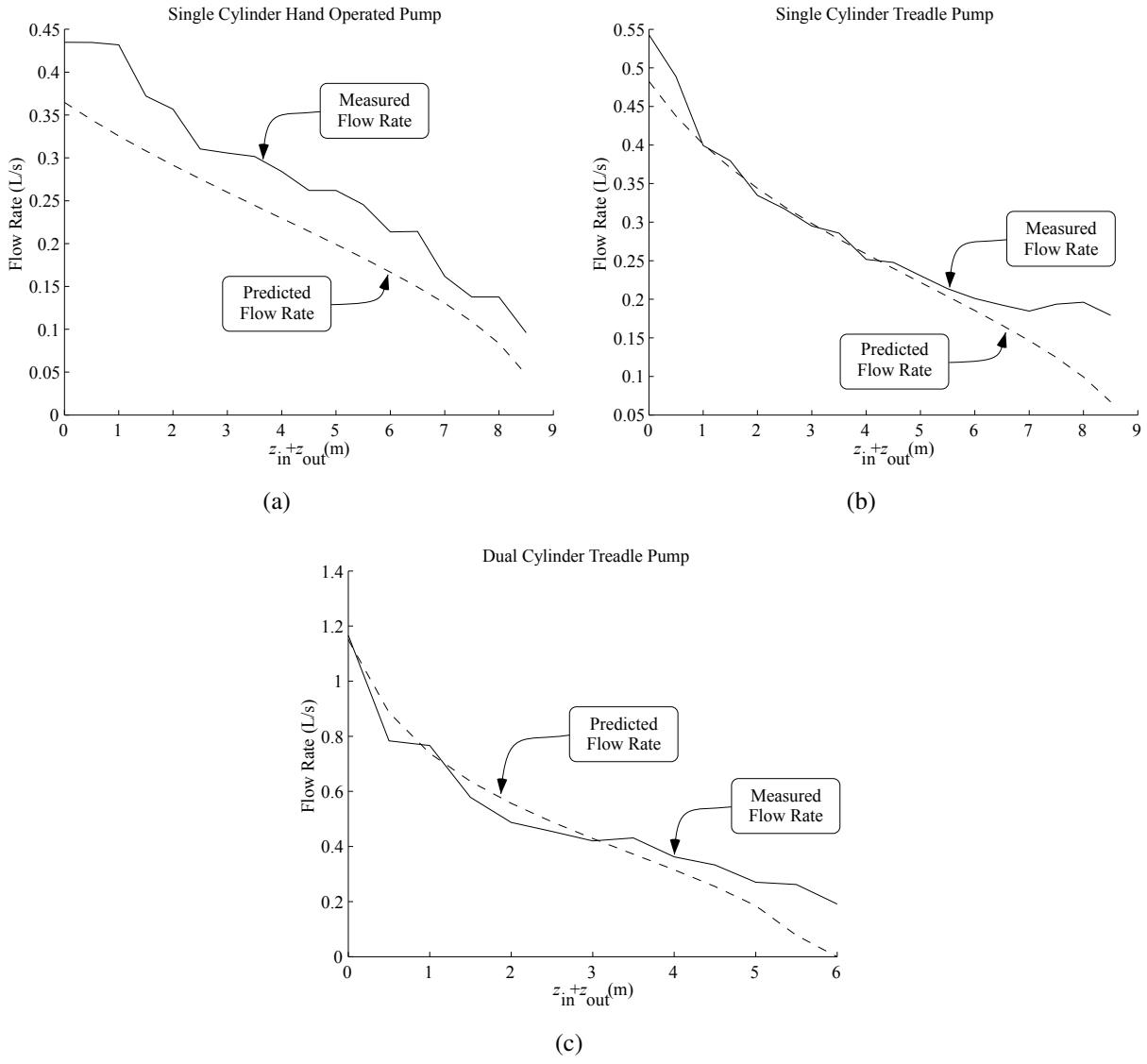

Figure 12.6: Comparison of the measured and predicted flow rate of the different configurations of the modular pump for values of z_{in} and z_{out} ranging from 0–4.25 meters (0–8.5 meters total elevation change between the inlet and outlet of the piping).

12.5.1 Performance: Optimization Objectives

As stated in Section 12.4.1, the selected optimization objectives were to minimize the sales price (S) and maximize the flow rate (Q) of the pump. As such, the measured and predicted values for Q and S of the pump platform and modules for the operating conditions used in the optimization method are presented in Table 12.8. From this table it can be seen that the measured S of the prototype, adjusted for assembly/production, is able to follow the same approximate trend

Table 12.8: Comparison of the measured ($[\,]_{\text{meas}}$) and predicted ($[\,]_{\text{pred}}$) sales price (S in US dollars) and flow rate (Q in L/s) of the pump platform ($i = 0$) and two modules ($i = 1, 2$).

i	Q_{meas} (\$)	Q_{pred} (\$)	S_{meas} (\$)	S_{pred} (\$)
0	$\sim$0.63	0.63	$\sim$40	42.30
1	$\sim$0.84	0.94	$\sim$20	17.15
2	$\sim$1.35	1.67	$\sim$25	23.62

predicted by the optimization. However, the measured and predicted flow rate for the prototype and theoretical design have errors starting at $\sim$0% error and ending at 19% error. Causes of this increasing error in the measured flow rate (Q_{meas}) between different pump configurations are likely due to: (i) pressure losses in the pistons from air leaking around the piston head, and (ii) differences between the assumed and measured operator stroke lengths (l_{s}) presented in Tables 12.3, 12.6, and 12.7.

In order to better determine the validity and accuracy of the analytical flow rate models, each configuration of the pump was also tested for values of z_{in} and z_{out} ranging from 0–4.25 meters (0–8.5 meters total elevation change between the inlet and outlet of the piping). In all, the hand operated and single cylinder treadle pump configurations were tested at eighteen combinations of z_{in} and z_{out}, and the dual cylinder treadle pump configuration was tested at thirteen combinations. The results of these tests in terms of the measured flow rate of the pump are presented in Figure 12.6. Also included in this figure is the predicted flow rate of the pump for the specified values of z_{in} and z_{out}, along with the values of l_{o}, l_{c}, n_{c}, l_{s}, and l_{t} presented in Tables 12.6 and 12.7. As indicated in Figure 12.6, the measured flow rate of the physical prototype is represented by the solid lines, and the predicted flow rate is represented by the dashed lines.

From the results in Figure 12.6(a), it can be seen that the platform pump design recorded a higher flow rate than that predicted by the analytical fluid model. Based on these results, the average difference between the measured and predicted flow rate for this configuration of the pump is 0.06 L/s. Similarly, for the plots provided in Figures 12.6(b) and (c), the average difference between the measured and predicted flow rate for the single and dual cylinder treadle pump configurations are 0.03 and 0.08 L/s respectively.

It is noted that there is a difference in the maximum flow rate values shown in Figure 12.6 compared to those shown in Figure 12.4. This is due to the setup required to perform the tests recorded in Figure 12.6. One example of changes in the setup that were not included in the execution of the optimization routines are 50 meter hoses used to draw the water from 4 meters and push it up to 4 meters. As a result, in the 100 meters of hose, there were additional losses in the system that were not considered in the previous optimizations. However, from the discussion of the differences between the predicted and measured flow rate of the pump, the models can still be used in the future to improve the optimization results, and subsequent pump performance to provide an overall better design for people living in poverty.

12.5.2 Performance: Additional Observations

Recall that the method described in Chapter 5 was used to determine the values of the key design variables. When developing concepts of how to make the pump with the desired modules, several challenges were encountered. In the original architectures shown in Figure 12.3, and in the early modular concepts that were considered, the cylinders were aligned below the treadles with the user unsafely positioned higher off the ground. An example of one of these modular concepts is provided in Figure 12.7. In order to keep the user as close to the ground as possible, the design was changed and the cylinders were repositioned above the treadles as shown in Figure 12.5. An unanticipated result of repositioning the cylinders with the pistons facing down was a loss in the efficiency of the piston seal that resulted in leaking. Unfortunately, this was not observed as a problem until tests were run trying to pull/push water more than two meters below/above the pump.

Due to the inherent physical exertion that is required to operate the pump, the physical endurance of the person operating the pump is an important issue. For the optimization results in Section 12.4.2, a constraint is used that limits the minimum time to complete a single pump stroke to 0.3 seconds, and was intended to address this issue. However, during the pump testing described in the previous subsection, it became clear that the physical endurance of the pump operator was not adequately considered and represented in the implemented optimization routine. Due to the number of strokes required to achieve the flow rate data and the subsequent results

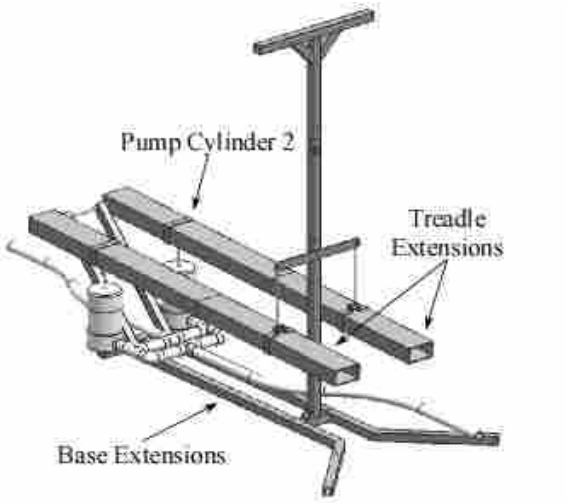

Figure 12.7: CAD model of one of the modular concepts showing the cylinders aligned below the treadles.

shown in Figure 12.6, it would not be physically sustainable for an extended period of time while using the dual-cylinder foot-operated pump configuration.

The major cause for this result stems from the evaluation of the flow rate (Q) in L/s. In the presented evaluations of Q in Equations 12.1-12.18 for the different pump configurations, the optimization searches for designs that result in the fastest L/s flow rate of water during a single stroke of the pump. As a result, the optimization increased the length of the treadles in order to increase the force applied to the piston head. However, without considering the amount/volume of water moving through the system over an extended period of time, the increased treadle lengths resulted in shorter strokes in the pistons. This in turn required the user to increase the number of strokes needed to move the same volume of water in a given time interval.

12.6 Prototype Informed Optimization Improvements & Results

The purpose of this section is to provide suggested improvements to the design of the modular pump. This includes (i) detailing changes to the optimization method inputs based on the observations and results presented in Section 12.5, and (ii) presenting the results of the improved optimization.

Table 12.9: Updated values of the fixed model inputs.

Parameter (units)	Value	Parameter (units)	Value
$l_{s,min}$ (m)	0.1524	$l_{s,max}$ (m)	0.4572
h_c (m)	0.1524	t_l (s)	0.1
φ	3.75	$M_m^{(k=1)}$ (%)	15
$M_m^{(k=2)}$	25	$M_m^{(k=3)}$ (%)	60
$t_{s,min}^{(k=1,2,3)}$ (s)	0.3	$t_{s,max}^{(k=1,2,3)}$ (s)	2.5

12.6.1 Optimization Model & Input Changes

Based on the results and observations presented in Section 12.5, changes to the optimization focus on the selected formulation of the optimization flow rate (Q) objective, and the model inputs used to optimize the modular pump configurations. As described in Section 12.5.2, by only considering the L/s flow rate of water during a single stroke, the optimization resulted in designs with small, fast piston strokes. To solve this problem the evaluation of Q was changed from considering the L/s of a single stroke, to the L/8-hr-day potential of the pump assuming the pump is used for 8 hours per day. Also, the length of the piston stroke (h_c) previously calculated in Equation 12.4, was changed to a model input. This required that the operator stroke length (l_s) be calculated and constrained to reasonable values. The values of h_c, and the upper/lower limits of l_s are provided in Table 12.9.

The new measure of Q and the calculation of l_s is obtained by respectively replacing Equations 12.18 and 12.4 with Equations 12.24 and 12.25 below.

$$\hat{Q} = \frac{1000 \cdot h_c \cdot A_c \cdot 8 \cdot 60^2}{t_s + t_l} \tag{12.24}$$

$$l_s = \left(\frac{l_o}{l_c}\right) \cdot h_c \tag{12.25}$$

where t_l is the pump operator's lag time between piston strokes. The assumed value of t_l is provided in Table 12.9.

Table 12.10: Updated values of the limits and step sizes of the selected discrete model inputs.

Variable (units)	Lower Limit	Upper Limit	Step Size
l_o (m)	0.25	.65	0.01
l_c (m)	0.15	0.2	0.01

To further improve the optimization results, and better reflect the costs associated with manufacturing the pump, the manufacturing margin (M_m) for each financial analysis model ($k = 1,2,3$) and the cost scaling factor (φ) were also changed. The updated values of M_m and φ for each pump configuration are provided in Table 12.9. Note that the initial ($k = 1$) value of M_m is lower then the value presented in Table 12.3. This was done to encourage individuals to purchase the initial pump. However, in order to ensure that making the pump would still be profitable for the manufacturer, the final value of M_m ($k = 3$) was set to result in an average M_m of 33%.

The only other changes to the model inputs for the optimization method were the upper/lower limits of the operator stroke time (t_s) for the hand operated pump ($k = 1$), the horizontal distance from the pivot to the operator (l_o), and from the pivot the pump cylinder (l_c). The limits for l_o and l_c are presented in Table 12.10, and were set to further focus the optimization algorithm on designs with increased flow rates as calculated in Equation 12.24. The new value of t_s for the hand operated pump was set to better reflect the speed that the operator can perform a stroke, and is provided in Table 12.9.

12.6.2 Optimization Results

In this section the optimization model and input changes described above are implemented in the method presented in Chapter 5 to identify an improved modular pump design. The new variable values of the platform and module designs identified through the method are presented in Tables 12.11 and 12.12 respectively. As in Section 12.4.2, l_t is the length of the i-th treadle extension (m) and $\hat{n}_c$ is the number of cylinders added by the i-th module. A representation of the predicted flow rate (L/8-hr-day) and sales price ($) for the three configurations of the pump are provided in Figure 12.8, along with the original theoretical optimization results and target pump

Table 12.11: Improved optimization variable and objective values of the platform pump design.

Variables			Objectives	
l_o (m)	l_c (m)	n_c	Q (L/8-hr-day)	S ($)
0.32	0.15	1	1.6681×10^4	40.82

Table 12.12: Variable and objective values of the modular pump configurations obtained by adding the i-th module design.

i	Variables			Objectives	
	l_t (m)	l_c (m)	$\hat{n}_c$	Q (L/8-hr-day)	S_m ($)
1	0.33	0.15	0	2.1278×10^4	53.05
2	0.14	0.15	1	4.4215×10^4	85.79

designs from Figure 12.4. Note that the presented flow rate values of the original optimization were obtained using Equation 12.24 as described in the previous subsection.

From the graphical results illustrated in Figure 12.8 and presented in Tables 12.11 and 12.12, it can be seen that the current optimization has improved the design in two ways. First, the sales price of the hand-operated (platform) and single-cylinder foot-operated pumps have respectively decreased by $\sim$4% and $\sim$11%, while maintaining approximately the same flow rate as the original optimization results. Second, the flow rate (L/8-hr-day) of the dual-cylinder foot-operated pump has increased by $\sim$25% of the original optimization results, while only increasing the predicted sales price by $\sim$3%.

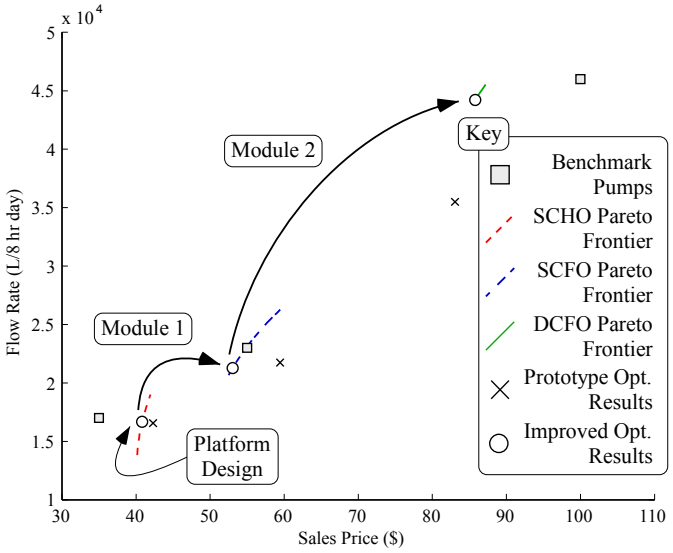

Figure 12.8: Graphical representation of the improved (○) and original prototype (×) optimization results for the modular pump configurations and the three benchmark non-modular water pumps. The Pareto frontiers corresponding to the single-cylinder hand-operated (SCHO), single-cylinder foot-operated (SCFO), and dual-cylinder foot-operated (DCFO) pump configurations are also illustrated.

CHAPTER 13. MODULAR PLYWOOD CART CASE STUDY

This chapter implements the unifying design approach presented in Chapter 11 in the identification of a modular plywood cart system for developing countries. Background for the motivation and selection of this example is provided in Sections 13.1–13.3, followed by the implementation of the selected design method in Section 13.4.

13.1 Step 1: Identify an Opportunity

As noted in Section 12.1, 75% of those individuals who are in extreme poverty are rural farmers [191]. As such, the ability to transport goods more efficiently would represent a potential means of increasing their income. In addition to these individuals, others could also benefit from the ability to obtain an inexpensive means of transporting goods and other cargo.

13.2 Step 2: Gather Information

One of the most commonly implemented ways for those in poverty to transport large quantities of goods is by using a human or animal drawn cart. Noting that increases in income will result in changes in what individuals view as affordable, preferences dictating the acceptable sales prices of carts for various cargo types/capacity will also change over time. In addition, the other sources of change for this case study include the cart structure analysis models and concepts due to various load scenarios (i.e., operation environments). These load scenarios come from the identification of three different types of cargo. A description of these cargo types are provided below.

(1) *Stackable Cargo:* This cargo is characterized by objects that can be stacked or placed next to each other, and only require a tie-down (i.e., rope or other lashing) to secure the cargo onto the cart. Examples of this cargo type include bricks, buckets, barrels, boxes, etc.

(2) *Low Density Non-Stackable Cargo:* This cargo is characterized by objects that are low in density, and can only be stacked if there is a structural aspect of the cart to contain the cargo within the boundaries of the cart bed (sides). Examples of this cargo type include foam, straw, clothing, etc.

(3) *High Density Non-Stackable Cargo:* This cargo is characterized by objects that are high in density, and again require a structural aspect of the cart to contain the cargo within the boundaries of the cart bed. Examples of this cargo type include soil, gravel, fresh produce, etc.

13.3 Step 3: Select a Design Method

In light of the focus of this dissertation, and the observed opportunity described above, the optimization-based modular-product design method presented in Chapter 9 [87] is used in this case study in the identification of a modular plywood cart. In order to identify a starting/reference point for the development of the modular cart system, Figure 13.1 presents non-modular concept plywood cart designs providing the structural elements identified in the cargo type definitions. The time sequence that these concepts are assumed to be desired, based on the relative costs of the concepts, is also illustrated in the figure by the assignment of $t = 1, 2, 3$ to the stackable cargo (Concept A – Flatbed Cart), low density non-stackable cargo (Concept B – Poles w/Cloth Sides Cart, Concept C – Wood Slats w/Cloth Sides Cart), and high density non-stackable cargo (Concept D – Wood Sided Cart) type concepts, respectively.

13.4 Step 4: Method Implementation in Identifying a Modular Plywood Cart

With a knowledge of the various cargo types and cart concepts being considered, the results and necessary information for implementation of the method presented in Chapter 9 are now provided.

Method Steps A & B: For this example the objectives being considered are to minimize the sales price (S) and to maximize the cart bed area or volumetric capacity (A and V respectively), depending on whether or not the concept has sides. In order to characterize the dynamic multiobjective design space, analysis models for each of the identified cart concepts are needed.

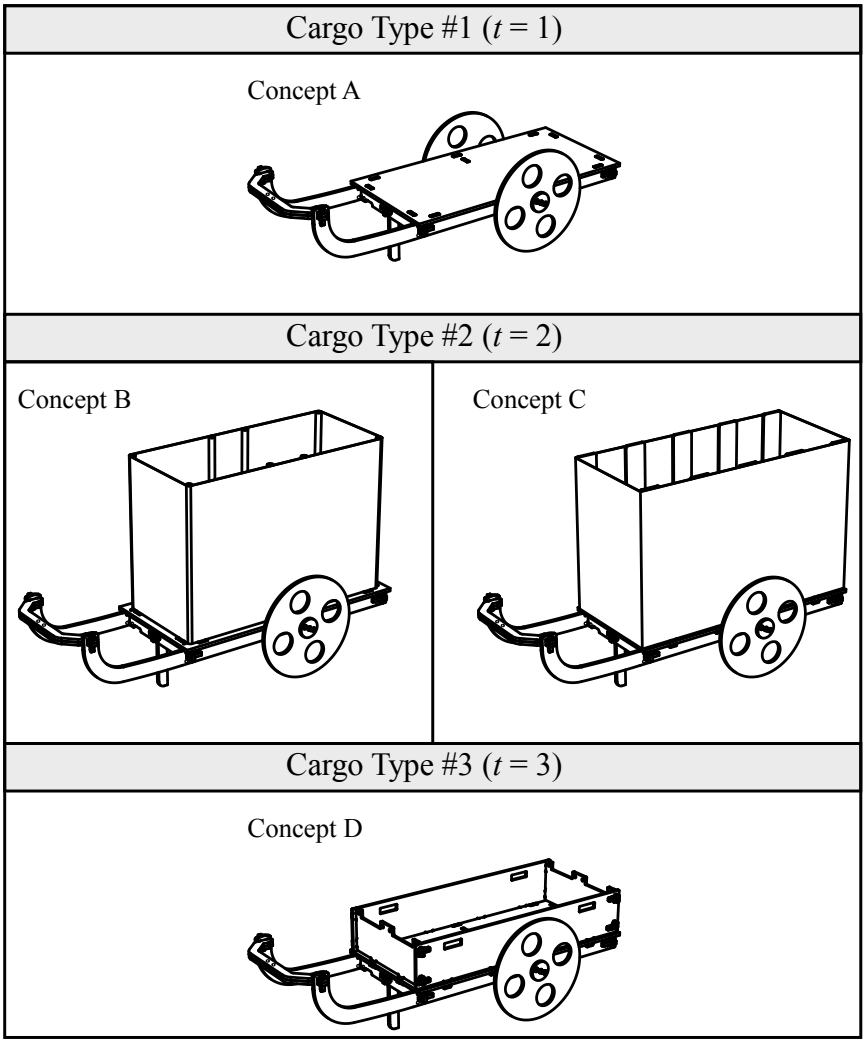

Figure 13.1: CAD models of concept plywood cart designs for each cargo type.

In addition to the models of S (sum of the material, machining, and distribution costs) and A or V, stress models of the frame (two different loading conditions), axle, and side concepts are developed. The first frame loading condition (Figure 13.2(a)) is applied to all concepts, assumes a maximum operational load (L) is uniformly distributed along the cart bed length (l_b), and is supported on the cart frame rails (long side members of the cart frame) by the reaction loads from the wheels (F_w) and cart operator (F_u) . The second frame loading condition is only applied to Concept D, assumes the same distributed load, but is now supported by the operator and the end of the cart frame (See Figure 13.2(b)) – simulates the operator lifting the front of the cart to dump out the load. For all of the concepts, the axle stress model looks at half of the axle (frame prevents

the center deflection of the axle), and applies the wheel load from Figure 13.2(a) as illustrated in Figure 13.2(c). For the three cart concepts with sides (Concepts B, C, and D), the assumed loads and boundary conditions used to determine the stress in the side structures are provided in Figures 13.2(d)–13.2(f) respectively.

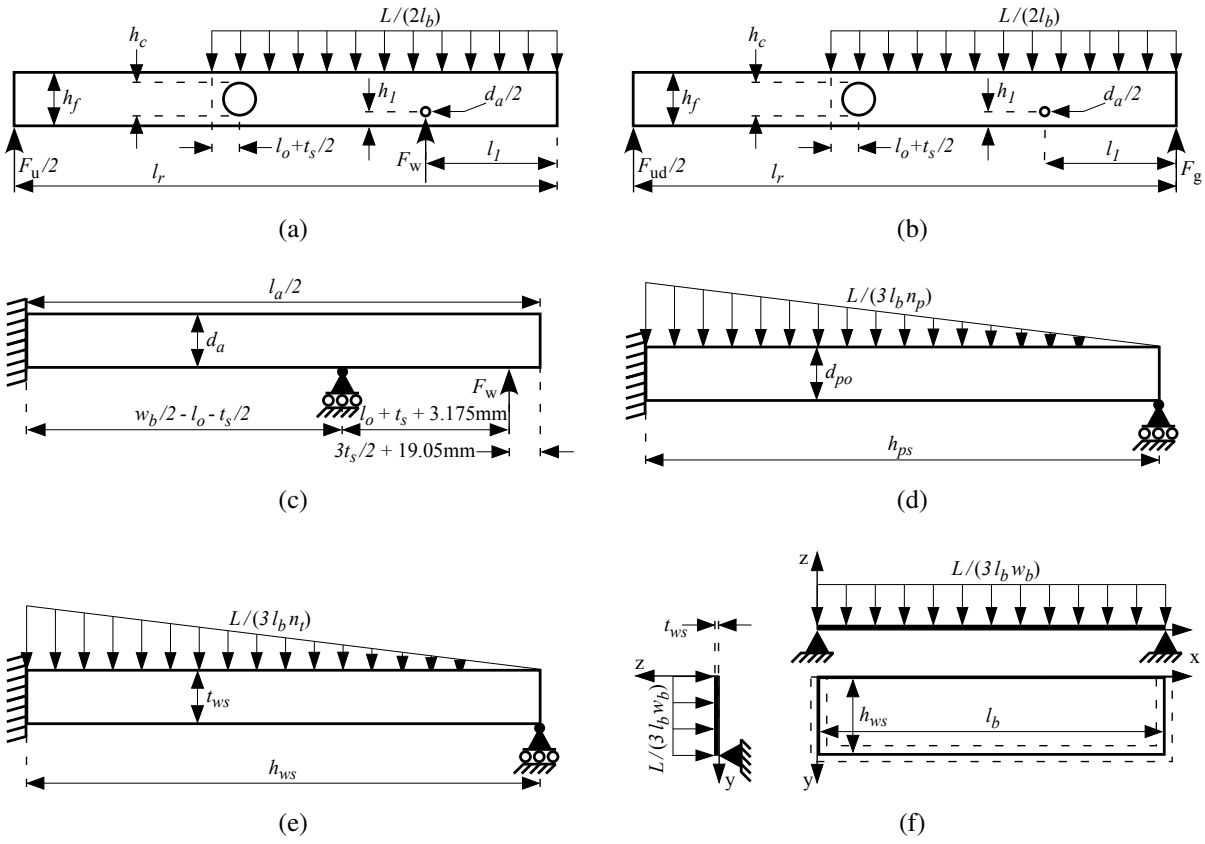

Figure 13.2: (a) Cart frame loading for Concepts A-D. (b) Cart frame loading for dumping (only used by Concept D). (c) Axle loading for Concepts A-D. (d) Cart bed sides loading for Concept B. (e) Cart bed sides loading for Concept C. (f) Cart bed sides loading for Concept D.

It should be noted that for each concept, the frame is connected without metal fasteners, and the axle passes through the rails. As a result, the beams in Figures 13.2(a)–(b) include stress concentrations in the form of circular holes to approximate the highest stress location cut-out for the implemented mortise and tenon joints (larger centered hole), and for the location of the axle (smaller non-centered hole). The formulas for both stress concentration factors come from Charts 4.88 and 4.89 of Pilkey and Pilkey 2008 [194].

Definitions of the design objects (variables) shown in Figure 13.2, and all other design objects pertaining to this example, are now provided:

l_r Cart frame rail length (mm)

h_r Overall height of the rails (mm)

l_o Length of the bed overhanging the frame (mm)

l_s Length of the plywood sheet (mm)

w_s Width of the structure plywood sheet (mm)

t_s Thickness of the structure plywood sheet (mm)

h_1 Axle center-height from the bottom edge of the rail (mm)

l_1 Axle center-distance from the rail end (mm)

d_a Diameter of the axle (mm)

L Maximum desired operational cart load (N)

l_b Length of the cart bed (mm)

w_b Width of the cart bed (mm)

h_c Height of the mortise cut-out in the rails (mm)

h_f Height of the cart frame beam members (mm)

F_u Reaction force applied by the operator (N)

F_w Reaction force applied by one wheel (N)

F_{ud} Reaction force applied by the operator when dumping the cart load (N)

F_g Reaction force applied by the ground when dumping the cart load (N)

l_a Length of the axle (mm)

d_{po} Outer pole diameter for Concept B (mm)

d_{pi} Inner pole diameter for Concept B (mm)

h_{ps} Height of Concept B sides (mm)

n_p Number of poles used in Concept B (mm)

h_{ws} Height of Concept C and D sides (mm)

t_{ws} Sheet thickness of Concept C and D sides (mm)

n_t Number of tenons securing the Concept C sides

$L_{\text{fail}}^{(i)}$ Cart failure load (N)

LF Load multiplier for calculating $L_{\text{fail}}^{(i)}$

h_u Average waist height of the cart operator (mm)

d_w Diameter of the plywood cart wheels (mm)

d_t Diameter of the router tool (mm)

f_r Feed rate of the router (mm/s)

ϕ_{mach} Hourly machining rate ($/hr)

ϕ_a Axle material price ($/mm)

ϕ_{p} Material price for pole sides ($/mm)

ϕ_{ws} Material price for the wood sides ($/mm^2)

C_{bwnp} Cost of bolts, washers, nuts, and pins ($)

σ_f Maximum frame stress (MPa)

σ_a Maximum axle stress (MPa)

σ_{ps} Maximum stress in pole sides (MPa)

σ_{ws} Maximum stress wood sides (MPa)

θ Bed angle while transporting cargo (rad)

$\bar{g}_1$ Calculated difference between $l_b/2$ and l_1 (mm)

$\bar{g}_2$ Calculated difference between l_r and l_b (mm)

$\bar{g}_3$ Calculated clearance of the Concept D sides above the wheels (mm)

$\bar{g}_4$ Calculated difference between l_s and l_r (mm)

$\bar{g}_5$ Calculated left-over sheet width (mm), assuming the rails/bed are cut as in Figure 13.3

A summary of each concept's design objects for $t = \{1,2,3\}$, along with the corresponding values of $x_l^{(k^{(t)})}$, $x_u^{(k^{(t)})}$, the diagonal entries in $\chi^{(k^{(t)})}$, the bounds of the uncertainty parameter domain (h), and the bounds of the anticipated regions of interest as defined in Section 9.4 (Step B) are presented in Appendix B. Using MATLAB's fmincon function, the dynamic s-Pareto frontier for each time step within the identified regions of interest was obtained (see Figure 13.4). From Figure 13.4, it can be seen that due to the changes in loading conditions, concepts, and required analysis models, the s-Pareto frontier does change. In addition, it should also be observed that although Concepts B and C are considered for $t = 2$, Concept C does not contribute to the s-Pareto

frontier for $t = 2$ because it is always dominated by Concept B in terms of the objectives for $t = 2$ to minimize the sales price (S) and maximize the volumetric cart capacity (V).

Method Steps C & D: In considering the differences between the concepts that comprise the dynamic s-Pareto frontier shown in Figure 13.4, a slot modular architecture [20] approach is selected for the modular cart development. The subsequent definitions of n_{m} and δ are as follows:

$$n_{\mathrm{m}} = 2 \tag{13.1}$$

$$\delta = \begin{bmatrix} 1 & 1 \\ 1 & 2 \\ 1 & 3 \end{bmatrix} \tag{13.2}$$

Using this knowledge of the desired modular progression and architecture, the modular cart system concept is developed. In order to reduce the cost of the modular system, the goal of the developed concept is to obtain all structural elements of the platform cart design (flat bed cart) from a single sheet of 19.05 mm or 28.58 mm plywood. The flat sheet part layout of this concept, including the necessary interface features for pole and box sides is illustrated in Figure 13.3. Also shown in Figure 13.3 are images of the CAD models of the assembled system configurations, the two modules (pole w/cloth and box side), and a picture of a preliminary physical prototype that was built and field tested in Peru to validate the modular system concept architecture (prototype created with 28.58 mm plywood).

Method Step E: In order to facilitate the modular system identification, the limits of the modular-system design objects ($\hat{x}_{u/l}$), the corresponding diagonal entries in $\hat{\chi}$, the domain of the modular-system uncertain parameters ($\hat{h}$), and the bounds of the uncertain areas of the regions of interest ($\hat{S}^{(i)}_{u/l,\mathrm{unc}}$) needed to evaluate Problem 9.2 are provided in Appendix B.

Optimization of the modular system is also performed using MATLAB's fmincon function, with the modular cart system design being directly selected using a weighted-sum aggregate objective function ($w_J = \{0.5, 1, 1\}$, $\hat{C} = \{\hat{A}^{(0)}, \hat{V}^{(1)}, \hat{V}^{(2)}\}$,$w_{\hat{C}} = 1.5$). The aggregate objective function and penalty function ($\hat{\Lambda}$) definitions used to evaluate *(P2)* are provided below:

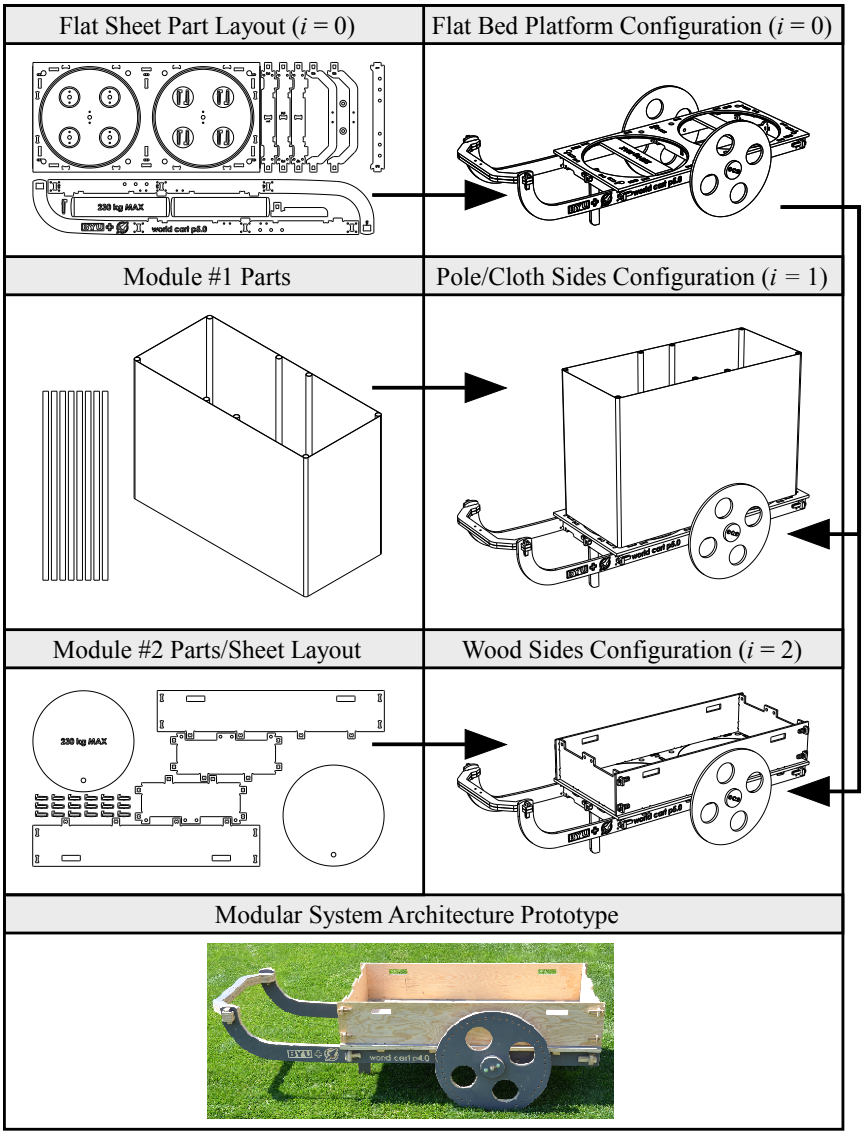

Figure 13.3: Illustrations of the modular cart system concept configurations, the flat sheet part layouts for the platform and module #2, the module #1 parts, and a preliminary physical prototype that was field tested in Peru.

$$J = \sum_{i=0}^{n_{\mathrm{m}}} \left(w_J^{(i)} \cdot \left(\hat{\Theta}^{(i)} + \hat{\Lambda}^{(i)} \right) - w_{\hat{C}} \cdot \hat{C}^{(i)} \right) \tag{13.3}$$

$$\hat{\Lambda}^{(i)} = \begin{cases} 1 - \left(\dfrac{\hat{V}^{(i)} - \hat{\mu}_{u,\mathrm{unc}}^{(i)}}{\hat{V}_u^{(i)} - \hat{\mu}_{u,\mathrm{unc}}^{(i)}} + 1 \right)^{-1} & , \hat{V}^{(i)} > \hat{\mu}_{u,\mathrm{unc}}^{(i)} \\ 1 - \left(\dfrac{\hat{\mu}_{l,\mathrm{unc}}^{(i)} - \hat{V}^{(i)}}{\hat{\mu}_{l,\mathrm{unc}}^{(i)} - \hat{V}_l^{(i)}} + 1 \right)^{-1} & , \hat{V}^{(i)} > \hat{\mu}_{l,\mathrm{unc}}^{(i)} \\ 0 & , \text{else} \end{cases} \tag{13.4}$$

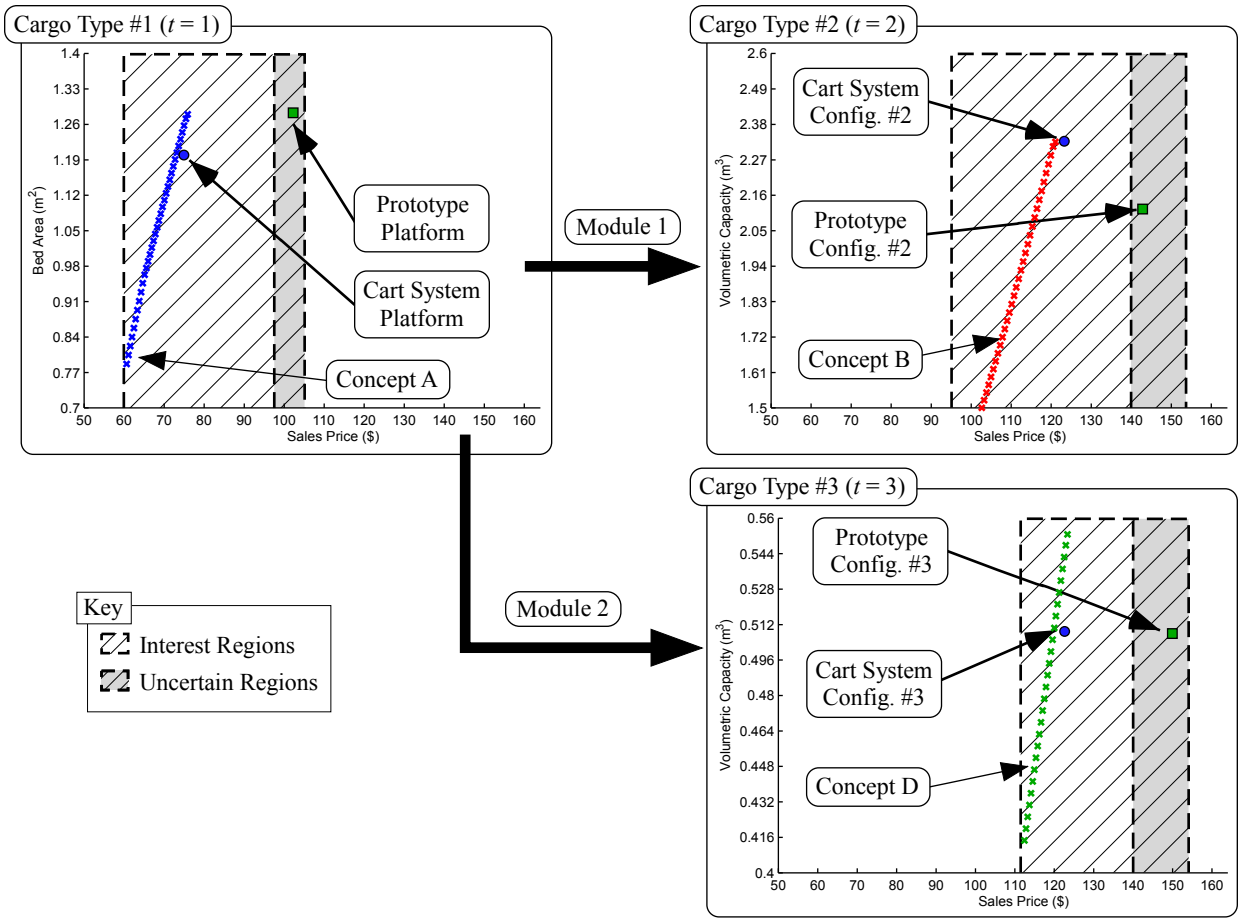

Figure 13.4: Representation of the s-pareto frontier obtained for each time-step (cargo type), along with the performance of each configuration of both the preliminary prototype in Figure 13.3 and the optimized modular cart system.

Figure 13.4 presents the objective space results for the optimized modular cart system and preliminary prototype. Although both systems are within the identified regions of interest, the prototype system has an average $\hat{\Theta}$ and $\hat{\Lambda}$ of 0.57 and 0.33, while the optimized system has averages of 0.04 and 0 respectively – represents $\sim$93% and 100% respective improvements. Figure 13.5 provides images of a physical prototype implementing the optimization results.

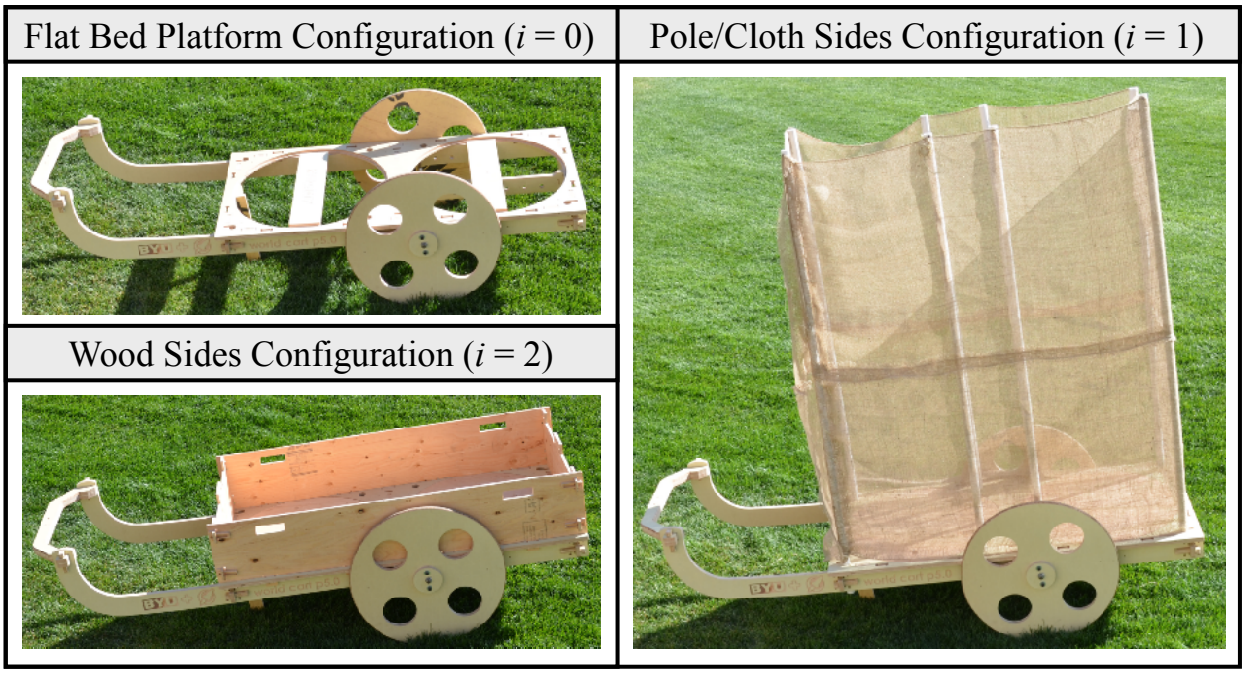

Figure 13.5: Images of a physical prototype created with 19.05 mm plywood implementing the modular cart system optimization results represented in Figure 13.4.

CHAPTER 14. CONCLUSIONS

This dissertation has addressed an important limitation of current methods of module-based product design in accounting for natural changes in customer needs (preferences), analysis models, design concepts, and implementation environments over time. In response to this limitation, a multiobjective optimization design method has been developed and demonstrated. The presented approach involves the strategic use of a series of optimization formulations that ultimately result in modular products that can adapt to changing preferences, concepts, models, and environments by moving from one design on the dynamic s-Pareto frontier to another through the addition or subtraction of a module.

One of the most common approaches used to address the challenge of satisfying a variety of preferences and operating environments is through the development of a family of products that provide diverse product performance. The strength of this approach is in the ability to provide a range of products that satisfy the *current* variation in customer needs across *multiple market segments*. An important element of the research presented in this dissertation is that changes in needs over time do not always require the significant changes in product performance that would result in a diversely performing product family. As a result, the objectives of traditional product family approaches to maximize both product family performance diversity and product commonality will not always be considered/satisfied. Thus, by overcoming these limitations the present approach enables the design of a new kind of product that is based on changes in preferences, concepts, models, and environments over time.

Development of the method presented in this dissertation was separated into four phases. The first phase of these developments focused on design cases where there is a *single* non-dynamic Pareto frontier (changes in concepts, models, and environments that effect the Pareto frontier are ignored), and resulted in a five-step design process. An example implementation of this first phase in the method development was provided through the design of a modular UAV. This example il-

lustrates the ability of the method to identify platform and module designs that provide the desired Pareto-optimal performance according to the changing objectives, parameters, and constraints over time identified within the problem description. The second phase in the method developments focused on the changes required to adapt the five-step process for single Pareto frontier cases to *multiple* Pareto frontier design cases. As a result, a six-step design process which implements the identification of a s-Pareto frontier was provided. To illustrate implementation of this second phase in the method development, the design of a hurricane and flood resistant modular residential structure was provided. Similar to the example of the UAV, the modular residential structure example demonstrates the ability of the method to design a product that is capable of traversing the s-Pareto frontier over time through the addition of modules based on predicted changes in preferences and operational environments that determine the selection of s-Pareto design over time.

The traditional optimization problem formulations that serve as the foundation to the first and second phase method developments are not well suited to allowing changes in concepts, models, and environments. To overcome these limitations, the third phase of developments focuses on identifying a generic optimization formulation capable of identifying the dynamic set of non-dominated designs that result from these changes. Implementation of this new dynamic-s-Pareto frontier problem formulation was illustrated through a simple aircraft design example that was inspired by the Lockheed C-130 Hercules. Finally, the fourth phase of method developments adapts the method resulting from the phase two developments to incorporate the new dynamic optimization formulation from the phase three developments, and allow for the identification of *modular systems* that account for changing preferences, environments, models, and concepts. Implementation of this method was then illustrated through the development of a modular truss system.

Noting that modular/adaptive products only represent one approach for dealing with changes in preferences, environments, models, and concepts, parallel research performed in the areas of collaborative products [4] (modular products created by combining two or more independently functional products) and design principle identification [5] were also described. In order to connect these different methods, the final research contributions gather the presented and parallel research developments into a unifying design approach, with two case studies presented to illustrate the implementation of this method in the development of a modular irrigation pump and a modular plywood cart for developing countries.

Through the variety of examples presented in this dissertation, it is seen that the modular product design method developed herein is broadly applicable to diverse applications. In the case of the UAV and Aircraft Examples, the method successfully provides designs based on known changes in mission profiles. In the case of the pump, cart, residential housing, and truss examples, the method was used to provide designs based on changes in the target customer's view of affordability and desired product/system performance. In addition, noting the inherent uncertainties related to the use of predicted future preferences, concepts, models, and environments, the cart and truss examples also illustrate the ability of the method to account for and incorporate uncertainty analysis.

Although the use of modularity is a key aspect of the work presented herein, there are consequences of using this design approach. Modularity necessitates the design of many different individual components where normally one single component could be used (i.e., redundant physical architectures occur at module interfaces) [17]. Although in the cases of the cart and water pump this allows for reconfiguration to facilitate the purchase of incremental upgrades by reducing the initial financial risk, the increased number of joints gives way to increased likelihood of structural failures at the module interfaces. For this reason, the decision of whether to develop a modular product, a set of independent products, a family of related products, or a single product that performs as best as possible in all situations is a complex decision.

Recognizing that one of the fundamental assumptions of the method developed herein is that the changes in customer needs over time are known, future research related to this dissertation should include the identification of methods for determining and quantifying the future needs of a product. One example of an approach for identifying these needs that was implemented in the pump case study, was to assume that the performance of current products on the market represented the customer preferences over time. As such, additional work should also look at developing methods for identifying those customer preferences that define anticipated regions of interest within the optimization design space. This is due to the inherent impact these regions have on the modular products identified, and the ability these products have to reduce the perceived financial risks of income generating products.

In current approaches of product development there are many methods available for determining the *present* customer needs of a product. The benefit of these methods comes in the ability

of the designer to characterize these needs and translate them into performance specifications and attributes that are used to guide the design of the product. However, as has been demonstrated in this dissertation, through the development of methods for determining and quantifying the *future* needs of a product, it is possible to translate these needs into performance specifications and attributes that are used to guide the design of products that adapt to satisfy changing needs over time. In the development of these methods of determining future customer needs, it is anticipated that many of the methods currently used for determining the current customer needs (e.g. focus groups, surveys, observation) could be adapted to provide the desired outcomes. In addition, more mathematical studies of the movement of customers between market segments and the emergence of additional market segments could be used to develop gradient based methods that would use previous information detailing the past changes in customer needs to forecast the future customer needs.

From the case studies presented in Chapters 12–13, an additional area of potential future work in relation to designing products for the developing world comes from an observed limitation of the modular product design optimization method presented in this dissertation. Specifically, the implemented method does not include a system of accounting for the social, environmental and political factors that determine the success of a product upon implementation in the developing world. Future work to be done in this area should focus on the identification of a metric that can measure, and potentially predict, how successfully a product accounts for the complexities of these social factors.

REFERENCES

[1] Trope, Y., and Liberman, N., 2000. "Temporal construal and time-dependent changes in preference." *Journal of Personality and Social Psychology,* **79**(6), pp. 876–889. 1

[2] Lewis, P. K., Tackett, M., and Mattson, C. A., 2012. "Considering dynamic pareto frontiers in decision making." In *8th AIAA Multidisciplinary Design Optimization Specialist Conference*, no. AIAA-2012-1849. 1, 16, 81

[3] Li, Y., Xue, D., and Gu, P., 2008. "Design for product adaptability." *Concurrent Engineering,* **16**(3), pp. 221–232. 1

[4] Morrise, J., Mattson, C. A., Lewis, P. K., and Magleby, S. P., 2011. "A method for designing collaborative products for poverty alleviation." In *ASME 2011 International Design Engineering Technical Conferences & Computers and Information in Engineering Conference*, no. DETC2011-47409. 4, 18, 19, 133

[5] Campbell, R., Lewis, P. K., and Mattson, C. A., 2011. "A method for identifying design principles for the developing world." In *ASME 2011 International Design Engineering Technical Conferences & Computers and Information in Engineering Conference*, no. DETC2011-48584. 4, 20, 21, 99, 133

[6] Mattson, C. A., and Magleby, S. P., 2001. "The influence of product modularity during concept selection of consumer products." In *Proceedings of the ASME DETC'01, ASME 2001 Design Engineering Technical Conferences, and Computers and Information in Engineering Conference*, no. DETC2001/DTM21712. 6

[7] Gonzalez-Zugasti, J., and Otto, K., 2000. "Modular platform-based product family design." In *Proceedings of the ASME Design Automation Conference*, no. DETC2000/DAC-14238. 6, 16, 17

[8] Magrab, E., 1997. *Integrated Product and Process Design and Development*. CRC Press. 6

[9] Jiao, J., and Tseng, M. M., 1999. "A methodology of developing product family architecture for mass customization." *Journal of Intelligent Manufacturing,* **10**, pp. 3–20. 6, 7

[10] Yearsley, J. D., and Mattson, C. A., 2008. "Product family design using a smart pareto filter." In *46th AIAA Aerospace Sciences Meeting and Exhibit*, no. AIAA 2008-909. 6, 7

[11] Yearsley, J. D., and Mattson, C. A., 2008. "Product family member and platform identification with concurrent variable and objective space smart pareto filtering." In *4th AIAA Multidisciplinary Design Optimization Specialist Conference*, no. AIAA-2008-2220. 6, 7, 16

[12] Yearsley, J. D., and Mattson, C. A., 2008. "Interactive design of combined scale-based and module-based product family platforms." In *Proceedings of 12th AIAA/ISSMO Multidisciplinary Analysis and Optimization Conference*, no. AIAA-2008-5819. 6, 7, 16, 47

[13] Wie, M. V., Greer, J., Campbell, M., Stone, R., and Wood, K., 2001. "Interfaces and product architecture." In *Proceedings of the ASME Design Theory and Methodology Conference*, no. DETC2001/DTM-21689. 6

[14] Dahmus, J. B., Gonzalez-Zugasti, J. P., and Otto, K. N., 2001. "Modular product architecture." *Design Studies,* **22**, pp. 409–424. 6, 7

[15] Gershenson, J. K., Prasad, G. J., and Allamneni, S., 1999. "Modular product design: a life-cycle view." *Journal of Integrated Design & Process Science,* **3**(4), pp. 13–26. 6

[16] Jose, A., and Tollenaere, M., 2005. "Modular and platform methods for product family design: literature analysis." *Journal of Intelligent Manufacturing,* **16**, pp. 371–390. 6

[17] Huang, C. C., 2000. "Overview of modular product development." *Proceedings of the National Science Council ROC(A),* **24**(3), pp. 149–165. 7, 134

[18] Baguley, P., Bramall, D., Maropoulos, P., and Page, T., 2004. "The automation of sustainability via re-use, modularization, and fuzzy logic." In *Design and Manufacturing for Sustainable Development 2004*, Professional Engineering Publishing. 7

[19] Pahl, G., and Beitz, W., 2007. *Engineering Design: A Systematic Approach*. Springer-Verlag. 7, 97

[20] Ulrich, K., and Eppinger, S., 2004. *Product Design and Development*., 4th ed. McGraw-Hill. 7, 8, 9, 20, 51, 58, 84, 97, 99, 128

[21] Tseng, M. M., and Jiao, J., 1998. "Design for mass customization by developing product family architecture." In *ASME International Design Engineering Technical Conference & Computers and Information in Engineering Conference*, no. DETC98/DFM-5717. 7

[22] de Weck, O. L., Suh, E. S., and Chang, D., 2003. "Product family and platform portfolio optimization." In *ASME IDETC/CIE 2003*, no. DETC03/DAC-48721. 7

[23] Star, M. K., 1965. "Modular production – a new concept." *Harvard Business Review,* **43**, November–December, pp. 131–142. 7

[24] Yang, T. G., Beiter, K. A., and Ishii, K., 2004. "Product platform development: An approach for products in the conceptual stages of design." In *In 2004 ASME International Mechanical Engineering Congress and RDD Expo*, no. IMECE2004-62171. 7, 64

[25] Meyer, M. H., 1997. "Revitalize your product lines through continuous platform renewal." *Research Technology Management,* **40**(2), pp. 17–28. 7

[26] Simpson, T. W., Maier, J. R. A., and Mistree, F., 1999. "A product platform concept exploration method for product platform design." In *Proceedings of the ASME Design Engineering Technical Conferences*, no. DETC99/DTM-8761. 7, 17

[27] Oyebode, A., 2004. "Modularity and quality." In *Proceedings From the 2nd Seminar on Development of Modular Products*, G. Erixon and P. Kenger, eds., pp. 19–24. 8

[28] Padamat, M., 2004. "Methods for modularisation." In *Proceedings From the 2nd Seminar on Development of Modular Products*, G. Erixon and P. Kenger, eds., pp. 121–126. 8

[29] Strong, M. B., Magleby, S. P., and Parkinson, A. R., 2003. "A classification method to compare modular product concepts." In *the ASME 2003 Design Engineering Technical Conferences*. 8, 9, 84, 90

[30] Khire, R. A., and Messac, A., 2008. "Selection-integrated optimization (SIO) methodology for optimal design of adaptive systems." *ASME Journal of Mechanical Design,* **130**(10), pp. 101401–101413. 9, 17, 64

[31] Olewnik, A., Brauen, T., Ferguson, S., and Lewis, K., 2004. "A framework for flexible systems and its implementation in multiattribute decision making." *Journal of Mechanical Design*. 9, 64

[32] Siddiqi, A., and de Weck, O. L., 2008. "Modeling methods and conceptual design principles for reconfigurable systems." *ASME Journal of Mechanical Design,* **130**, pp. 101102–101116. 9, 64

[33] Balling, R. J., 2000. "Pareto sets in decision-based design." *Engineering Valuation and Cost Analysis,* **3**, pp. 189–198. 10

[34] Das, I., 1999. "A preference ordering among various pareto optimal alternatives." *Structural and Multidisciplinary Optimization,* **18**(1), Aug., pp. 30–35. 10, 11

[35] Kasprzak, E. M., and Lewis, K. E., 2000. "An approach to facilitate decision tradeoffs in pareto solution sets." *Engineering Valuation and Cost Analysis,* **3**, pp. 173–187. 10

[36] Li, Y., Fadel, G. M., and Wiecek, M. M., 1998. "Approximating pareto curves using the hyper-ellipse." In *Proceedings of the 7th AIAA/USAF/NASA/ISSMO Symposium on Multidisciplinary Analysis and Optimization*, no. AIAA-98-4961. 10

[37] Mattson, C. A., and Messac, A., 2003. "Concept selection using s-pareto frontiers." *AIAA Journal,* **41**(6), pp. 1190–1204. 10, 11, 12, 13, 15, 16, 43, 72

[38] Mattson, C. A., and Messac, A., 2005. "Pareto frontier based concept selection under uncertainty, with visualization." *OPTE: Optimization and Engineering,* **6**(1), pp. 85–115. 10

[39] Park, K. W., and Grierson, D. E., 1999. "Pareto-optimal conceptual design of the structural layout of buildings using a multicriteria genetic algorithm." *Computer-Aided Civil and Infrastructure Engineering,* **14**, pp. 163–170. 10

[40] Tappeta, R. V., Renaud, J. E., Messac, A., and Sundaraj, G. J., 2000. "Interactive physical programming: Tradeoff analysis and decision making in multidisciplinary optimization." *AIAA Journal,* **38**(5), May, pp. 917–926. 10

[41] Wu, J., and Azarm, S., 2001. "Metrics for quality assessment of a multiobjective design optimization solution set." *ASME Journal of Mechanical Design,* **123**, March, pp. 18–25. 10

[42] Messac, A., 1996. "Physical programming: Effective optimization for computational design." *AIAA Journal,* **34**(1), pp. 149–158. 10

[43] Frischknecht, B. D., Peters, D. L., and Papalambros, P. Y., 2011. "Pareto set analysis: local measures of objective coupling in multiobjective design optimization." *Structural and Multidisciplinary Optimization,* **43**(5), pp. 617–630 DOI: 10.1007/s00158-010-0599-2. 10

[44] Messac, A., and Mattson, C. A., 2004. "Normal constraint metthod with guarentee of even representation of complete pareto frontier." *AIAA Journal,* **42**(10), pp. 2101–2111. 10, 12

[45] Todoroki, A., and Sekishiro, M., 2008. "Modified efficient global optimization for a hat-stiffened composite panel with buckling constraint." *AIAA Journal,* **46**(9), September, pp. 2257–2264 DOI: 10.2514/1.34548. 10

[46] Gurnani, A. P., and Lewis, K., 2008. "Using bounded rationality to improve decentralized design." *AIAA Journal,* **46**(12), December, pp. 3049–3059 DOI: 10.2514/1.35776. 10

[47] Miettinen, K. M., 1999. *Nonlinear Multiobjective Optimization*. International Series in Operations Research & Management Science. Kluwer Academic Publishers. 10, 11

[48] Messac, A., and Mattson, C. A., 2002. "Generating well-distributed sets of pareto points for engineering design using physical programming." *Optimization and Engineering,* **3**(4), pp. 431–450 Kluwer Academic Publishers. 10

[49] Steuer, R. E., 1986. *Multiple Criteria Optimization, Theory Computations and Applications*. John Wiley & Sons, Inc., New York. 10, 11

[50] Belegundu, A., and Chandrupatla, T., 1999. *Optimization Concepts and Applications in Engineering*. Prentice Hall, New Jersey. 10, 11

[51] Chen, W., Wiecek, M. M., and Zhang, J., 1999. "Quality utility - a compromise programming approach to robust design." *ASME Journal of Mechanical Design,* **121**, June. 11, 28, 78

[52] Pareto, V., 1964. *Cour dEconomie Politique*., the first edition in 1896 ed. Librarie Droz, Geneve. 11

[53] Das, I., 1999. "On characterizing the kneeof the pareto curve based on normal-boundary intersection." *Structural Optimization,* **18**(2/3), pp. 107–115. 11

[54] Di Barba, P., 2001. "A fast evolutionary method for identifying non-inferior solutions in multicriteria shape optimization of a shielded reactor." *International Journal for Computation and Mathematics in Electrical and Electronic Engineering,* **20**(3), pp. 762–776. 11, 12

[55] Mattson, C. A., Mullur, A. A., and Messac, A., 2004. "Smart pareto filter: Obtaining a minimal representation of multiobjective design space." *Engineering Optimization,* **36**(4), pp. 721–740. 11, 12

[56] Montusiewicz, J., and Osyczka, A., 1990. "A decomposition strategy for multicriteria optimization with application to machine tool design." *Engineering Costs and Production Economics,* **20**, pp. 191–202. 11

[57] Abraham, S. G., Rau, B. R., and Schriber, R., 2000. Fast design space exploration through validity and quality filtering of subsystem designs Tech. Rep. HPL–2000–98,, Hewlett Packard. 11

[58] Cheng, F. Y., and Li, D., 1998. "Genetic algorithm development for multiobjective optimization of structures." *AIAA Journal,* **36**(6), pp. 1105–1112. 11, 12

[59] Messac, A., Ismail-Yahaya, A., and Mattson, C. A., 2003. "The normalized normal constraint method for generating the pareto frontier." *Structural and Multidisciplinary Optimization,* **25**(2), pp. 86–98. 11, 15

[60] Wiecek, M., Blouin, V. Y., Fadel, G. M., Engau, A., Hunt, B., and Singh, V., 2009. *Multi-scenario Multi-Objective Optimization in Engineering Design*., XV ed., Vol. 618 Springer Lecture Notes in Economics and Mathematical Systems LNEMS volume of MOPGP. 14, 15

[61] Bulut, G., 2001. Robust multi-scenario optimization of an air expeditionary force structure applying scatter search to the combat forces assessment model Tech. rep., DTIC Document. 14

[62] Laird, C. D., and Biegler, L. T., 2008. "Large-scale nonlinear programming for multi-scenario optimization." In *Modeling, Simulation and Optimization of Complex Processes*, H. G. Bock, E. Kostina, H. X. Phu, and R. Rannacher, eds. Springer Berlin Heidelberg, pp. 323–336. 14

[63] Taniguchi, F., Yamada, T., and Kataoka, S., 2008. "Heuristic and exact algorithms for the maxmin optimization of the multi-scenario knapsack problem." *Computers & Operations Research,* **35**(6), pp. 2034–2048 ¡ce:title¿Part Special Issue: OR Applications in the Military and in Counter-Terrorism¡/ce:title¿. 14

[64] Christoforidis, M., Aganagic, M., Awobamise, B., Tong, S., and Rahimi, A., 1996. "Long-term/mid-term resource optimization of a hydrodominant power system using interior point method." *Power Systems, IEEE Transactions on,* **11**(1), February, pp. 287–294. 14

[65] Aissi, H., Bazgan, C., and Vanderpooten, D., 2009. "Min-max and min-max regret versions of combinatorial optimization problems: A survey." *European Journal of Operational Research,* **197**(2), pp. 427–438. 14

[66] Zavala, V. M., Laird, C. D., and Biegler, L. T., 2008. "Interior-point decomposition approaches for parallel solution of large-scale nonlinear parameter estimation problems." *Chemical Engineering Science,* **63**(19), pp. 4834–4845 ¡ce:title¿Model-Based Experimental Analysis¡/ce:title¿. 14

[67] Sanchez Marin, F. T., and Gonzalez, A. P., 2003. "Global optimization in path synthesis based on design space reduction." *Mechanism and Machine Theory,* **38**(6), pp. 579–594. 14, 15

[68] Balling, R. J., 2009. *Computer Structural Analysis*., Vol. I BYU Academic Publishing. 14, 56, 90, 94

[69] Nelson, S., Parkinson, M., and Papalambros, P., 2001. "Multicriteria optimization in product platform design." *ASME Journal of Mechanical Design,* **123**(2), pp. 199–204. 15, 16, 17

[70] Fonsecay, C. M., and Fleming, P. J., 1995. "An overview of evolutionary algorithms in multiobjective optimization." *Evolutionary Computation,* **3**(1), pp. 1–16. 15

[71] Rosenbrock, H. H., 1960. "An automatic method for finding the greatest or least value of a function." *The Computer Journal,* **3**, p. 175. 15

[72] Fletcher, R., 1981. *Practical Methods of Optimization: Vol. 2: Constrained Optimization*. John Wiley & Sons. 15

[73] Box, M. J., 1966. "A comparison of several current optimization methods, and the use of transformations in constrained problems." *The Computer Journal,* **9**(1), pp. 67–77. 15

[74] Fischer, A., 1992. "A special newton-type optimization method." *Optimization,* **24**(3 & 4), pp. 269–284. 15

[75] Lewis, P. K., Murray, V. R., and Mattson, C. A., 2010. "Identification of modular product platforms and modules that account for changing consumer needs." In *6th AIAA Multidisciplinary Design Optimization Specialist Conference*, no. AIAA-2010-2836. 16, 23

[76] Lewis, P. K., Murray, V. R., and Mattson, C. A., 2010. "An engineering design strategy for reconfigurable products that support poverty alleviation." In *the ASME 2010 International Design Engineering Technical Conferences & Computers and Information in Engineering Conference*, no. DETC2010-28739. 16, 103

[77] Lewis, P. K., Murray, V. R., and Mattson, C. A., 2010. "Accounting for changing consumer needs with s-pareto frontiers." In *the 13th AIAA/ISSMO Multidisciplinary Analysis Optimization Conference*, no. AIAA-2010-9039. 16, 43

[78] Lewis, P. K., Murray, V. R., and Mattson, C. A., 2011. "A design optimization strategy for creating devices that traverse the Pareto frontier over time." *Structural and Multidisciplinary Optimization,* **43**(2), February, pp. 191–204 DOI 10.1007/s00158-010-0555-1. 16, 23, 58, 64

[79] Lewis, P. K., and Mattson, C. A., 2011. "Effect of alternate aggregate objective functions on selecting target s-pareto designs for modular products." In *7th AIAA Multidisciplinary Design Optimization Specialist Conference*, no. AIAA-2011-2151. 16, 43

[80] Lewis, P. K., and Mattson, C. A., 2012. "A method for developing systems that traverse the pareto frontiers of multiple system concepts through modularity." *Structural and Multidisciplinary Optimization,* **45**(4), pp. 467–478. 16, 43, 64, 83, 104

[81] Lewis, P. K., and Mattson, C. A., 2012. "Multiobjective optimization of modular systems that traverse dynamic s-pareto frontiers." In *14th AIAA/ISSMO Multidisciplinary Analysis Optimization Conference*, no. AIAA-2012-5441. 16, 77

[82] Wood, C. D., Lewis, P. K., and Mattson, C. A., 2012. "Modular product optimization to alleviate poverty: An irrigation pump case study." In *the ASME 2012 International Design Engineering Technical Conferences & Computers and Information in Engineering Conference*, no. DETC2012-71171. 16

[83] Curtis, S. K., Mattson, C. A., Hancock, B. J., and Lewis, P. K., 2012. "Dynamic multiobjective optimization formulation." In *8th AIAA Multidisciplinary Design Optimization Specialist Conference*, no. AIAA-2012-1848. 16, 64, 65, 66

[84] Curtis, S. K., Mattson, C. A., Hancock, B. J., and Lewis, P. K., 2012. "Divergent exploration in design with a dynamic multiobjective optimization formulation." *Structural and Multidisciplinary Optimization,* **Accepted 21 Oct. 2012**. 16, 64, 65, 66

[85] Lewis, P. K., Wood, C. D., and Mattson, C. A., 2012. "Modular product optimization to alleviate poverty: An irrigation pump case study." *International Journal of Product Development,* **Under Review**. 16

[86] Lewis, P. K., Tackett, M., and Mattson, C. A., 2012. "Considering dynamic pareto frontiers in decision making." *Optimization and Engineering,* **Under Review**. 16

[87] Lewis, P. K., and Mattson, C. A., 2012. "An optimization-based method for designing modular systems that traverse dynamic s-pareto frontiers." *Structural and Multidisciplinary Optimization,* **Under Review**. 16, 77, 123

[88] Mattson, C. A., and Lewis, P. K., 2011. "Modular product design in engineering-based poverty alleviation." In *Proceedings of the 2011 NSF Engineering Research and Innovation Conference* Grant # CMMI-0954580. 16

[89] Yigit, A. S., Ulsoy, A. G., and Allahverdi, A., 2002. "Optimizing modular product design for reconfigurable manufacturing." *Journal of Intelligent Manufacturing,* **13**, pp. 309–316. 16

[90] Cakmakci, M., and Ulsoy, A. G., 2000. "Qualification of coupling in modular design problems." In *Proceedings of the 2000 Japan-USA Symposium on Flexible Automation*. 16

[91] Ulrich, K., and Seering, W., 1989. "Synthesis of schematic descriptions in mechanical design." *Research in Engineering Design,* **1**, pp. 3–18. 16

[92] Fujita, K., Sakaguchi, H., and Akagi, S., 1999. "Product variety deployment and its optimization under modular architecture and module commonalization." In *ASME Design Engineering Technical Conferences – Design for Manufacturing*, no. DETC99/DFM-8923. 16, 17

[93] Martin, M. V., and Ishii, K., 2002. "Design for variety: developing standardized and modularized product platform architectures." *Research in Engineering Design,* **13**(4), pp. 213–235 DOI 10.1007/s00163-002-0020-2. 16, 47

[94] Ericsson, A., and Erixon, G., 1999. *Controlling design variants: modular product platforms*. ASME Press. 16

[95] Conner, C. G., De Kroon, J. P., and Mistree, F., 1999. "A product variety evaluation method for a family of cordless drill transmissions." In *Proceedings of the ASME Design Engineering Technical Conferences*, no. DETC99/DAC-8625. 16, 17

[96] Gonzalez-Zugasti, J. P., Otto, K. N., and Baker, J. D., 1998. "A method for architecting product platforms with an application to interplanetary mission design." In *Proceedings of the ASME Design Engineering Technical Conferences*, no. DETC98/DAC-5608. 16

[97] Fujita, K., Akagi, S., Yoneda, T., and Ishikawa, M., 1998. "Simultaneous optimization of product family sharing system structure and configuration." In *Proceedings of the ASME Design Engineering Technical Conferences*, no. DETC98/DFM-5722. 16

[98] Fellini, R., Kokkolaras, M., Michelena, N., Papalambros, P., Perez-Duarte, A., Saitou, K., and Fenyes, P., 2004. "A sensitivity-based commonality strategy for family products of mild variation, with application to automotive body structures." *Structural and Multidisciplinary Optimization,* **27**, pp. 89–96. 16, 17

[99] DSouza, B., and Simpson, T. W., 2003. "A genetic algorithm based method for product family design optimization." *Engineering Optimization,* **35**(1), pp. 1–18. 17

[100] Simpson, T. W., Chen, W., Allen, J. K., and Mistree, F., 1996. "Conceptual design of a family of products through the use of the robust concept exploration method." In *6th AIAA/USAF/NASA/ISSMO Symposium on Multidisciplinary Analysis and Optimization*, Vol. 2, pp. 1535–1545. 17

[101] Nayak, R., Chen, W., and Simpson, T. W., 2002. "Variation-based methodology for product family design." *Engineering Optimization,* **34**(1), pp. 65–81. 17

[102] Mistree, F., Hughes, O. F., and Bras, B. A., 1993. "The compromise decision support problem and the adaptive linear programming algorithm." In *Structural Optimization: Status and Promise*, M. P. Kamat, ed. AIAA, Washington, D.C., pp. 247–286. 17

[103] Fellini, R., Papalambros, P. Y., and Weber, T., 2000. "Application of a product platform design process to automotive powertrains." In *Proceedings of the 8th AIAA/USAF/NASA/ISSMO Symposium on Multidisciplinary Analysis and Optimization*, no. AIAA2000-4849. 17

[104] Parkinson, M., Reed, M., Kokkolaras, M., and Papalambros, P., 2005. "Robust truck cabin layout optimization using advanced driver variance models." In *Proceedings of the 2005 ASME International Design Engineering Technical Conferences and Computers and Information in Engineering Conference*, Vol. 2, pp. 1103–1109. 17

[105] Roser, C., and Kazmer, D., 2000. "Flexible design methodology." In *Proceedings of the ASME Design for Manufacturing Conference*, no. DETC00/DFM-14016. 17

[106] Ferguson, S., and Lewis, K., 2004. "Effective development of flexible systems in multidisciplinary optimization." In *Collection of Technical Papers – 10th AIAA/ISSMO Multidisciplinary Analysis and Optimization Conference*, Vol. 1, pp. 100–112. 17

[107] Chen, W., Allen, J. K., Tsui, K.-L., and Mistree, F., 1996. "A procedure for robust design: Minimizing variations caused by noise factors and control factors." *ASME Journal of Mechanical Design,* **118**(4), pp. 478–485. 17

[108] Gunawan, S., and Azarm, S., 2005. "Multi-objective robust optimization using a sensitivity region concept." *Structural and Multidisciplinary Optimization,* **29**(1), pp. 50–60. 17

[109] Morrise, J., 2011. "Collaborative products: A design methodology with application to engineering-based poverty alleviation." Master's thesis, Brigham Young University, August. 18, 19

[110] Wasley, N. S., Lewis, P. K., and Mattson, C. A., 2012. "Designing products for optimal collaborative performance with application to engineering-based poverty alleviation." In *the ASME 2012 International Design Engineering Technical Conferences & Computers and Information in Engineering Conference*, no. DETC2012-71209. 19, 20

[111] Kotonya, G., and Sommerville, I., 1995. Requirements engineering with viewpoints Tech. rep., Lancaster University Computing Department. 20

[112] Suh, N. P., 1990. *The Principles of Design*. Oxford University Press. 20

[113] Ramachandran, D., Kam, M., Chiu, J., Canny, J., and Frankel, J., 2007. "Social dynamics of early stage co-design in developing regions." In *CHI 2007*. 20

[114] Singleton, D., 2003. "Poverty alleviation: the role of the engineer." *The ARUP Journal*, pp. 3–9. 20

[115] United Nations, 2010. The millennium development goals report 2010 Tech. rep. 20

[116] The World Bank, 2010. World development indicators 2010 Tech. rep. 20, 102

[117] Campbell, R. D., Lewis, P. K., and Mattson, C. A., 2011. "A method for identifying design principles for the developing world." *ASME Journal of Mechanical Design,* **Under Review**. 21, 99

[118] Gonzalez, L. F., Periaux, J., Damp, L., and Srinivas, K., 2007. "Evolutionary methods for multidisciplinary optimization applied to the design of UAV systems." *Engineering Optimization,* **39**(7), pp. 773–795. 33

[119] Jun, S., Jeon, Y. H., Rho, J., and Lee, D. H., 2006. "Application of collaborative optimization using genetic algorithm and response surface method to an aircraft wing design." *Journal of Mechaical Science and Technology,* **20**(1), January, pp. 133–146. 33

[120] Rajagopal, S., and Ganguli, R., 2008. "Conceptual design of long endurance uav using kriging approximation and multi-objective genetic algorithm." *Aeronautical Journal,* **112**(1137), pp. 653–662. 33

[121] Viswamurthy, S. R., and Ganguli, R., 2009. "Optimal placement of piezoelectric actuated trailing-edge flaps for helicopter vibration control." *Journal of Aircraft,* **26**(1), pp. 244–253. 33

[122] Viswamurthy, S. R., and Ganguli, R., 2007. "Optimal placement of trailing edge flaps for helicopter vibration reduction using response surface methods." *Engineering Optimization,* **39**(2), pp. 185–202. 33

[123] Nigam, N., and Kroo, I., 2008. "Control and design of multiple unmanned air vehicles for a persistent surveillance task." In *12th AIAA/ISSMO Multidisciplinary Analysis and Optimization Conference*, no. AIAA-2008-5913. 36, 39, 68, 70

[124] Wakayama, S., and Kroo, I., 1995. "Subsonic wing planform design using multidisciplinary optimization." *Journal of Aircraft,* **32**(4), July–August, pp. 746–753. 36

[125] International Organization for Standardization (ISO), 1975. "International standard atmosphere." No. ISO 2533:1975. 39

[126] Shelquist Engineering, 2009. "Air density and density altitude calculations." *http://wahiduddin.net/calc/density_altitude.htm*, June. 39

[127] Otto, K., and Wood, K., 2001. *Product Design: Techniques in Reverse Engineering and New Product Development*. Prentice Hall. 51, 99

[128] Fay, M., Ghesquiere, F., and Solo, T., 2003. "Natural disasters and the urban poor." *en breve,* **32**, October, pp. 1–4. 54

[129] Favela, V. D., 2009. "Houses put to flood and hurricane test." *Inter Press Service*, September. 54

[130] Cheng, F. Y., and Li, D., 1996. "Multiobjective optimization of structures with and without control." *Journal of Guidance, Control, and Dynamics,* **19**(2), pp. 392–397. 57, 74

[131] Messac, A., 2000. "From dubious construction of objective functions to the application of physical programming." *AIAA Journal,* **38**(1), pp. 155–163. 57, 62, 63, 74

[132] Messac, A., Puemi-Sukam, C., and Melachrinoudis, E., 2000. "Aggregate objective functions and pareto frontiers: Required relationships and practical implications." *Optimization and Engineering,* **1**, pp. 171–188. 63

[133] Simpson, T. W., 1998. "Product platform design and optimization: Status and promise." *Artificial Intelligence for Engineering Design, Analysis and Manufacturing,* **18**(1), pp. 3–20. 64

[134] Blackwell, T., and Branke, J., 2004. "Multi-swarm optimization in dynamic environments." In *Applications of Evolutionary Computing*, Vol. 3005 of *Lecture Notes in Computer Science*. Springer Berlin / Heidelberg, pp. 489–500 10.1007/978-3-540-24653-4_50. 64

[135] Hatzakis, I., and Wallace, D., 2006. "Dynamic multi-objective optimization with evolutionary algorithms: a forward-looking approach." In *Proceedings of the 8th annual conference on Genetic and evolutionary computation*, GECCO '06, ACM, pp. 1201–1208. 64

[136] Trautmann, H., and Mehnen, J., 2009. "Preference-based pareto optimization in certain and noisy environments." *Engineering Optimization,* **41**(1), pp. 23–38. 64

[137] Heintz, C., 2002. "Aircraft design made easy." *EAA Experimenter Magazine*, November. 68, 70

[138] Bowman, M. W., 1999. *Lockheed C-130 Hercules*. Crowood Press. 68

[139] Smith, P. C., 2001. *Lockheed C-130 Hercules: The World's Favourite Military Transport*. Airlife Press. 68

[140] Frangopol, D. M., and Corotis, R. B., 1996. "Reliability-based structural system optimization: State-of-the-art verses state-of-the-practice." *Proceedings of the Twelfth Conference on Analysis and Computation*, April, pp. 67–78. 78

[141] Thanedar, P. B., and Kodiyalam, S., 1991. "Structural optimization using probabilistic constraints." In *AIAA/ASME/ASCE/AHS Structures, Structural Dynamics, and Materials Conference*, no. AIAA-91-0922-CP. 78

[142] Melchers, R. E., 1999. *Structural Reliability: Analysis and Prediction*. Ellis Horwood Series in Civil Engineering. John Wiley & Sons, New York. 78

[143] Parkinson, A., Sorensen, C., and Pourhassan, N., 1995. "A general approach for robust optimal design." *ASME Journal of Mechanical Design,* **115**, pp. 74–80. 78

[144] Chen, W., Sahai, A., Messac, A., and Sundaraj, G. J., 2000. "Exploring the effectiveness of physical programming in robust design." *ASME Journal of Mechanical Design,* **122**(2), June, pp. 155–163. 78

[145] Su, J., and Renaud, J. E., 1997. "Automatic differentiation in robust optimization." *AIAA Journal,* **35**(6), pp. 1072–1079. 78

[146] Taguchi, G., 1993. *Taguchi on Robust Technology Development: Bringing Quality Engineering Upstream*. ASME Press, New York. 78

[147] Messac, A., and Ismail-Yahaya, A., 2002. "Multiobjective robust design using physical programming." *Structural and Multidisciplinary Optimization,* **23**(5), pp. 357–371. 78

[148] Chen, W., and Wassenaar, H. J., 2001. "An approach to decision-based design." In *Proceedings of DETC'01, ASME 2001 Design Engineering Technical Conference and Computers and Information in Engineering Conference*, no. DETC2001/DMT-21683. 78

[149] DeVor, R. E., Chang, T. H., and Sutherland, J. W., 1992. *Statistical Quality Design and Control: Contemporary Concepts and Methods*. Prentice Hall, New Jersey, pp. 525–535. 78

[150] Koch, P. N., 2002. "Probabilistic design: Optimizing for six sigma quality." In *43rd AIAA/ASME/ASCE/AHS Structures, Structural Dynamics, and Materials Conference*, no. AIAA–2002–1471. 78

[151] Halton, J. H., 1960. "On the efficiency of certain quasi-random sequences of points in evaluating multi-dimensional integrals." *Numerische Mathematik,* **2**, pp. 84–90. 78

[152] Hammersley, J. M., 1960. "Monte carlo methods for solving multivariate problems." *Annals of the New York Academy of Science,* **86**, May, pp. 844–874. 78

[153] Owen, A. B., 1998. "Latin supercube sampling for very high-dimensional simulations." *ACM Transactions on Modeling and Computer Simulations,* **86**(1), January, pp. 71–102. 78

[154] Hutcheson, R. S., and McAdams, D. A., 2010. "A hybrid sensitivity analysis for use in early design." *Journal of Mechanical Design,* **132**(11), November, p. 111007. 78

[155] Xiong, F., Guo, K., and Zhou, W., 2011. "Uncertainty propagation techniques in probabilistic design of multilevel systems." In *2011 International Conference on Quality, Reliability, Risk, Maintenance, and Safety Engineering*, pp. 874–878. 78

[156] Li, G., and Zhang, K., 2011. "A combined reliability analysis approach with dimension reduction method and maximum entropy method." *Structural and Multidisciplinary Optimization,* **43**(1), pp. 121–134. 78

[157] Larson, B., Anderson, T. V., and Mattson, C. A., 2010. "System behavioral model verification for concurrent design modeling." In *13th AIAA/ISSMO Multidisciplinary Analysis and Optimization Conference*, no. AIAA-2010-9104. 78

[158] Evans, J. W., Zawadzki, R. J., Jones, S. M., Olivier, S. S., and Werner, J. S., 2009. "Error budget analysis for an adaptive optics optical coherence tomography system." *Optics Express,* **17**(16), August, pp. 13768–13784. 78

[159] Hamaker, H. C., 1995. "Improved estimates of the range of errors on photomasks using measured values of skewness and kurtosis." *Proceedings of SPIE,* **2621**(198(1995)), March. 78

[160] Hayes, B., 2003. "A lucid interval." *American Scientist,* **91**(6), November-December, pp. 484–488. 78

[161] Box, G. E., and Tiao, G. C., 1992. *Bayesian Inference in Statistical Analysis*. Wiley, Hoboken, NJ, April ISBN: 9780471574286. 78

[162] Microsoft Research, 2011. Basics of bayesian inference and belief networks, July. 78

[163] Lombardi, M., and Haftka, R. T., 1998. "Anti-optimization technique for structural design under load uncertainties." *Computer Methods in Applied Mechanics and Engineering,* **157**(1-2), pp. 19–31. 78

[164] Gurav, S. P., Goosen, J. F. L., and vanKeulen, F., 2005. "Bounded-but-unknown uncertainty optimization using design sensitivities and parallel computing: Application to mems." *Structural Optimization and Computational Mechanics,* **83**(14), pp. 1134–1149. 78

[165] Glancy, C., 1999. "A second-order method for assembly tolerance analysis." In *Proceedings of the 1999 ASME Design Engineering Technical Conferences*, no. DAC-8707 in DETC99. 78

[166] Vardeman, S. B., 1994. *Statistics for Engineering Problem Solving*. PWS Publishing Company, Boston, MA ISBN: 0-534-92871-4. 78

[167] Jackson, P. S., 1982. "A second-order moments method for uncertainty analysis." *IEEE Transactions on Reliability,* **R-31**(4), October, pp. 382–384. 78

[168] Krishnan, V., and Ulrich, K. T., 2001. "Product development decisions: A review of the literature." *Management Science,* **47**(1), January, pp. 1–21. 97

[169] Rice, M., Kelley, D., Peters, L., and "O'C"onnor, G. C., 2001. "Radical innovation: Triggering initiation of opportunity recognition and evaluation." *R & D Management,* **31**(4), October, pp. 409–420. 98

[170] Ardichvili, A., and Cardozo, R. N., 2000. "A model of the entrepreneurial opportunity recognition process." *Journal of Enterprising Culture,* **8**(2), June, pp. 103–119. 98

[171] Ardichvili, A., Cardozo, R. N., and Ray, S., 2003. "A theory of entrepreneurial opportunity identification and development." *Journal of Business Venturing,* **18**(1), January, pp. 105–123. 98

[172] Park, J. S., 2005. "Opportunity recognition and product innovation in entrepreneurial hi-tech start-ups: a new perspective and supporting case study." *Technovation,* **25**, pp. 739–752. 98

[173] Zahra, S. A., Korri, J. S., and Yu, J., 2005. "Cognition and international entrepreneurship: implications for research on international opportunity recognition and exploitation." *International Business Review,* **14**(2), April, pp. 129–146. 98

[174] Baron, R. A., and Ensley, M. D., 2006. "Opportunity recognition as the detection of meaningful patterns: Evidence from comparisons of novice and experienced entrepreneurs." *Management Science,* **52**(9), September, pp. 1331–1344. 98

[175] Hills, G. E., and Singh, R. P., 2004. "Opportunity recognition." In *Handbook of Entrepreneurial Dynamics: The Process of Business Creation*, W. B. Gartner, K. G. Shaver, N. M. Carter, and P. D. Reynolds, eds. Sage Publications, ch. 24. 98

[176] Kakati, M., 2003. "Success criteria in high-tech new ventures." *Technovation,* **23**(5), pp. 447–457. 98

[177] Arenius, P., and De Clercq, D., 2005. "A network-based approach on opportunity recognition." *Small Business Economics,* **24**(3), pp. 249–265. 98

[178] SocialVentureCanvas.com, 2012. Social venture canvas: A too to build lean, validated, impactful, and innovative social ventures Online. 98

[179] Urban, G., and Hauser, J., 1993. *Design and Marketing of New Products*. Prentice Hall, Englewood Cliffs, NJ. 99

[180] Leonard-Barton, D., 1995. "Wellsprings of knowledge." *Boston: Harvard Business School Press*. 99

[181] Sanders, E., 2002. "Ethnography in npd research: How applied ethnography can improve your npd research process." *Visions*, April. 99

[182] Griffin, A., and Hauser, J., 1993. "The voice of the customer." *Marketing Science,* **12**(1), pp. 1–27. 99

[183] Iansiti, M., and Stein, E., 1995. "Understanding user needs." In *Harvard Business School*. 99

[184] Pulman, M., Moore, W., and Wardell, D., 2002. "A comparison of quality function deployment and conjoint analysis in new product design." *Journal of Product Innovation Management,* **19**, pp. 354–364. 99

[185] World Resources Institute and International Finance Corporation, 2007. The next 4 billion: Market size and business strategy at the base of the pyramid Tech. rep., World Bank, June http://rru.worldbank.org/thenext4billion. 102, 103

[186] Fisher, M., 2006. "Income is development." *Innovations Journal,* **Winter 2006**, pp. 9–30. 102, 103

[187] International Development Enterprises, 2008. *Rural Wealth Creation: Strategic Directions for IDE*. 102, 103

[188] Prahalad, C. K., 2005. *The Fortune at the Bottom of the Pyramid: Eradicating Poverty Through Profits*. Wharton School Publishing. 102

[189] Polak, P., 2005. "The big potential of small farms." *Scientific American,* **293**(3). 102

[190] KickStart, 2009. *Our 5 Step Process*. http://www.kickstart.org/what-we-do/step-02.php. 102, 103

[191] The Mulago Foundation, 2012. One acre fund: Planting prosperity, June. 102, 122

[192] Johnson, N. G., Hallam, A., Bryden, M., and Conway, S., 2006. "Sustainable and market-based analysis of cooking technologies in developing countries." In *Proceeding of the ASME International Mechanical Engineering Congress and Exposition*, no. IMECE2006-15375. 103

[193] Munson, B. R., Young, D. F., and Okiishi, T. H., 2006. *Fundamentals of Fluid Mechanics*., fifth ed. John Wiley & Sons. 106, 109

[194] Pilkey, W. D., and Pilkey, D. F., 2008. *Peterson's Stress Concentration Factors*., 3 ed. John Wiley & Sons Inc. 125

APPENDIX A. AIRCRAFT EXAMPLE DYNAMIC S-PARETO FORMULATION INPUTS

For the aircraft design example presented in Chapter 8 there are three concepts. The variable values for these different concepts are presented in Tables A.1 – A.3. The units and descriptions of these variables are given in Section 8.1. The rows of the tables at each time-step are the values of the diagonal matrix ($\chi^{(k^{(t)})}$) and design object limits ($x_l^{(k^{(t)})}$, $x_u^{(k^{(t)})}$) for the corresponding concept. For example, the rows corresponding $\chi_{i,i}$, x_l, and x_u for Concept 1 at $t = 1$ represent the $\chi_{i,i}^{(1^{(1)})}$ values of equation 7.5, $x_l^{(1^{(1)})}$ values of equation 7.3, and $x_u^{(1^{(1)})}$ values of equation 7.3, respectively.

Table A.1: Values of the objective identifiers and design object limits for aircraft Concept 1 (k = 1)

		φ	$C_{L,fd}$	$C_{L,c}$	b	V_{turn}	r_f	r_{eu}	$V_{s,fd}$	$V_{s,c}$	E	W_c	Z_{cr}	Z_{sp}	V_{cr}	V_{sp}	g	ρ	W	P	$\hat{T}_{lost}$
$t=1$	$\chi_{i,i}$	0	0	0	0	–	0	0	0	0	0	0	0	0	0	0	0	0	1	1	–
	x_l	95	2.2	1.1	30	–	0.40	1.4	45	50	3	450	13e3	5e3	90	120	32.2	0.0584	0	75	–
	x_u	125	2.5	1.4	50	–	0.40	1.4	45	50	3	450	13e3	5e3	90	120	32.2	0.0584	1500	120	–
$t=2$	$\chi_{i,i}$	0	0	0	0	–	0	0	0	0	0	0	0	0	0	0	0	0	1	1	–
	x_l	95	2.2	1.1	30	–	0.40	1.4	45	50	3	430	11e3	5e3	90	110	32.2	0.0584	0	75	–
	x_u	125	2.5	1.4	50	–	0.40	1.4	45	50	3	430	11e3	5e3	90	110	32.2	0.0584	1500	120	–
$t=3$	$\chi_{i,i}$	–	–	–	–	–	–	–	–	–	–	–	–	–	–	–	–	–	–	–	–
	x_l	–	–	–	–	–	–	–	–	–	–	–	–	–	–	–	–	–	–	–	–
	x_u	–	–	–	–	–	–	–	–	–	–	–	–	–	–	–	–	–	–	–	–

Table A.2: Values of the objective identifiers and design object limits for aircraft Concept 2 (k = 2)

		φ	$C_{L,fd}$	$C_{L,c}$	b	V_{turn}	r_f	r_{eu}	$V_{s,fd}$	$V_{s,c}$	E	W_c	Z_{cr}	Z_{sp}	V_{cr}	V_{sp}	g	ρ	W	P	$\hat{T}_{lost}$
$t=1$	$\chi_{i,i}$	0	0	0	0	–	0	0	0	0	0	0	0	0	0	0	0	0	1	1	–
	x_l	85	1.8	1.1	25	–	0.4	1.4	45	50	3	450	13e3	5e3	90	120	32.2	0.0584	0	75	–
	x_u	110	2.1	1.4	45	–	0.4	1.4	45	50	3	450	13e3	5e3	90	120	32.2	0.0584	1500	120	–
$t=2$	$\chi_{i,i}$	0	0	0	0	–	0	0	0	0	0	0	0	0	0	0	0	0	1	1	–
	x_l	85	1.8	1.1	25	–	0.36	1.4	45	50	3	430	11e3	5e3	90	110	32.2	0.0584	0	75	–
	x_u	110	2.1	1.4	45	–	0.36	1.4	45	50	3	430	11e3	5e3	90	110	32.2	0.0584	1500	120	–
$t=3$	$\chi_{i,i}$	0	0	0	0	0	0	0	0	0	0	0	0	0	0	0	0	0	1	1	1
	x_l	85	1.8	1.1	25	90	0.36	1.4	45	50	3.5	402	12e3	7e3	90	90	32.2	0.0584	0	75	6.9e-4
	x_u	110	2.1	1.4	45	115	0.36	1.4	45	50	3.5	402	12e3	7e3	90	90	32.2	0.0584	1500	120	8e-4

Table A.3: Values of the objective identifiers and design object limits for aircraft Concept 3 ($k = 3$)

		φ	$C_{\mathrm{L,fd}}$	$C_{\mathrm{L,c}}$	b	V_{turn}	r_{f}	r_{eu}	$V_{\mathrm{s,fd}}$	$V_{\mathrm{s,c}}$	E	W_{c}	Z_{cr}	Z_{sp}	V_{cr}	V_{sp}	g	ρ	W	P	$\hat{T}_{\mathrm{lost}}$
$t = 1$	$\chi_{i,i}$	–	–	–	–	–	–	–	–	–	–	–	–	–	–	–	–	–	–	–	–
	x_l	–	–	–	–	–	–	–	–	–	–	–	–	–	–	–	–	–	–	–	–
	x_u	–	–	–	–	–	–	–	–	–	–	–	–	–	–	–	–	–	–	–	–
$t = 2$	$\chi_{i,i}$	0	0	0	0	–	0	0	0	0	0	0	0	0	0	0	0	0	1	1	–
	x_l	75	1.5	1.1	20	–	0.30	1.4	45	50	3	430	11e3	5e3	90	110	32.2	0.0584	0	75	–
	x_u	90	1.8	1.4	35	–	0.30	1.4	45	50	3	430	11e3	5e3	90	110	32.2	0.0584	1500	120	–
$t = 3$	$\chi_{i,i}$	0	0	0	0	0	0	0	0	0	0	0	0	0	0	0	0	0	1	1	1
	x_l	75	1.5	1.1	20	90	0.30	1.4	45	50	3.5	402	12e3	7e3	90	90	32.2	0.0584	0	75	6.9e-4
	x_u	90	1.8	1.4	35	115	0.30	1.4	45	50	3.5	402	12e3	7e3	90	90	32.2	0.0584	1500	120	8e-4

APPENDIX B. CART EXAMPLE OPTIMIZATION FORMULATION INPUTS

A summary of each non-modular plywood cart concept's design objects for $t = \{1,2,3\}$, along with the corresponding values of $x_l^{(k^{(t)})}$, $x_u^{(k^{(t)})}$, and the diagonal entries in $w^{(k^{(t)})}$ needed to evaluate Problem 9.1 are provided in Tables B.1 and B.2. It should be noted that the bounds of the anticipated regions of interest as defined in Section 9.4 (Step B) are presented in Table B.1 as the listed values of $S_l^{(k^{(t)})}$ and $S_u^{(k^{(t)})}$. In addition, for this example it is assumed the values of $y^{(k^{(t)})}$ have bounded uncertainties that result in the domain (h) of the uncertain parameters (c) being defined as $c_l^{(k^{(t)})} \leq c^{(k^{(t)})} \leq c_u^{(k^{(t)})}$. The values of $c_l^{(k^{(t)})}$ and $c_u^{(k^{(t)})}$ needed to evaluate Problem 9.1 are also provided in Table B.2.

Limits of the modular-system design objects ($\hat{x}_{u/l}$), the corresponding diagonal entries in $\hat{w}$, the domain limit vectors of the modular-system uncertain parameters ($\hat{c}_{u/l}$), and the bounds of the uncertain areas of the regions of interest ($\hat{S}^{(i)}_{u/l,\text{unc}}$) needed to evaluate Problem 9.2 are provided in Table B.3.

Table B.1: Values of $z_{l/u}$ and the objective identifiers (diagonal entries in $\chi^{(k^{(t)})}$) for the cart example evaluation of Problem 9.1.

	$t=1$			$t=2$						$t=3$		
	$k=1$			$k=1$			$k=2$			$k=1$		
z (units)	χ	z_l	z_u	χ	z_l	z_u	χ	z_l	z_u	χ	z_l	z_u
S (\$)	1	60	105	1	95	153	1	95	153	1	112	154
A (m^2)	-1	0.697	1.333	–	–	–	–	–	–	–	–	–
V (m^3)	–	–	–	-1	1.147	2.327	-1	1.147	2.327	-1	0.229	0.557
L_{fail} (N)	0	4448.2	22241	0	4448.2	22241	0	4448.2	22241	0	4448.2	22241
σ_f (MPa)	0	0	76.532	0	0	76.532	0	0	76.532	0	0	76.532
σ_a (MPa)	0	0	344.7	0	0	344.7	0	0	344.7	0	0	344.7
σ_{ps} (MPa)	–	–	–	0	0	99.63	–	–	–	–	–	–
σ_{ws} (MPa)	–	–	–	–	–	–	0	0	76.532	0	0	76.532
θ (rad)	0	0	0.297	0	0	0.297	0	0	0.297	0	0	0.297
F_u (N)	0	0	444.8	0	0	444.8	0	0	444.8	0	0	444.8
F_{ud} (N)	–	–	–	–	–	–	–	–	–	0	0	2224.1
$\bar{g}_1$ (mm)	0	0	∞	0	0	∞	0	0	∞	0	0	∞
$\bar{g}_2$ (mm)	–	–	–	–	–	–	–	–	–	0	0	∞
$\bar{g}_3$ (mm)	0	686	762	0	686	762	0	686	762	0	686	762
$\bar{g}_4$ (mm)	0	0	∞	0	0	∞	0	0	∞	0	0	∞
$\bar{g}_5$ (mm)	0	0	∞	0	0	∞	0	0	∞	0	0	∞

Table B.2: Values of $y_{l/u}$, $c_{l/u}$, and the objective identifiers (diagonal entries in $\chi^{(k^{(t)})}$) for the cart example evaluation of Problem 9.1.

	$t=1$					$t=2$										$t=3$				
	$k=1$					$k=1$					$k=2$					$k=1$				
y (units)	χ	y_l	y_u	c_l	c_u	χ	y_l	y_u	c_l	c_u	χ	y_l	y_u	c_l	c_u	χ	y_l	y_u	c_l	c_u
d_a (mm)	0	19.05	19.05	-0.051	0	0	19.05	19.05	-0.051	0	0	19.05	19.05	-0.051	0	0	19.05	19.05	-0.051	0
l_b (mm)	0	1143	1625.6	-0.254	0.254	0	1143	1625.6	-0.254	0.254	0	1143	1625.6	-0.254	0.254	0	1143	1625.6	-0.254	0.254
w_b (mm)	0	609.6	812.8	-0.254	0.254	0	609.6	812.8	-0.254	0.254	0	609.6	812.8	-0.254	0.254	0	609.6	812.8	-0.254	0.254
h_f (mm)	0	95.25	107.95	-0.254	0.254	0	95.25	107.95	-0.254	0.254	0	95.25	107.95	-0.254	0.254	0	95.25	107.95	-0.254	0.254
l_1 (mm)	0	508	711.2	-0.254	0.254	0	508	711.2	-0.254	0.254	0	508	711.2	-0.254	0.254	0	508	711.2	-0.254	0.254
h_1 (mm)	0	25.4	34.9	-0.254	0.254	0	25.4	34.9	-0.254	0.254	0	25.4	34.9	-0.254	0.254	0	25.4	34.9	-0.254	0.254
t_s (mm)	0	19.05	28.58	-1.778	0	0	19.05	28.58	-1.778	0	0	19.05	28.58	-1.778	0	0	19.05	28.58	-1.778	0
w_s (mm)	0	1193.8	1193.8	-1.588	0	0	1193.8	1193.8	-1.588	0	0	1193.8	1193.8	-1.588	0	0	1193.8	1193.8	-1.588	0
l_s (mm)	0	2438.4	2438.4	-1.588	0	0	2438.4	2438.4	-1.588	0	0	2438.4	2438.4	-1.588	0	0	2438.4	2438.4	-1.588	0
l_o (mm)	0	38.1	38.1	0	0	0	38.1	38.1	0	0	0	38.1	38.1	0	0	0	38.1	38.1	0	0
d_t (mm)	0	9.525	9.525	0	0	0	9.525	9.525	0	0	0	9.525	9.525	0	0	0	9.525	9.525	0	0
f_r (mm/s)	0	50.8	50.8	0	0	0	50.8	50.8	0	0	0	50.8	50.8	0	0	0	50.8	50.8	0	0
L (N)	0	2224.1	2224.1	0	0	0	2224.1	2224.1	0	0	0	2224.1	2224.1	0	0	0	2224.1	2224.1	0	0
LF	0	2	100	0	0	0	2	100	0	0	0	2	100	0	0	0	2	100	0	0
h_c (mm)	0	47.625	53.975	-0.255	0.254	0	47.625	53.975	-0.255	0.254	0	47.625	53.975	-0.255	0.254	0	47.625	53.975	-0.255	0.254
h_u (mm)	0	889	889	0	0	0	889	889	0	0	0	889	889	0	0	0	889	889	0	0
ϕ_{mach} (\$/hr)	0	20	20	0	0	0	20	20	0	0	0	20	20	0	0	0	20	20	0	0
ϕ_a (\$/m)	0	4.10	4.10	0	0	0	4.10	4.10	0	0	0	4.10	4.10	0	0	0	4.10	4.10	0	0
C_{bwnp} (\$)	0	2	2	0	0	0	2	2	0	0	0	2	2	0	0	0	2	2	0	0
l_r (mm)	0	1828.8	2333.6	-0.255	0.254	0	1828.8	2333.6	-0.255	0.254	0	1828.8	2333.6	-0.255	0.254	0	1828.8	2333.6	-0.255	0.254
h_r (mm)	0	254	574.7	-0.255	0.254	0	254	574.7	-0.255	0.254	0	254	574.7	-0.255	0.254	0	254	574.7	-0.255	0.254
d_w (mm)	0	508	762	-0.255	0.254	0	508	762	-0.255	0.254	0	508	762	-0.255	0.254	0	508	762	-0.255	0.254
h_{ps} (mm)	–	–	–	–	–	0	1219.2	1828.8	-0.255	0.254	–	–	–	–	–	–	–	–	–	–
n_p	–	–	–	–	–	0	8	8	0	0	–	–	–	–	–	–	–	–	–	–
d_{po} (mm)	–	–	–	–	–	0	33.4	33.4	-0.127	0.127	–	–	–	–	–	–	–	–	–	–
d_{pi} (mm)	–	–	–	–	–	0	26.24	26.24	-0.127	0.127	–	–	–	–	–	–	–	–	–	–
ϕ_{p} (\$/m)	–	–	–	–	–	0	2.38	2.38	0	0	–	–	–	–	–	–	–	–	–	–
h_{ws} (mm)	–	–	–	–	–	–	–	–	–	–	0	254	939.8	-0.254	0.254	0	302.2	304.8	-0.254	0.254
n_t (mm)	–	–	–	–	–	–	–	–	–	–	0	8	8	0	0	–	–	–	–	–
t_{ws} (mm)	–	–	–	–	–	–	–	–	–	–	0	12.7	12.7	-0.178	0	0	12.7	12.7	-0.178	0
w_{st} (mm)	–	–	–	–	–	–	–	–	–	–	0	38.1	50.8	-0.254	0.254	0	38.1	50.8	-0.254	0.254
ϕ_{ws} (\$/m^2)	–	–	–	–	–	–	–	–	–	–	0	30	30	0	0	0	30	30	0	0

Table B.3: Limit values of the modular-system design objects ($\hat{x}_{u/l}$), uncertain parameter domain limits ($\hat{c}_{u/l}$), and the corresponding diagonal entries in $\hat{w}^{(i)}$ needed to evaluate Problem 9.2.

$\hat{x}$	$\hat{w}^{(0)}$	$\hat{w}^{(1)}$	$\hat{w}^{(2)}$	x_l	x_u	c_l	c_u
$\hat{d}_a$	0	0	0	19.05	19.05	-0.051	0
$\hat{l}_b$	0	0	0	1143	1625.6	-0.254	0.254
$\hat{w}_b$	0	0	0	609.6	812.8	-0.254	0.254
$\hat{h}_f$	0	0	0	95.25	107.95	-0.254	0.254
$\hat{l}_1$	0	0	0	508	711.2	-0.254	0.254
$\hat{h}_1$	0	0	0	25.4	34.9	-0.254	0.254
$\hat{t}_s$	0	0	0	19.05	28.58	-1.778	0
$\hat{w}_s$	0	0	0	1193.8	1193.8	-1.588	0
$\hat{l}_s$	0	0	0	2438.4	2438.4	-1.588	0
$\hat{l}_o$	0	0	0	38.1	38.1	0	0
$\hat{d}_t$	0	0	0	9.525	9.525	0	0
$\hat{f}_r$	0	0	0	50.8	50.8	0	0
$\hat{L}$	0	0	0	2224.1	2224.1	0	0
$\hat{LF}$	0	0	0	2	100	0	0
$\hat{h}_c$	0	0	0	47.625	53.975	-0.255	0.254
$\hat{h}_u$	0	0	0	889	889	0	0
$\hat{\phi}_{\text{mach}}$	0	0	0	20	20	0	0
$\hat{\phi}_a$	0	0	0	4.10	4.10	0	0
$\hat{C}_{\text{bwnp}}$	0	0	0	2	2	0	0
$\hat{l}_r$	0	0	0	1828.8	2333.6	-0.255	0.254
$\hat{h}_r$	0	0	0	254	574.7	-0.255	0.254
$\hat{d}_w$	0	0	0	508	762	-0.255	0.254
$\hat{h}_{ps}$	–	0	–	1219.2	1828.8	-0.255	0.254
$\hat{n}_p$	–	0	–	8	8	0	0
$\hat{d}_{po}$	–	0	–	33.4	33.4	-0.127	0.127
$\hat{d}_{pi}$	–	0	–	26.24	26.24	-0.127	0.127
$\hat{\phi}_{\text{p}}$	–	0	–	2.38	2.38	0	0
$\hat{h}_{ws}$	–	–	0	302.2	304.8	-0.254	0.254
$\hat{t}_{ws}$	–	–	0	12.7	12.7	-0.178	0
$\hat{\phi}_{\text{ws}}$	–	–	0	30	30	0	0
$\hat{S}^{(0)}$	1	–	–	60	105	–	–
$\hat{A}^{(0)}$	-1	–	–	0.697	1.333	–	–
$\hat{L}^{(i)}_{\text{fail}}$	0	0	0	4448.2	22241	–	–
$\hat{\sigma}^{(i)}_f$	0	–	0	0	76.532	–	–
$\hat{\sigma}_a$	0	–	–	0	344.7	–	–
$\hat{\theta}$	0	–	–	0	0.297	–	–
$\hat{F}_u$	0	–	–	0	444.8	–	–
$\hat{\bar{g}}_1$	0	–	–	0	∞	–	–
$\hat{\bar{g}}_2$	–	–	0	0	∞	–	–
$\hat{\bar{g}}_3$	0	–	–	686	762	–	–
$\hat{\bar{g}}_4$	0	–	–	0	∞	–	–
$\hat{\bar{g}}_5$	0	–	–	0	∞	–	–
$\hat{S}^{(1)}$	–	1	–	95	153	–	–
$\hat{V}^{(1)}$	–	-1	–	1.147	2.327	–	–
$\hat{\sigma}_{ps}$	–	0	–	0	99.63	–	–
$\hat{S}^{(2)}$	–	–	1	112	154	–	–
$\hat{V}^{(2)}$	–	–	-1	0.229	0.557	–	–
$\hat{\sigma}_{ws}$	–	–	0	0	76.532	–	–
$\hat{F}_{ud}$	–	–	0	0	2224.1	–	–
$\hat{\bar{g}}_6$	–	–	0	0	0	–	–
$\hat{\bar{g}}_7$	–	–	0	0	∞	–	–